

AD-A146 879

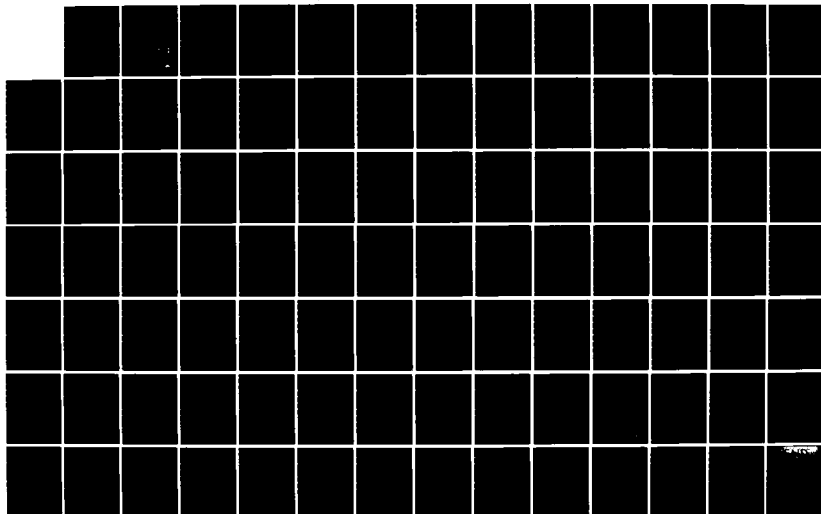
SIGNAL ANALYSIS OF VISUAL EVOKED RESPONSES(U)
SCIENTIFIC SYSTEMS INC CAMBRIDGE MA W JARISCH ET AL.
DEC 83 USAFSAM-TR-83-38 F33615-81-C-0602

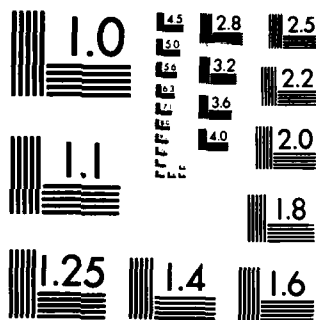
1/1

UNCLASSIFIED

F/G 6/16

NL





OPY RESOLUTION TEST CHART

12

Report USAFSAM-TR-83-38

AD-A146 879

SIGNAL ANALYSIS OF VISUAL EVOKED RESPONSES

Wolfram Jarisch, Ph.D.

Kia Hsu, Ph.D.

Scientific Systems, Inc.
54 Rindge Avenue Extension
Cambridge, Massachusetts 02140

DTIC
ELECTE
OCT 30 1984
B

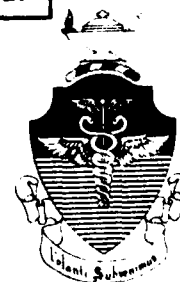
December 1983

Final Report for Period 1 January 1981 - 1 February 1982

Approved for public release; distribution is unlimited.

Prepared for

USAF SCHOOL OF AEROSPACE MEDICINE
Aerospace Medical Division (AFSC)
Brooks Air Force Base, Texas 78235-5000



DTIC FILE COPY

84 10 28 155

NOTICES

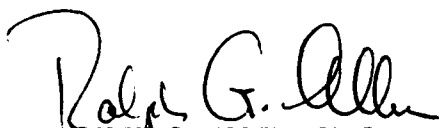
This final report was submitted by Scientific Systems, Inc., 54 Rindge Avenue Extension, Cambridge, Massachusetts, under contract F33615-81-C-0602, job order 7757-02-75, with the USAF School of Aerospace Medicine, Aerospace Medical Division, AFSC, Brooks Air Force Base, Texas. Dr. Ralph G. Allen (USAFSAM/RZV) was the Laboratory Project Scientist-in-Charge.

When Government drawings, specifications, or other data are used for any purpose other than in connection with a definitely Government-related procurement, the United States Government incurs no responsibility or any obligation whatsoever. The fact that the Government may have formulated or in any way supplied the said drawings, specifications, or other data, is not to be regarded by implication, or otherwise in any manner construed, as licensing the holder, or any other person or corporation; or as conveying any rights or permission to manufacture, use, or sell any patented invention that may in any way be related thereto.

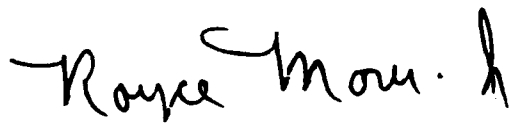
The voluntary informed consent of the subjects used in this research was obtained in accordance with AFR 169-3.

The Office of Public Affairs has reviewed this report, and it is releasable to the National Technical Information Service, where it will be available to the general public, including foreign nationals.

This report has been reviewed and is approved for publication.


RALPH G. ALLEN, Ph.D.
Project Scientist


DONALD N. FARRER, Ph.D.
Supervisor


ROYCE MOSER, Jr.
Colonel, USAF, MC
Commander

UNCLASSIFIED

SECURITY CLASSIFICATION OF THIS PAGE

REPORT DOCUMENTATION PAGE

1a. REPORT SECURITY CLASSIFICATION UNCLASSIFIED		1b. RESTRICTIVE MARKINGS	
2a. SECURITY CLASSIFICATION AUTHORITY		3. DISTRIBUTION/AVAILABILITY OF REPORT Approved for public release; distribution is unlimited.	
2b. DECLASSIFICATION/DOWNGRADING SCHEDULE		4. PERFORMING ORGANIZATION REPORT NUMBER(S)	
5. MONITORING ORGANIZATION REPORT NUMBER(S) USAFSAM-TR-83-38		6a. NAME OF PERFORMING ORGANIZATION Scientific Systems, Inc.	
6b. OFFICE SYMBOL (If applicable)		7a. NAME OF MONITORING ORGANIZATION USAF School of Aerospace Medicine (RZV)	
6c. ADDRESS (City, State and ZIP Code) 54 Rindge Avenue Extension Cambridge, Massachusetts 02140		7b. ADDRESS (City, State and ZIP Code) Aerospace Medical Division (AFSC) Brooks Air Force Base, Texas 78235	
8a. NAME OF FUNDING/SPONSORING ORGANIZATION		8b. OFFICE SYMBOL (If applicable)	
9. PROCUREMENT INSTRUMENT IDENTIFICATION NUMBER F33615-81-C-0602		10. SOURCE OF FUNDING NOS.	
8c. ADDRESS (City, State and ZIP Code)		PROGRAM ELEMENT NO. 62202F	TASK NO. 02
11. TITLE (Include Security Classification) SIGNAL ANALYSIS OF VISUAL EVOKED RESPONSES		PROJECT NO. 7757	WORK UNIT NO. 75
12. PERSONAL AUTHOR(S) Jarisch, Wolfram R., Ph.D.; and Hsu, Kia, Ph.D.			
13a. TYPE OF REPORT Final Report	13b. TIME COVERED FROM 1-1-81 TO 2-1-82	14. DATE OF REPORT (Yr., Mo., Day) 1983 December	15. PAGE COUNT 96
16. SUPPLEMENTARY NOTATION			
17. COSATI CODES		18. SUBJECT TERMS (Continue on reverse if necessary and identify by block number)	
FIELD	GROUP	SUB GR.	
06	05		
05	10		
19. ABSTRACT (Continue on reverse if necessary and identify by block number) This study was undertaken in support of the USAF School of Aerospace Medicine's (USAFSAM) goal of assessing the effect of visual stimuli upon the flier. The main objective was to reduce the variability (variance, or coefficient of variation) of estimates of visual evoked responses. For this purpose, USAFSAM had previously collected data from <u>Macaca mulatta</u> . These data have been used in this report, together with new data collected from human volunteers by the authors. The method of approach, based on modern statistical analysis, lead to the development of software which was subsequently installed on DEC 11/34 computers at the USAFSAM Laser Effects Branch. An up to sixteen-fold reduction of the coefficients of variation (stimulus present) and a more than three-fold reduction in variance (stimulus absent), compared to results of earlier classic fast-Fourier-transform methods, can be ascribed to a particular hierarchical matched filter and a maximum likelihood estimation technique.			
20. DISTRIBUTION/AVAILABILITY OF ABSTRACT UNCLASSIFIED/UNLIMITED <input checked="" type="checkbox"/> SAME AS RPT. <input type="checkbox"/> DTIC USERS <input type="checkbox"/>		21. ABSTRACT SECURITY CLASSIFICATION UNCLASSIFIED	
22a. NAME OF RESPONSIBLE INDIVIDUAL Ralph G. Allen, Ph.D.		22b. TELEPHONE NUMBER (Include Area Code) (512) 536-3622	22c. OFFICE SYMBOL USAFSAM/RZV

P R E F A C E

As Project Scientist of Contract F33615-81-C-0602, I would like to acknowledge Ms. Ena Borden Shaw (of our Medical Editing Function) for the outstanding manner in which she critically, and expertly edited this technical report. It was through the technical skill, dedication, and patience of Ms. Shaw, that the USAF School of Aerospace Medicine and Scientific Systems, Inc., were able to produce a useful document.

Ralph G. Allen

RALPH G. ALLEN, Ph.D.

(Contract Monitor)

Chief, Visual Sciences Function,
Vulnerability Assessment Branch,
Radiation Sciences Division,
USAF School of Aerospace Medicine



Accession For	
NTIS GRA&I	<input checked="checked" type="checkbox"/>
DTIC TAB	<input type="checkbox"/>
Unannounced	<input type="checkbox"/>
Justification	
By	
Distribution/	
Availability Codes	
Dist	Avail and/or Special
A-1	

CONTENTS

	<u>Page</u>
1. OBJECTIVE OF VISUAL EVOKED RESPONSE STUDY	9
2. NATURE OF THE PROBLEM	11
3. APPROACH TO REDUCING THE VARIABILITY OF ESTIMATES OF THE VER	15
3.1 Stimulus Conditions	15
3.2 Subject Preparation	15
3.3 Data Collection	15
4. THE DATA FROM <u>MACACA MULATTA</u>	17
4.1 The Database	17
4.2 Graphic Display of the VER	19
4.3 Modeling Approach for Data Processing	23
4.3.1 Removal of 60 Hz and Harmonics	23
4.3.2 Effect of Removal of ECG	24
4.3.3 Method of Construction of an ECG Template	24
4.3.4 Clipping of Data	30
4.3.5 Modeling the EEG and Segmenting	30
4.3.6 Generating a VER Template	31
4.3.7 Smoothing the VER Template	31
4.4 The Matched Filter Approach for <u>Macaca Mulatta</u>	31
4.5 Conclusions About Data from <u>Macaca Mulatta</u>	35
5. ANALYSIS OF RAW DATA FROM <u>MACACA MULATTA</u>	39
5.1 Covariance Structure	39
5.2 Properties of the VER and the EEG	39
5.3 The Spectral Properties of the ECG	42
5.4 The 60-Hz Noise	42
5.5 Conclusion	45
6. HUMAN SUBJECTS	46
6.1 Recording Techniques	46
6.2 Comparison of Variability of VER Estimates	47
6.2.1 The FFT-Method	52
6.2.2 The Matched Filter Approach for the Human Subjects	52
6.2.3 Integrated Information of Response Estimates	53

CONTENTS (Cont'd)

	<u>Page</u>
6.3 Technical Aspects of Matched Filter Approach for Human Subject Data.....	57
6.3.1 Estimating the Template	57
6.3.2 The Matched Filter for the Human Subjects	60
6.4 Integration of Information from Individual Information Channels.....	60
7. SOME BASIC STUDIES AND PROPERTIES OF THE HUMAN VER	68
7.1 The Concept of Variability	68
7.2 Relation of Fundamental and Harmonic Frequencies	69
7.3 The Effect of Blinking	69
7.4 Study of Segmenting	74
8. DISCUSSION	76
REFERENCES	77
APPENDIXES:	
1.1. Statistics for FFT Method, Center Electrode, No Stimulus--for Female Subject	81
1.2. Statistics for FFT Method, Center Electrode, With Stimulus--for Female Subject	82
1.3. Statistics for FFT Method, Center Electrode, No Stimulus--for Male Subject	83
1.4. Statistics for FFT Method, Center Electrode, With Stimulus--for Male Subject	84
2.1. Statistics for Matched Filter Method, Center Electrode, No Stimulus--for Female Subject	85
2.2. Statistics for Matched Filter Method, Center Electrode, With Stimulus--for Female Subject	86
2.3. Statistics for Matched Filter Method, Center Electrode, No Stimulus--for Male Subject	87
2.4. Statistics for Matched Filter Method, Center Electrode, With Stimulus--for Male Subject	88

APPENDIXES (Cont'd)

	<u>Page</u>
3.1. Statistics for Matched Filters, All Electrodes, Both Stimuli--for Female Subject	89
3.2. Example of Augmenting Data for Approximate Likelihood Estimation, All Channels--for Female Subject	90
3.3. Statistics for Matched Filters, All Electrodes, Both Stimuli--for Male Subject	92
3.4. Example of Augmenting Data for Approximate Maximum Likelihood Estimation, All Channels--for Male Subject	93
4.1. Usefulness of Variability Measure--for Female Subject	95
4.2. Usefulness of Variability Measure--for Male Subject	96

I L L U S T R A T I O N S

Figure No.

2.1. Example of EEG and VER data, supplied by the U.S. Air Force ..	12
2.2. Lead arrangement for recording of VER and EEG	13
4.1. Arrangement of electrodes and five channels for data file #2..	18
4.2. Integral response (VER) at the reversal rate of 4 Hz and the first harmonic at 8 Hz	20
4.3. Integral response from the matched filter approach	21
4.4. Modification of the plots in Figure 4.2	22
4.5. The raw data, the estimated 60-Hz component, and the data after removal of the 60-Hz noise	25
4.6. Scheme for the determination of the ECG template	26
4.7. Example of the average ECG in channel #1 and standard deviation of ECG	26
4.8. The effect of the removal of the 60-Hz noise and the ECG	27
4.9. Comparison of spectral components of the VER and the ECG	28
4.10. Comparison of spectral components of VER and ECG after removal of the average ECG	29

ILLUSTRATIONS (Cont'd)

	<u>Page</u>
4.11. Estimation of fiducial point and template	30
4.12. A preliminary study of AR(2) models of the EEG, without stimulus	32
4.13. A template of the VER obtained by synchronous averaging using preprocessed data	33
4.14. The smoothed VER template, after removal of higher harmonics and of all frequencies other than a multiple of the reversal rate.....	34
4.15. The matched filter approach applied to the VER signal for estimation of its amplitude	34
4.16. Result of matched filter with $\alpha_1 = .99$, $\alpha_2 = 0$	36
4.17. Comparison of transformed template with original template....	37
4.18. Output of matched filter while a stimulus was applied	38
5.1. Slow components of EEG with 3-sec period; autocorrelation ...	40
5.2. Strong serial dependency of ECG	40
5.3. Cross-correlation between two channels shows strong 60-Hz noise which extends undiminished over some 30 sec	41
5.4. The coherence between the stimulus and the VER + EEG	41
5.5. The coherence within and between the two hemispheres	43
5.6. Average ECG and standard deviation of the ECG in channel 2..	44
6.1. Arrangement of epidural electrodes in <u>Macaca mulatta</u>	48
6.2. New arrangement, for reduced common mode of VER, based on analysis of previous USAFSAM recordings.....	48
6.3. Raw data in presence of 15-Hz reversal-rate stimulus	49
6.4. Specification of channels	50
6.5. Example of high-pass filtered signal from center electrode ..	50
6.6. Summary of VER processing	51

ILLUSTRATIONS (Cont'd)

	<u>Page</u>
6.7. Sequence of 20 experimental measurements for a <u>female</u> <u>subject</u>	54
6.8. Sequence of 20 experimental measurements for a <u>male</u> <u>subject</u>	55
6.9. Raw templates for <u>male subject</u>	58
6.10. Smoothed templates for <u>male subject</u>	59
6.11. The matched filter approach applied to the VER signal for estimation of its amplitude	61
6.12. Output from matched filter	62
6.13. How error in the assumed independent variable, x , yields a biased regression line for assumed dependent variable, y ..	64
6.14. Simple model for the relation between visual evoked response, x_j , and stimulus, y	66
6.15. A more realistic model for the relation between visual evoked response, x_j , and stimulus, y	66
7.1. Autocorrelation and cross-correlation of amplitude of 15-Hz and 30-Hz components, when estimated from 1-sec segments of data.....	70
7.2. Random walk, in complex plane of the integrated 15-Hz com- ponent, when stimulus is absent	71
7.3. Comparison of phase angle of VER with and without blinking [for <u>female subject</u>]	72
7.4. Comparison of phase angle of VER with and without blinking [for <u>male subject</u>]	73

Table No.

6.1. Standard deviations of individual estimates	56
--	----

SIGNAL ANALYSIS OF VISUAL EVOKED RESPONSES

1. OBJECTIVE OF VISUAL EVOKED RESPONSE STUDY

The objective of the present work was to provide means to improve and extend results regarding the interpretation of the visual evoked response (VER), as reported in relevant literature and as previously achieved by the Laser Effects Branch, Radiation Sciences Division, of the U.S. Air Force School of Aerospace Medicine (USAFSAM). Our effort has been undertaken in support of the Air Force goal of assessing the effect of visual stimuli upon the flier.

To assess the effects of visual stimuli, USAFSAM had previously recorded data from Macaca mulatta. The data obtained were multi-electrode tracings, covering primarily the area 17 (primary visual cortex). The experimental setup was geared to obtaining modulation transfer functions for variable contrast levels during macular stimulation (narrow field-of-view).

During the analysis of these data, the USAF realized the inadequacy of conventional Fourier Analysis of VERs based on the raw data; for very long recordings had to be used to achieve a reliable estimation of the modulation transfer function. Similarly, long tracings were necessary for the inference of the psychophysical contrast level--the psychophysical contrast threshold, in particular.

Our objective was to extract the relevant information from the data by alternative means and in a more efficient manner. In other words, the present objective required the tools of modern signal analysis which were geared to reducing the effect of various noise mechanisms and to enhancing the underlying signals. Emphasis was to be placed on schemes which would be simple and robust. The schemes were to be automated in the form of algorithms which would permit the USAF to obtain the desired information in-house. [In this context, the reader is referred to a discussion of important aspects of signal processing of VERs in the preceding work by Gustafson, Eterno, and Jarisch(5).]

The material in much of this report is presented in the following order:

- (a) the background of problem;
- (b) the highlights of results (e.g., improvements);
- (c) the processing of information; and
- (d) the analysis which motivated the processing.

This format will be of assistance to those individuals who are only interested in using these algorithms. These readers will quickly find what they can expect in terms of improved signal extraction without working their way



through all the intricacies that led to the particular processing method. For the motivation behind these algorithms, refer to the technical details following the main results.

The one exception to this format is that we discuss the data (obtained in previous research) from Macaca mulatta before the processing of human subject data. Our reasons were that: we received the data from Macaca mulatta first; and, these earlier data permitted a more general discussion of aspects of signal analysis.

2. NATURE OF THE PROBLEM

The interest of the Air Force was in the study of: initially, animal VERS; and, later, human subject VERS. For obvious reasons, the data recorded from human subjects were restricted to scalp electrode recordings. By contrast, in the animal preparations, epidural bipolar electrode recordings (with a tip separation, at any given site, in the millimeter range), were possible. However, to emulate the human subject data, the USAF decided to provide us, at first, with epidural monopolar recordings of Macaca mulatta. These data were expected to exhibit properties that might also be encountered in the human subject -- thus providing, within the given time constraint, an easily accessible basis for an evaluation of our processing techniques.

Preliminary evaluation of these data by USAFSAM indicated that, in contrast to bipolar recordings, they exhibit a complex relationship between the visual stimuli and the estimated VERS. The most important difficulties encountered were:

- (a) high variability of the VER under fixed experimental conditions; and
- (b) low signal-to-noise ratio.

To extract the desired information, we had to:

- (a) separate the signal from the noise, as well as possible; and
- (b) reduce the variability through proper combination of information channels.

The problems at hand were further complicated by the fact that well-defined quantitative or qualitative models, for the desired underlying information carrying signals, did not exist. The problem of information extraction was therefore more difficult. Fortunately, however, modern signal analysis addresses precisely these problems in a systematic fashion.

For the convenience of the reader, an example of some data is given and is briefly discussed. Data previously recorded from Macaca mulatta and supplied by the USAF are shown in Fig. 2.1. Channels #1 - #8 represent the voltages recorded with the arrangement of electrodes as shown in Fig. 2.2; channel #9 merely represents the control for the phase of the pattern reversal. The following features of the tracings are striking:

The VERS are not discernible by the naked eye. The tracings contain strong components of the electrocardiogram (ECG) in all channels. Observe that these tracings coincide, over periods of several seconds, with a given phase of the control signal in channel #9.

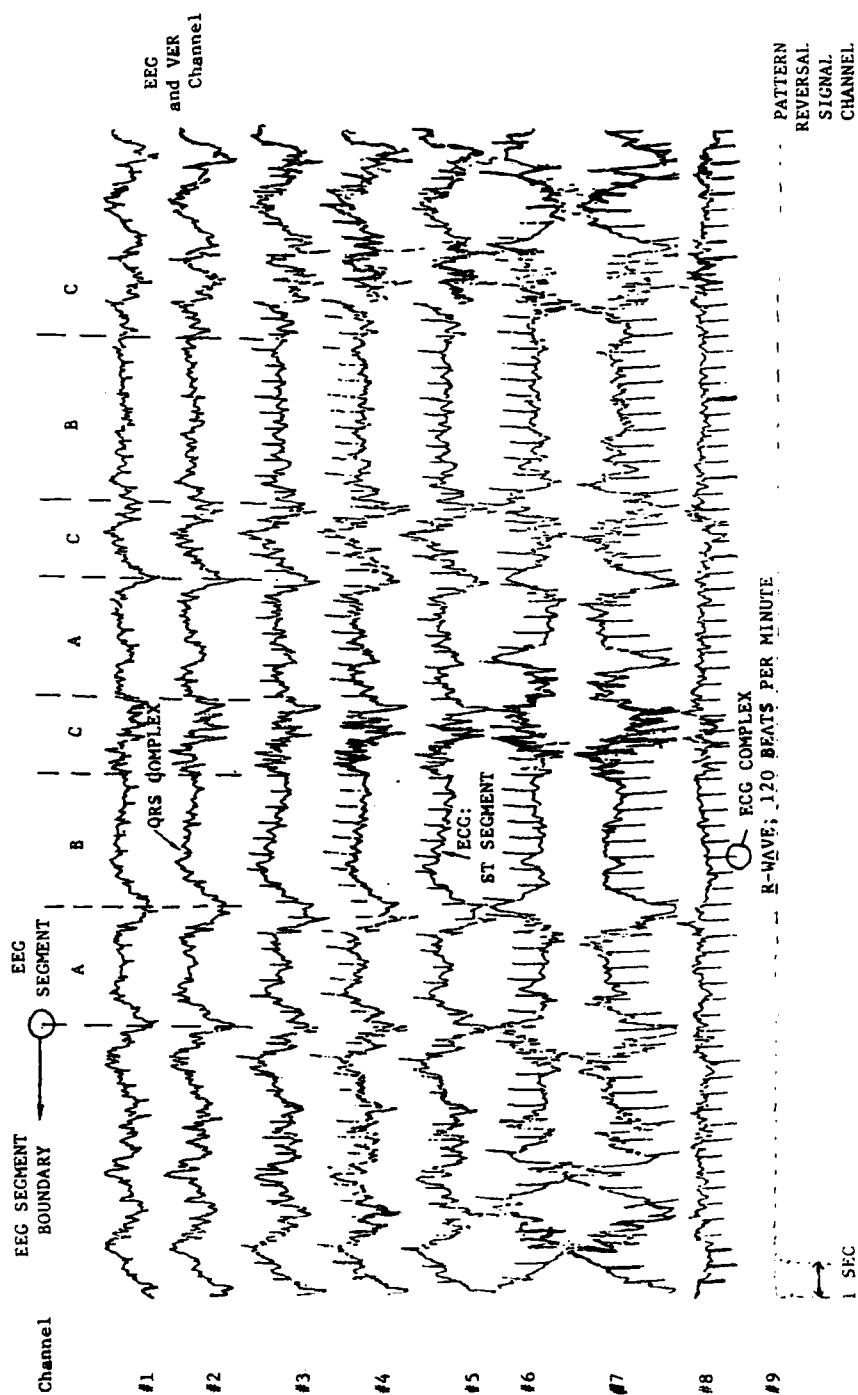


Figure 2.1. Example of EEG and VER data, supplied by the U.S. Air Force. Channels #1-8 correspond to leads (as shown in Fig. 2.2); Channel #2 carries invisible VERs; and Channel #9 is the control signal of pattern reversal.

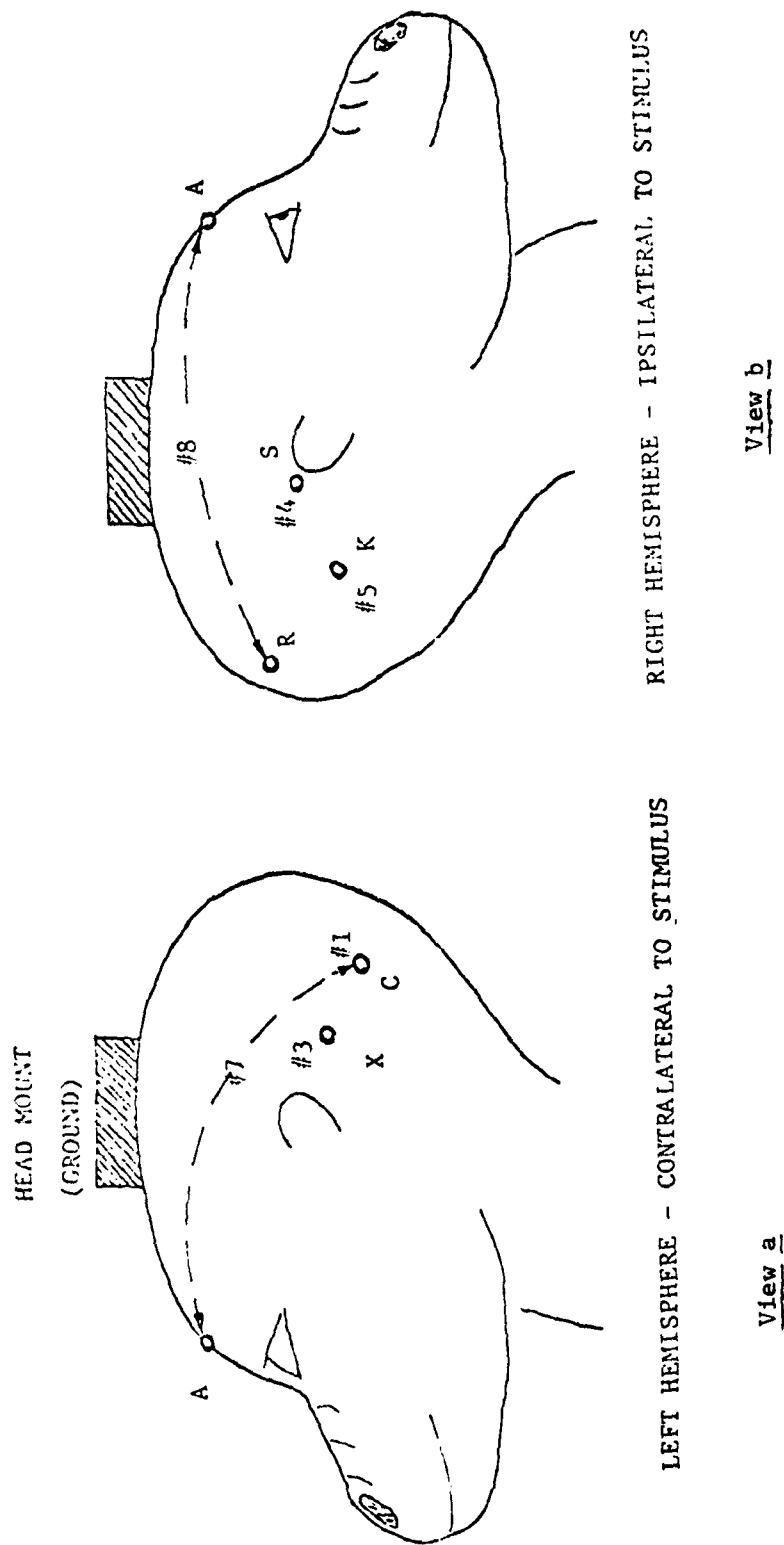


Figure 2.2: Views a and b. Lead arrangement for recording of VER and EEG. (Relation to channels in Fig. 2.1 is indicated by numbers.)

All traces show simultaneous changes of similar patterns of the electroencephalographic (EEG) background activity.

The distinct EEG background patterns may belong to a finite population; a systematic relationship also appears to exist between the administered drug level (Nembutal) and the duration and prevalence of certain of these patterns (not visible in Fig. 2.1).

A further feature concerning the VER, although not visible in these tracings, is also of importance. From various studies we know that the response to a single stimulus consists of several wavelets (4). Each of these wavelets exhibits different degrees of variability in terms of amplitude and phase, typically increasing with added time after the stimulus. All of these features of the data determined the approach we had to take and the attention we had to devote to detail.

3. APPROACH TO REDUCING THE VARIABILITY OF ESTIMATES OF THE VER

The study of the VER was particularly interesting because both Macaca mulatta and human data were included. Some important differences exist in the experimental conditions and in the characteristics of the data. Here, we give a brief overview of these differences. The detailed discussion of the individual approaches and studies of these data are reserved for subsequent sections of this report.

3.1 STIMULUS CONDITIONS

The stimulus was provided by a computer-controlled TV display. For the present experiments a colorless checkerboard pattern, of 4 degrees squared with 4 checks per degree, was used. The reversal rate for stimulating the Macaca mulatta had been 4 Hz; but, for the human subject data, the reversal rate was increased to 15 Hz. Also, the Macaca mulatta had been stimulated monocularly; but, for the human subject, both eyes were used.

3.2 SUBJECT PREPARATION

In the earlier research, the Macaca mulatta was sedated by Nembutal, and the pupil was dilated with atropine. To avoid any motion artifacts, the eye and the eyelid of the monkey were arrested with sutures; the eye was kept moist with a spraying device. Conversely, the human volunteers were unrestrained and used binocular vision.

3.3 DATA COLLECTION

The data from the Macaca mulatta were recorded from 5 epidural electrodes spaced horizontally, 10 mm apart, to cover the foveal representations on the two hemispheres. (Note that considerable anatomical differences exist, between Macaca mulatta and man, in the mapping of the foveal area into the primary visual cortex.) In the human subjects, 3 scalp electrodes were placed above the (believed) location of the calcarine fissure and were spaced horizontally 30 mm apart.

The data were bandpass-filtered with a lower corner frequency of 0.3 Hz (6 dB/octave); the upper corner frequency was 300 Hz (6 dB/octave) for the data from the Macaca mulatta, and 100 Hz (12 dB/octave) for the human subject data. For the Macaca mulatta the sampling frequency was 512 samples/sec; and, for the human subjects, 256 samples/sec. (Unfortunately, the upper corner frequency of the data from the Macaca mulatta was higher than the Nyquist frequency.) Note that the measurement of the differential voltages between the electrodes was arranged differently for the two types of data, as explained in more detail in section 6.1.

In section 4, we introduce the data formerly obtained from the Macaca mulatta. Then, in section 5, we present a number of interesting findings; and, in section 6, we turn to the modification of the recording and analysis approach for the human subjects. In section 7, some basic studies for these subjects are given. Finally, in section 8, we address some ideas on improving experimental conditions for refining the current modeling approach.

4. THE DATA FROM MACACA MULATTA

Scientific Systems, Inc., was provided with several minutes worth of earlier data, obtained with and without stimulus, and sampled before and after the subject (Macaca mulatta) had been blinded, transiently, by a flash. Even though our new data processing scheme has now been tried without any fine tuning, considerable improvement in the estimation of visual evoked responses has been achieved. Furthermore, we found some interesting results which suggested the usefulness of the combination of VER and instantaneous variability in assessing visual performance.

4.1 THE DATABASE

For the development of our basic software we were provided with data previously recorded by the USAF. These data represent potentials from 5 epidural electrodes, aligned horizontally above the visual cortex. The electrodes were spaced 10 mm apart, and potentials were recorded relative to the left ear (Fig. 4.1). The data had been preamplified with Grass preamplifiers (.3 Hz - 300 Hz), recorded on FM-tape and, at replay, digitized with 512 samples/sec.

For the development of our software, we concentrated on a dataset with, approximately, the following stimulus conditions:

<u>Time</u>	<u>Conditions</u>
0 - 60 sec	: Blank screen
60 - 180 sec	: Stimulus
180 - 420 sec	: Flash, followed by 240 sec of stimulus

The stimulus consisted of a 4-degree visual field with a reversing checkerboard pattern. The reversal rate (rectangular modulation) of the stimulus was 4/sec at 30% contrast. At T = 180 sec, a .85-Joule flash was discharged, causing a transient blinding of the subject. Throughout the experiment, only the right eye of the subject was kept open, fixed, and artificially moistened. Nembutal was administered as a sedative.

We selected these data from five similar sets, because they provided not only the largest database but also numerous artifacts with which we would eventually have to cope. They appeared to provide, also, a more reliable database when compared with the first set, as one might expect various gains settings to be better adjusted the second time.

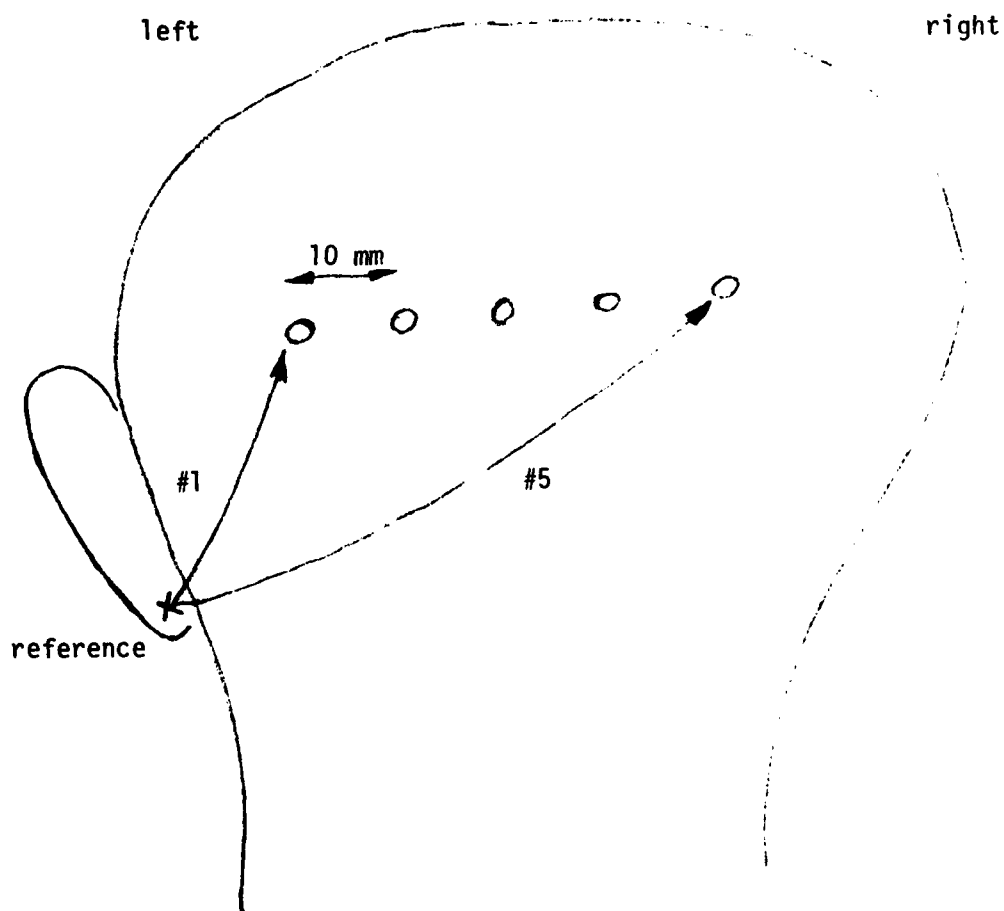


Figure 4.1. Arrangement of electrodes and five channels for data file #2 (monkey).

4.2 GRAPHIC DISPLAY OF THE VER

An important criterion in assessing the performance of data analysis is the capability to discern stimulus conditions. For this purpose, we emulated the previous USAFSAM data processing and compared it with ours.

Previous processing by USAFSAM was based on the amplitudes of the frequencies of the VER, the fundamental at the reversal rate (here, 4 Hz), and its harmonics. However, we display the data in a slightly different way than in earlier USAFSAM studies--rather than plotting the amplitude over short consecutive data windows, per se, we display the cumulative sum of these amplitudes: i.e.,

$$R(T) = \sum_{t=0}^T a(t) \quad (4.1)$$

(not power, since eq. 4.1 is more robust).

The idea here is that a consistent change of the amplitude would build up an integral response, while random changes would tend to cancel. However, the amplitudes will always be positive quantities; so, even without stimulus, the foregoing sum will show some buildup. Upon stimulation, however, one would expect a faster buildup (increase in slope). This idea is displayed in Fig. 4.2.

Next, we proceed to the cumulative output of our matched filter approach. The details of this method are explained in section 4.4. At the moment observe, in Fig. 4.3, the clear onset of a stimulus at $T = 60$ sec, compared with the display in Fig. 4.2. This comparison gives the first hint of the way in which we will proceed.

Regarding Fig. 4.2, one may argue that the onset of a stimulus is obscured because, visually, a change of slope in a display is hard to judge. To cope with such an argument, we produced the plot in Fig. 4.4 (modified from Fig. 4.2), by removing the average slope, which is present without a stimulus. Although this step appears to bring some improvement (additional information has been used, however), the integrated VER appears less clear in Fig. 4.4 than in Fig. 4.3.

Here observe also that, in Fig. 4.3, with the onset of the stimulus ($T = 60$ sec), the integral response forms a much smoother graph. The fact that such a change in character is not apparent in Fig. 4.4 can, in itself, be utilized to assess visual response.

In summary, by plotting the cumulative response, we demonstrated the superior performance of the new matched filter approach. In section 5, we discuss the individual steps of the new approach as well as some preprocessing of the data.

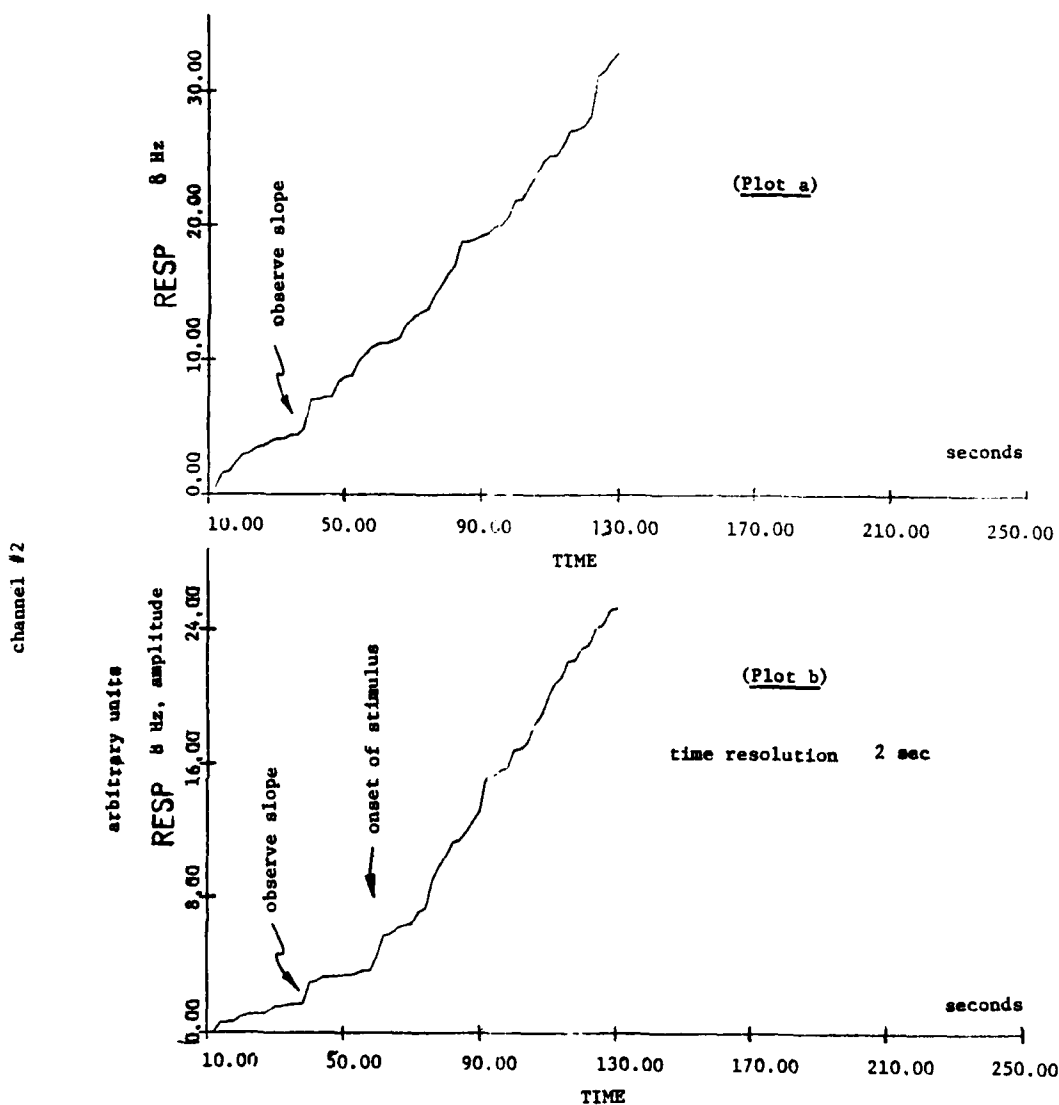


Figure 4.2: Plots a and b. Integral response (VER) at the reversal rate of 4 Hz and the first harmonic at 8 Hz. Stimulus onset is at about $T = 60$. Observe the large variability of the response, before and after onset of the stimulus.

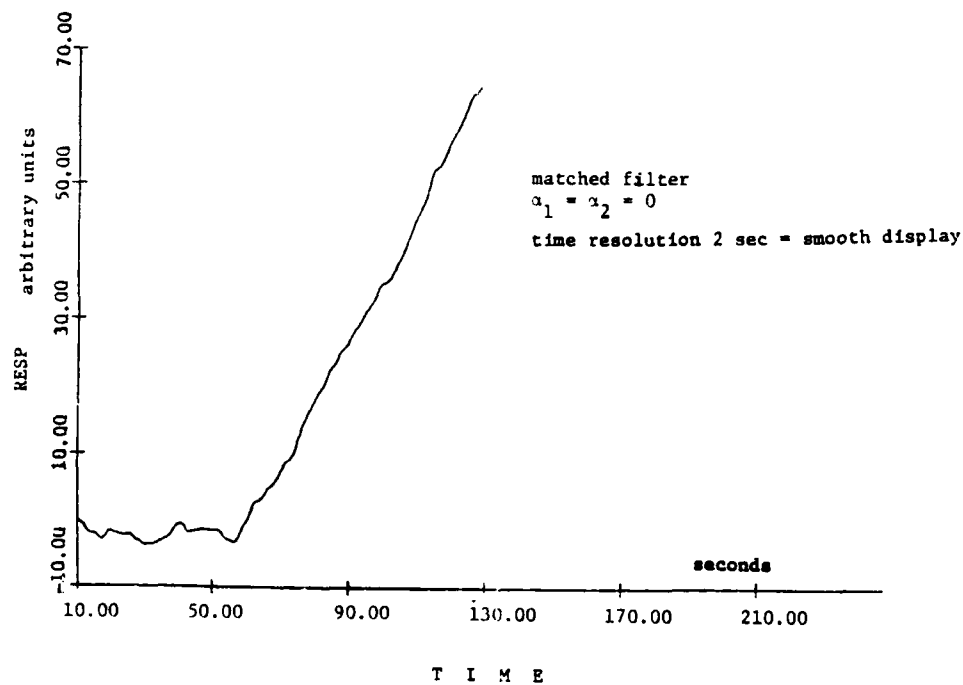


Figure 4.3. Integral response from the matched filter approach. Observe the clear onset of a VER at $T = 60$ sec. The integral response appears to become smoother once the stimulus is present. This change of the quality of the response may be of use for assessing visual processing.

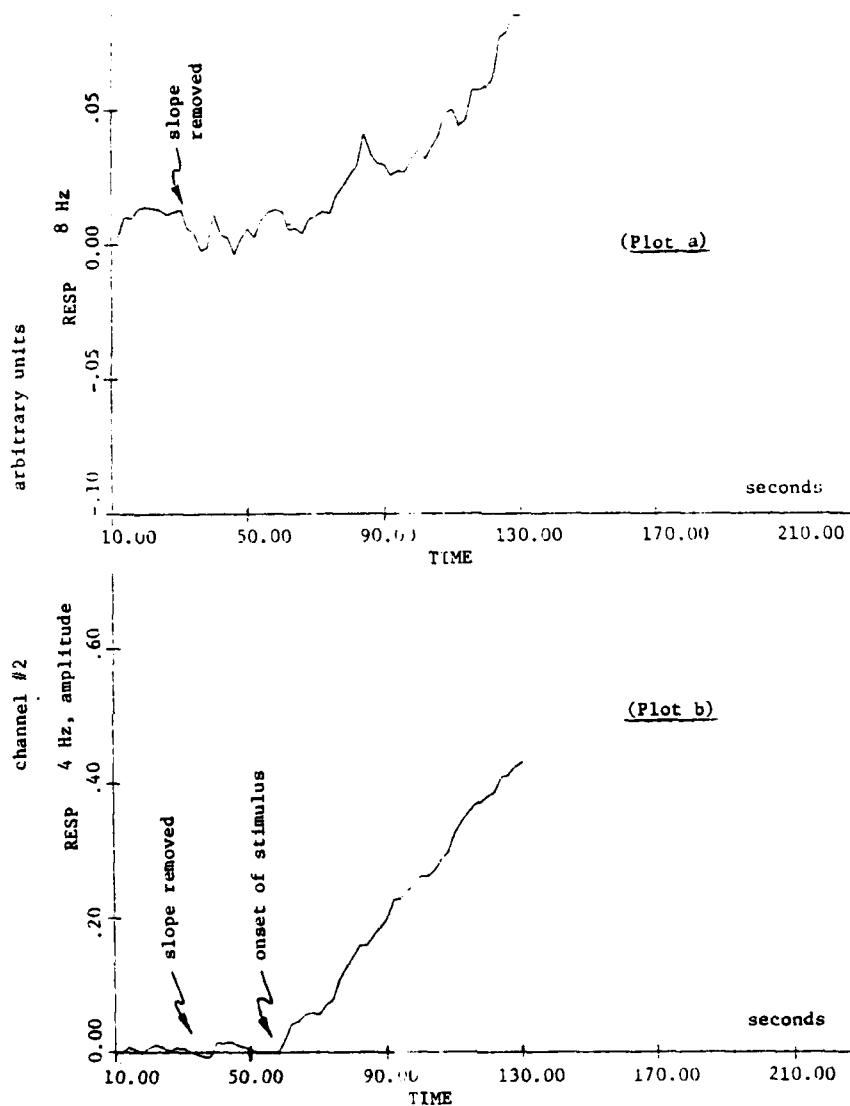


Figure 4.4: Plots a and b. Modification of the plots in Figure 4.2. Here, the average slope of the integral response during a nonstimulus period has been removed. Although this step enhances the onset of the VER, the variability of the response estimate remains high. Also, no change is apparent in the character of the response curve (e.g., reduced variability).

4.3 MODELING APPROACH FOR DATA PROCESSING

The philosophy of our data processing consists, in general, of three parts:

- (a) removal of artifacts (modeling of artifacts);
- (b) transformation of data (modeling of EEG); and
- (c) extraction of signal (modeling of VER).

4.3.1 Removal of 60 Hz and Harmonics

Power-line noise (60 Hz) and its harmonics impose some interferences in EEG/VER recording. For better analyses of the VER to be performed, these artifacts have to be removed from the raw data. A robust adaptive filter has been developed to achieve this purpose. The mechanics of the filter are quite straightforward. First, a trigonometric identity is employed:

$$\sin(\theta+\delta) = 2\sin\theta\cos\delta - \sin(\theta-\delta) \quad (4.2)$$

It represents the phase change between digital samples for a sinusoidal signal. Equation 4.2 can be used to calculate the sinusoidal amplitude at the next sample time (phase equal $\theta + \delta$) in terms of the amplitude at the previous two samples (phases of θ and $\theta - \delta$). Multiplication of (4.2) by the amplitude magnitude results in:

$$a_{i+1} = 2a_i\cos\delta - a_{i-1} \quad (4.3)$$

where a_i represents the time series of alternating current (a.c.) interference amplitudes. If we denote the digitized source signal sequence by x_i , then the difference, $x_i - a_i$, should be a null apart from a possible constant offset (in our case, this offset is EEG/VER background at sample i). The previous difference, $x_{i-1} - a_{i-1}$, is the best available estimate of this offset. In equation 4.4:

$$f = (x_i - a_i) - (x_{i-1} - a_{i-1}) \quad (4.4)$$

The quantity f will be null if the interference amplitude is properly estimated by a_i . Thus, f should be used as a positive feedback element. Based on equation 4.3, the logic followed is:

if $f > \Delta$, increase a_i by a small fixed amount,

if $f < -\Delta$, decrease a_i by a small fixed amount,

where Δ is a small positive number.

This logic is implemented in EEG/VER analysis, with the results shown in Fig. 4.5. The result is quite robust in the sense that, if a_1 is overestimated or underestimated, f will tend to be negative or positive, thus causing a_1 to be decremented or incremented in a cautious fashion. The feedback loop is stable. In addition, the adaption of the filter to changing condition is reasonably rapid.

4.3.2 Effect of Removal of ECG

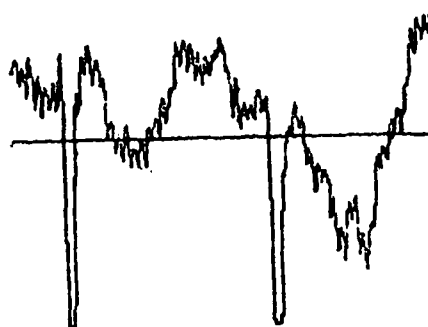
In our data (FILE 2), the ECG is a prominent feature on all five channels. The spectrum of the nonperiodic ECG extends from about 2 Hz well into the 80-Hz region. From some spectral analysis, we concluded that energy in the 20- to 40-Hz region should provide good information (high signal-to-noise) for the generation of ECG fiducial points. Thus, we decided to look at bursts of energy around 30 Hz. We use the scheme shown in Fig. 4.6 for the detection of R-waves. In order to avoid confusion with P-waves, we check over a 200-ms window for the presence of other bursts of energy; if none occur, the detected local maximum is associated with a data window from which the average ECG is computed (Fig. 4.7).

A second pass through the data subtracts the average ECG whenever its presence is detected. In Fig. 4.8, one can see the effect of this process: after an initial startup period, the ECG and the 60 Hz, plus its harmonics, are removed from the data.

The power at the fundamental frequency and low-order harmonics is comparable or even larger than the signal of interest--the VER (Fig. 4.9). Observe that a slight change in heart rate could result in a strong interference of the ECG with the VER. For this reason, the ECG had to be removed. A typical result of such removal is shown in Fig. 4.10. Note the drastic change of the amplitude of the fundamental frequency (2 Hz) and the first harmonic (4 Hz), next to the fundamental reversal rate of the VER. Thus, our scheme appears to provide a good safeguard against any interference of the ECG with the VER.

4.3.3 Method of Construction of an ECG Template

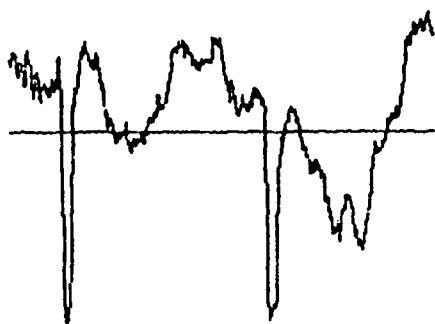
The construction of the template for the ECG requires some pre-processing of data, and is based on an iterative refinement of estimation. Thus, we pass the raw data first through a high-pass filter to extract the high-frequency component of the ECG. Any clipping of the data due to the analog-to-digital (A/D) converter is currently detected in the high-pass filtered version of the data; and the data corresponding to clipping are excluded from further processing. Following this signal conditioning, preliminary fiducial points for the ECG are computed by use of the accumulated velocity, v .



(Raw data)



(Estimated 60-Hz component)



(Data after removal of 60-Hz noise)

Channel 4

Channel 5

Figure 4.5. (From top to bottom) The raw data, the estimated 60-Hz component, and the data after removal of the 60-Hz noise.

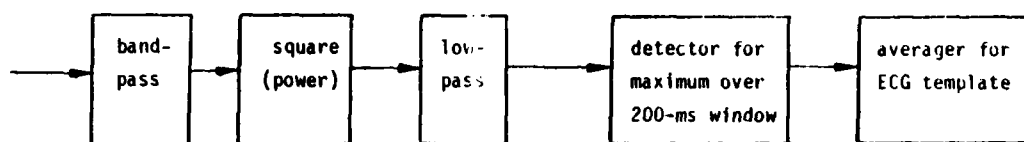


Figure 4.6. Scheme for the determination of the ECG template. This scheme does not depend on the shape of the ECG, since power in the neighborhood of 30 Hz is observed. The 200-ms window serves the rejection of local maxima induced by P-waves; thus, trigger points are associated with R-waves.

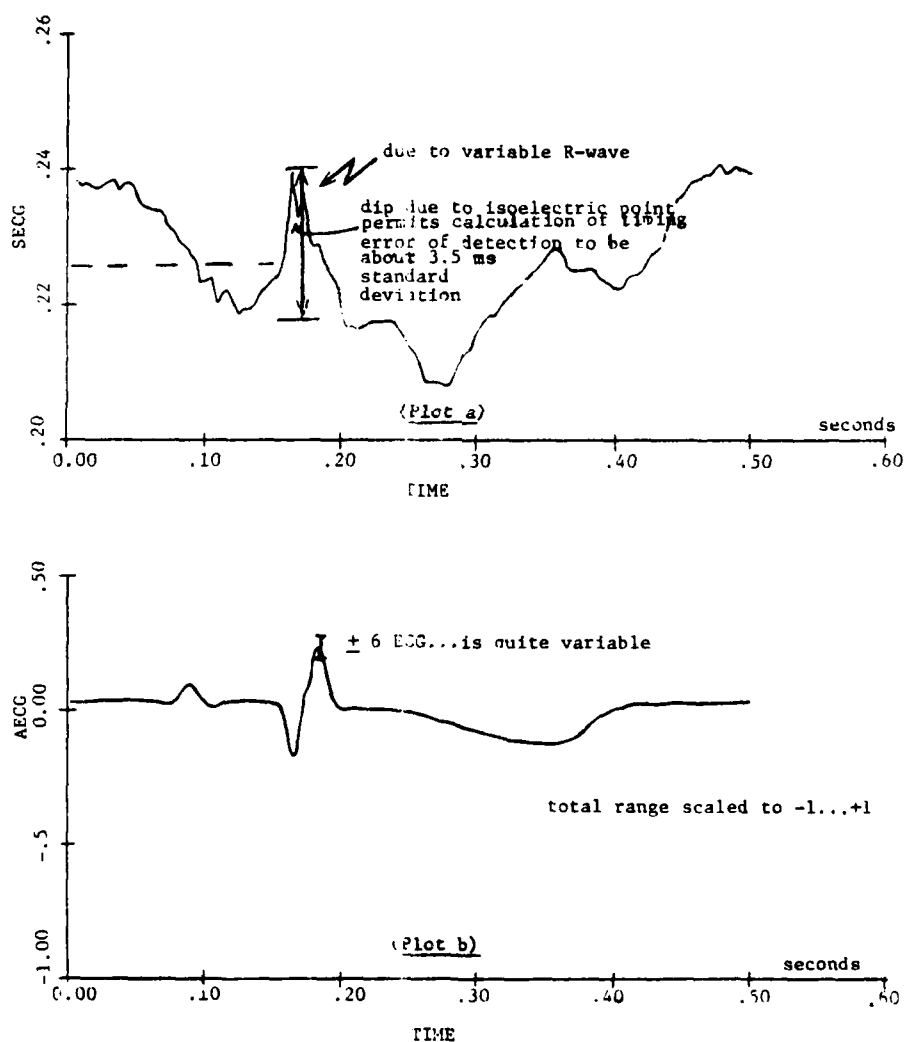


Figure 4.7: Plots a and b. Example of the average ECG in channel #1 (= template) and standard deviation of ECG (without removal of baseline). From the shape of these two plots, one can estimate a timing uncertainty for the detection of the R-wave in the order of 3-ms standard deviation.

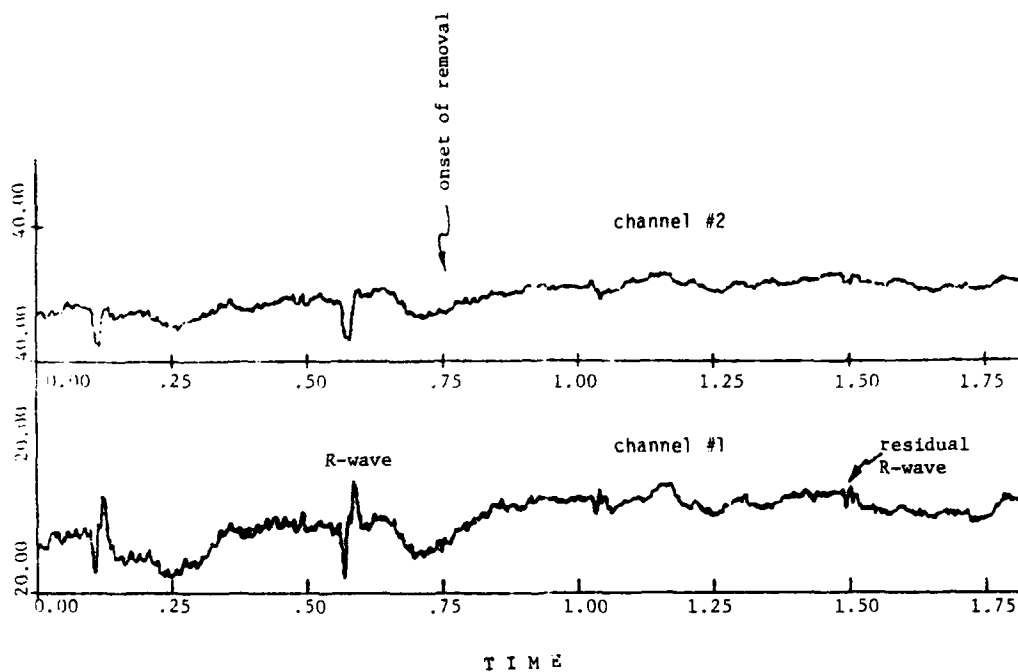


Figure 4.8. The effect of the removal of the 60-Hz noise and the ECG. The graphs show the processed data before and after the activation of the 60 Hz and ECG removal.

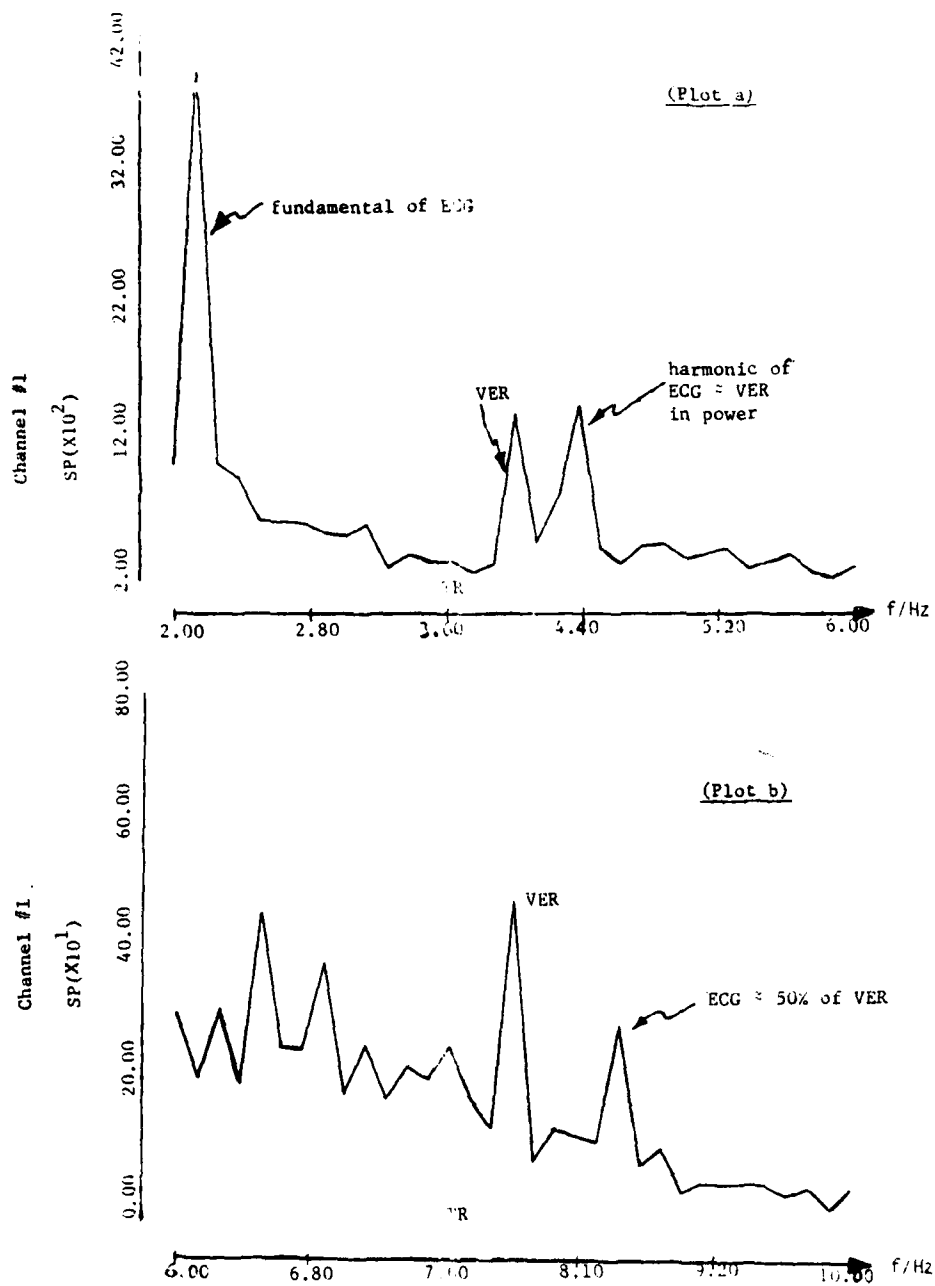


Figure 4.9: Plots a and b. Comparison of spectral components of the VER and the ECG. (Observe the dominance of ECG spectral components.)

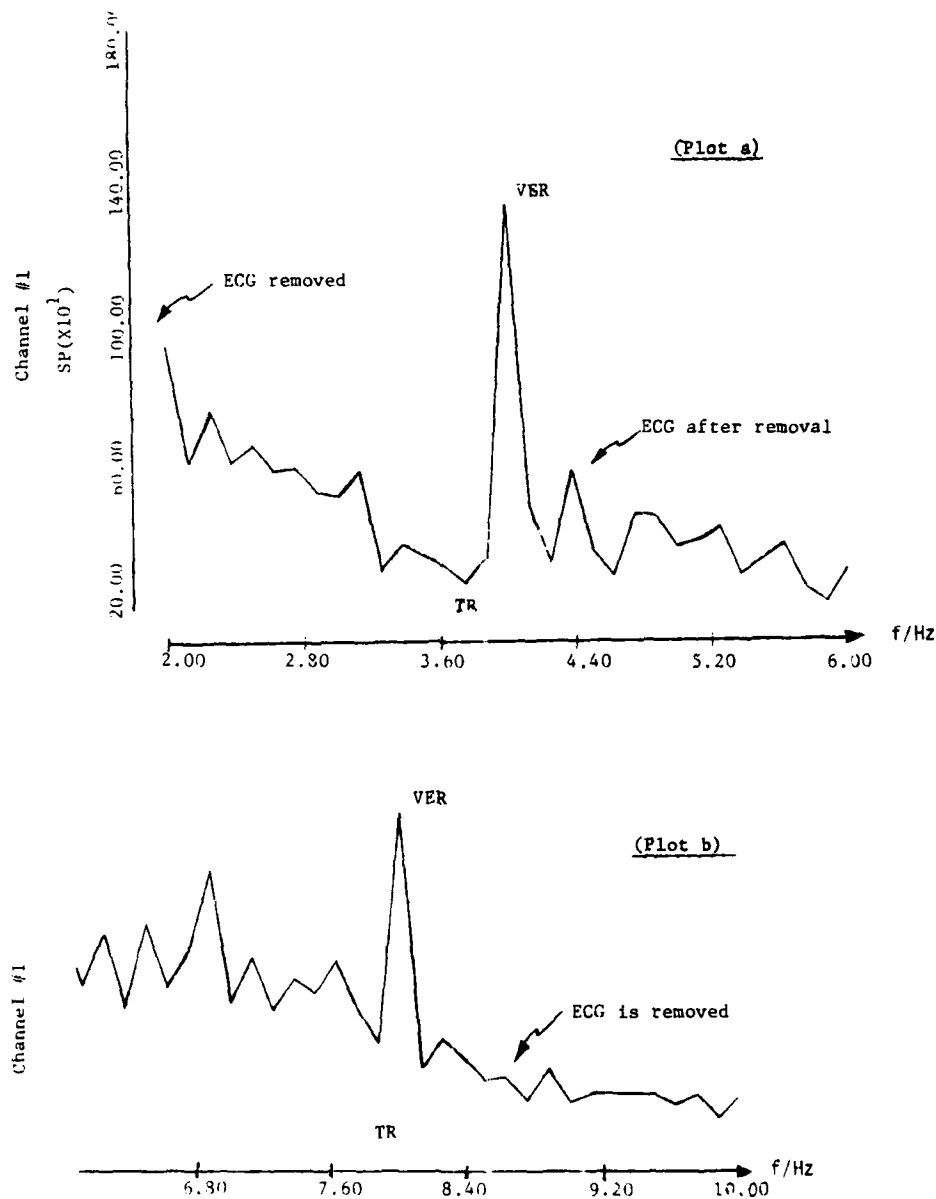


Figure 4.10: Plots a and b. Comparison of spectral components of VER and ECG after removal of the average ECG. (Note the suppression of the ECG fundamental and first harmonics components.)

Thus, we use the five velocities of the ECG in the channels by computing:

$$v = \sum_{i=1}^5 w_i \cdot v_i \quad (4.5)$$

For these data the relevant weights, w , are chosen by hand, on the basis of subjective confidence in the clarity of the ECG-wavelets.

Next, a preliminary template is computed for each channel by use of these preliminary fiducial points. The templates are moved over the data and adjusted with respect to their shape and fiducial point, as shown in Fig. 4.11.

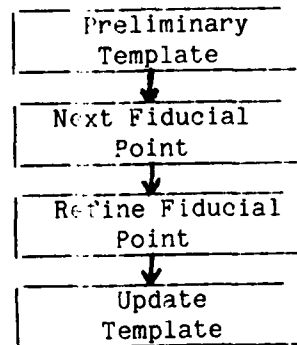


Figure 4.11. Estimation of fiducial point and template.

4.3.4 Clipping of Data

All programs disregard data points associated with clipping and (mainly at the QRS-complex) adjust the weight of estimates accordingly. For our data, the estimates derived in this way (by regarding clipped data as missing) are biased estimates; but the bias tends to be small compared to the sample variability and does not, at this time, justify any correction.

4.3.5 Modeling the EEG and Segmenting

Visual examination of data which are free of 60 Hz and the ECG indicates that a second autoregressive model might allow a good description of segments of the EEG. From our preliminary studies, we found that a

nonstationary first-order model, of the type:

$$y_t = y_{t-1} + \epsilon_t \quad (4.6)$$

$$E[\epsilon_t] = 0$$

$$\text{var}[\epsilon_t] = \sigma^2 \text{ for segment \# } k$$

provides a statistically good approximation (that is, on 95% confidence level, e.g., only 5% of all models are not well described) for a few seconds worth of data. The distribution of the autoregressive coefficients α_1 and α_2 is given in Fig. 4.12. A clustering around $\alpha_1 = 1$, $\alpha_2 = 0$ (equivalent to eq. 4.6), is apparent.

We note that these coefficients were estimated by regarding as missing data the clipped data and data near R-waves of the ECG. We note also that the data displayed correspond to a sampling rate of 256 samples/sec. The variance of the EEG appears to form two groups: one with very large variance, and one with little variance (Fig. 4.12). The estimate of the variance within each segment of the EEG is anticipated to permit, later, the proper weighing of the estimated VER in order to minimize variability of response estimates.

4.3.6 Generating a VER Template

The generation of a template for the VER is based, at this time, on averaging in synchrony with the reference channel. When clipping occurs, corresponding data sections are again treated as missing data (Fig. 4.13).

4.3.7 Smoothing the VER Template

From simple models of the VER, we know that only integer multiple frequencies of the reversal rate (RR) can be contained in the VER. For this reason, we select from the averaged VER only those characteristic frequencies to generate a smoothed VER template. As a processing option, the number of harmonics can be selected. So far, we select an RR of 4 Hz and harmonics up to 16 Hz. Thus, in this case, the VER is represented by 8 parameters--2 for each characteristic frequency (real and imaginary parts). The result of this smoothing is shown in Fig. 4.14. This smoothed template is used as the reference for the matched filter.

4.4 THE MATCHED FILTER APPROACH FOR MACACA MULATTA

A well-known fact is that the matched filter is optimal in the least squares sense for estimating the (unknown) amplitude of a waveform with known shape embedded in white noise. Shown in Fig. 4.15 is the data processing, using this matched filter, substituting the estimated and smoothed VER for the "known" waveform.

CHANNEL 2

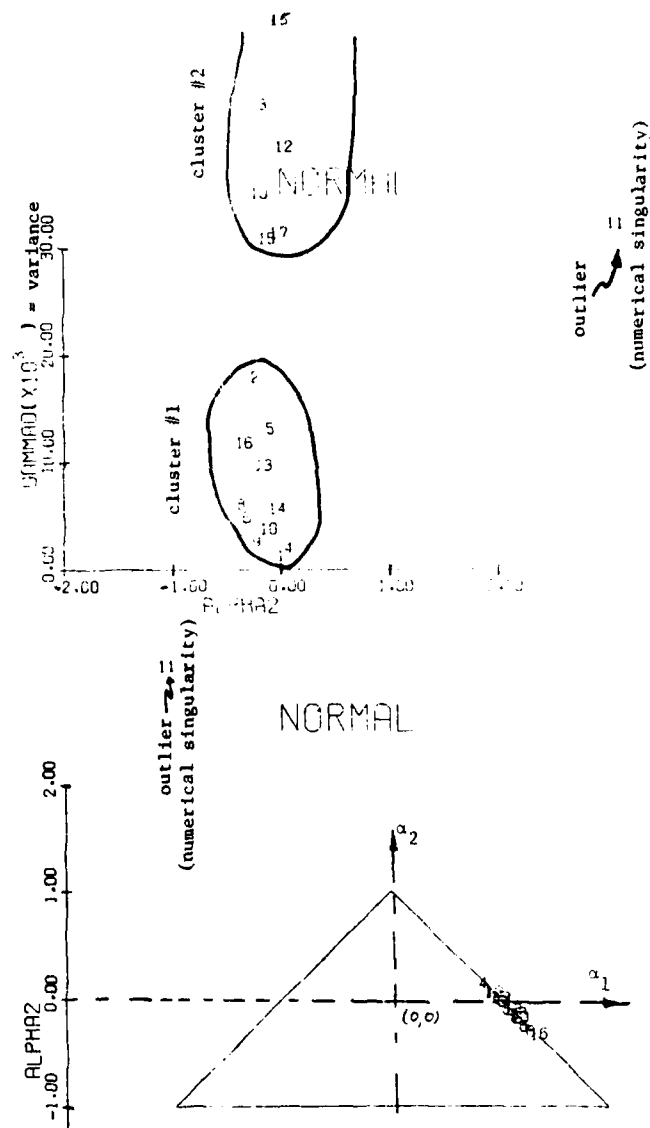


Figure 4.12. A preliminary study of autoregressive AR (2) models of the EEG, without stimulus. The autoregressive coefficients cluster for different segments at $\alpha_1 = 1$, $\alpha_2 = 0$. The variance of these processes may, however, form two groups.

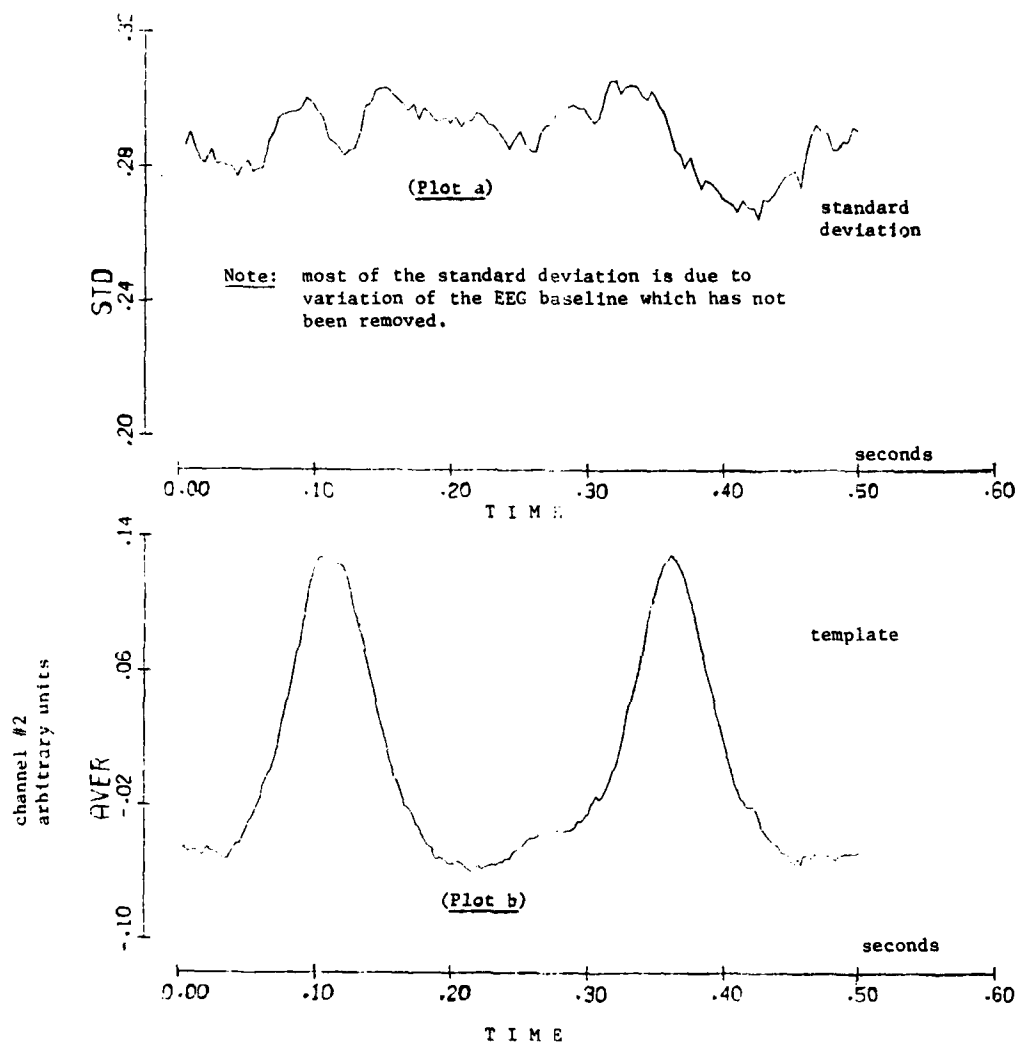


Figure 4.13: Plots a and b. A template of the VER obtained by synchronous averaging using preprocessed data (free of ECG and 60 Hz). Clipping of data has been taken into account.

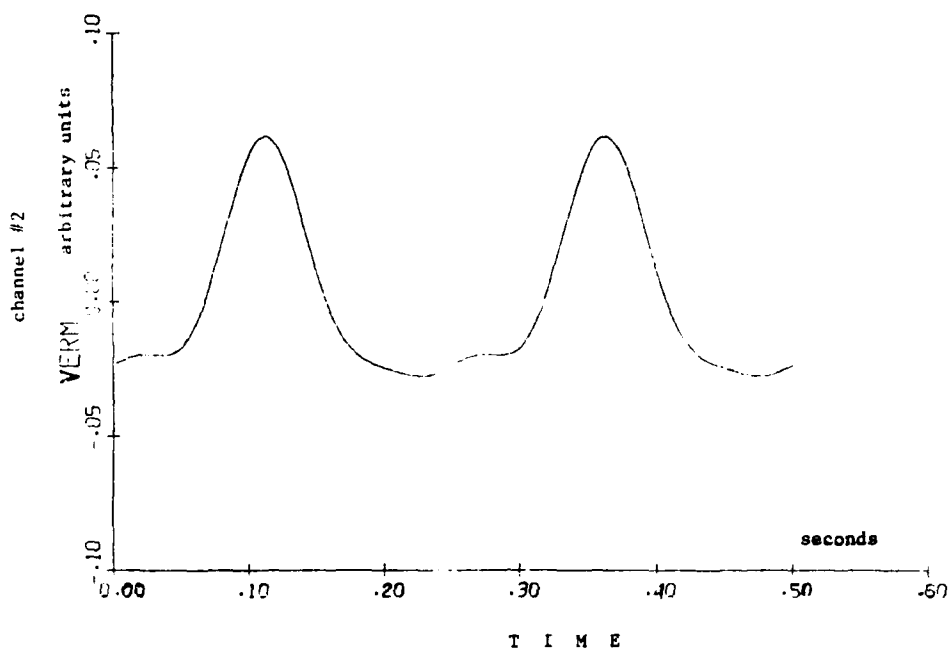


Figure 4.14. The smoothed VER template, after removal of higher harmonics and of all frequencies other than a multiple of the reversal rate.

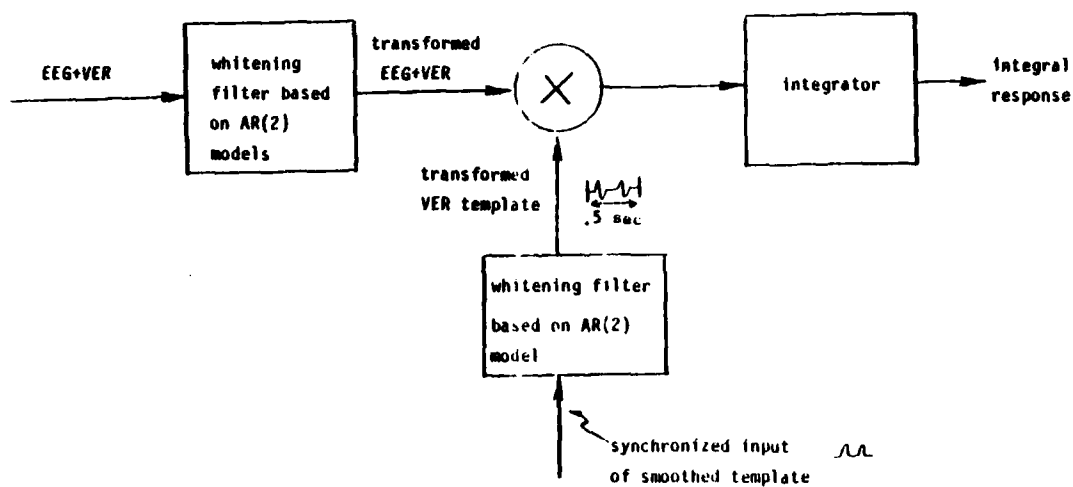


Figure 4.15. The matched filter approach applied to the VER signal for estimation of its (integrated) amplitude.

To generate the necessary white background noise, we transform our data to the innovation sequence generated from estimated autoregressive models. From preliminary studies of segmenting we simply choose: $\alpha_1 = .99$, $\alpha_2 = 0$; or, for comparison, $\alpha_1 = \alpha_2 = 0$. From visual examination of results we cannot, at the present time, see a significant change of the estimated strength of the VER (aside from differences in some fine detail associated chiefly with the finer resolution display of .5 sec). Compare the result of the integral response of Fig. 4.3 with that of Fig. 4.16. Note, however, that the two templates which were matched against the (transformed) data look quite different in these two cases (Fig. 4.17).

Two observations, regarding outputs of the integral response of the matched filter, deserve attention:

First, one can observe a reduced variability of the output when the subject was stimulated. This observation suggests combining the variance and the amplitude estimate for assessing stimulus condition. Some more spectral estimates, for comparing the EEG background (one of the components introducing variability into estimates) with and without stimulus, will be useful in clarifying our observations further.

A second observation (Fig. 4.18) deserves further study--the recovery of the VER, some 10 sec after the flash at $T = 180$ sec, appears to be rather abrupt. Not much of a "slow" recovery is detectable. This behavior is reminiscent of the recovery of an amplifier with feedback gain control after overdriving it with an impulse.

4.5 CONCLUSIONS ABOUT DATA FROM MACACA MULATTA

Removal of the EEG background from the signal channel by use of neighboring channels (as suggested in our original proposal) turned out not to be useful, because the VER is contained in all channels. Hence, by use of the originally proposed regression model, one would not only eliminate EEG background but also--to an unpredictable degree--the VER. Thus, we proceeded with a separate processing of individual channels. Furthermore, we have reason to believe that fewer electrodes collect most of the relevant information; e.g., using only the outputs from a pair of channels from the left and right hemispheres may be sufficient. The combination will depend on the correlation structure of the outputs of our matched filters (one for each hemisphere).

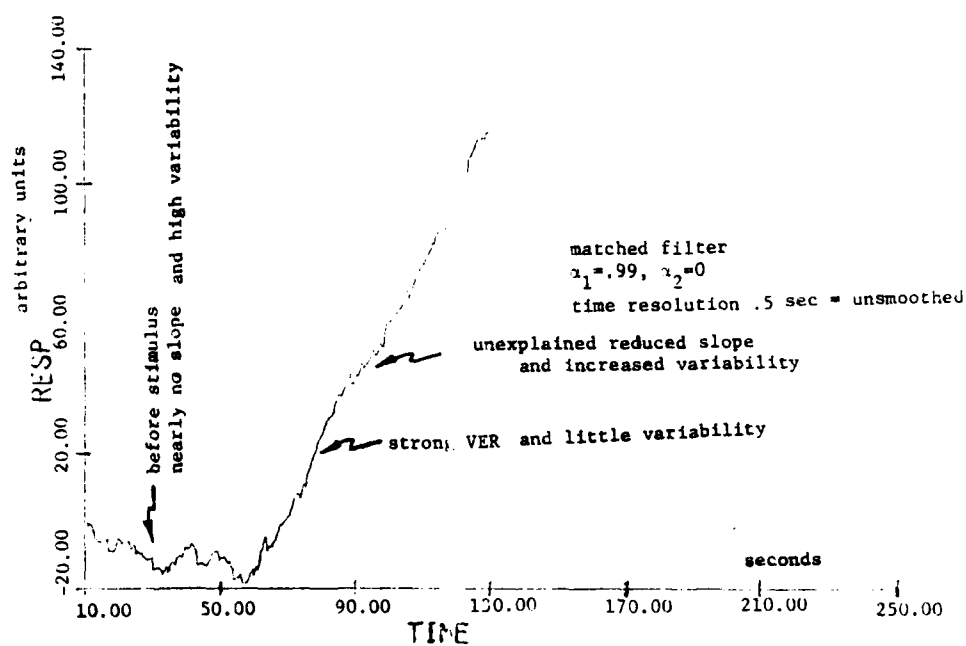


Figure 4.16. Result of matched filter with $\alpha_1 = .99, \alpha_2 = 0$. The integral response is plotted with .5 sec resolution.

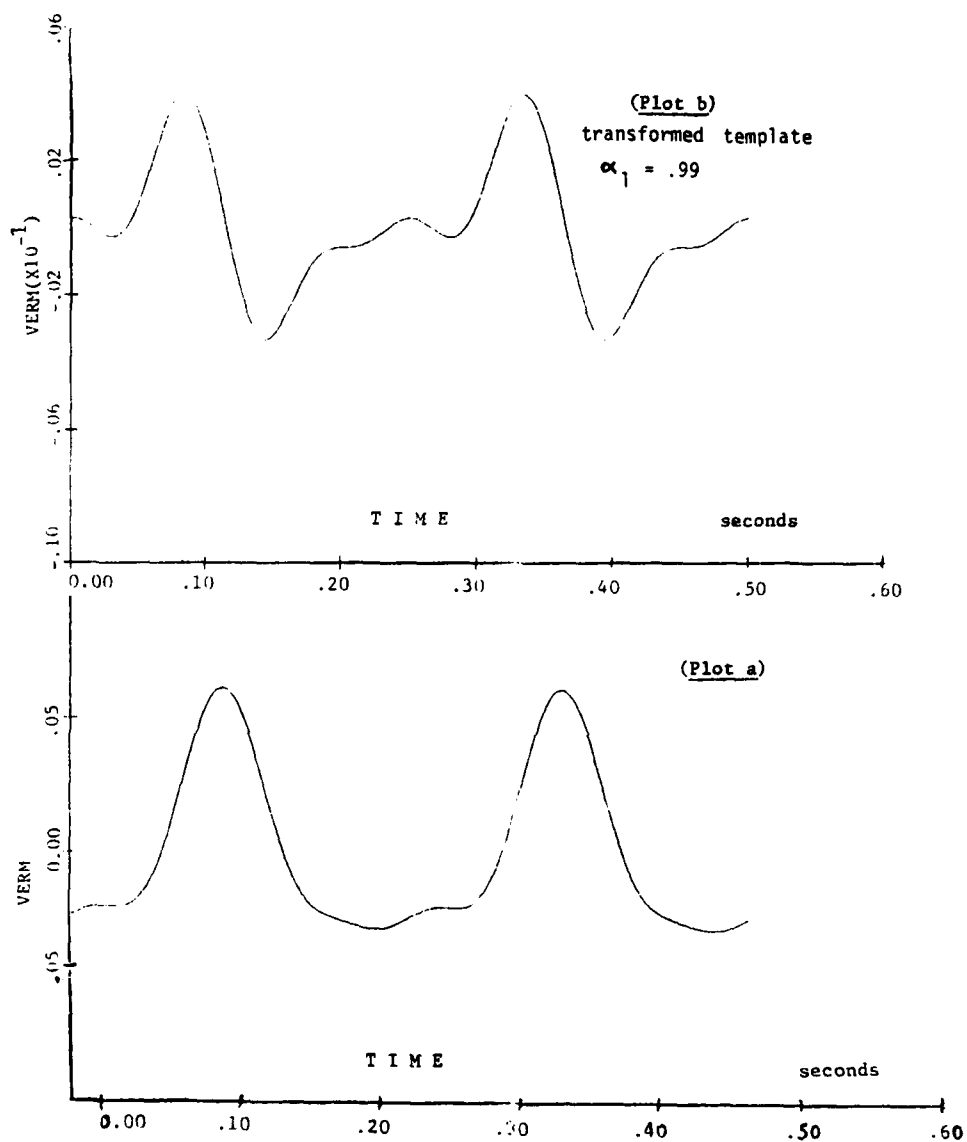


Figure 4.17: Plots a and b. Comparison of transformed template with original template.

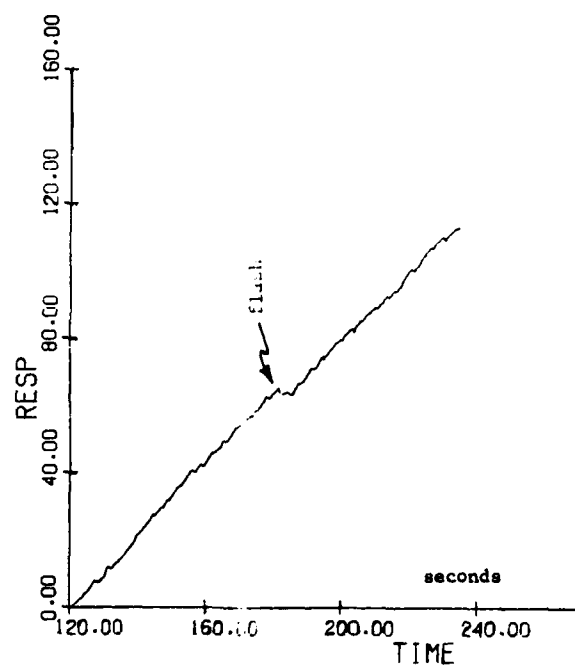


Figure 4.18. Output of matched filter while a stimulus was applied. A flash ($T = 180$ sec) blinded the subject transiently, thus suppressing the VER.

5. ANALYSIS OF RAW DATA FROM MACACA MULATTA

Some Basic Properties

Before we began designing our data processing scheme, we analyzed our data by spectral analysis, by auto- and cross-correlation, and by spectral methods. Even though our eventual data processing scheme is rather a time domain estimation technique, we found the spectral analysis to be more revealing for assessing gross properties of the data, mainly because:

- a. The VER is a periodic signal.
- b. The noise introduced by the EEG is a near-periodic process.
- c. The 60-Hz noise and its harmonics provide relatively pure spectral lines.

Our observations concerning these processes are presented in the following material.

5.1 COVARIANCE STRUCTURE

At least three components of the signal are of interest, and these are shown in Figures 5.1 - 5.3:

- a. a slow component with a period of some 3 sec;
- b. a strong serial dependency of the ECGs; and
- c. a strong 60-Hz signal (and, presumably, harmonics).

The slow component could be associated with the .3-Hz filter cutoff frequency prior to A/D conversion, or could be physiological (e.g., related to respiration).

Next, the ECG serial dependency is interesting, as it suggests the possibility of a better way to remove the ECG by modeling its serial dependency with a simple model, perhaps by a low-order autoregressive model.^a

Finally, observe the strong 60-Hz signal (and its harmonics). Such strong signals have to be removed.

5.2 PROPERTIES OF THE VER AND THE ECG

As a first step, we tried to assess the properties of the VER. For this purpose, we examined the coherence between stimulus, x , and the recorded brain potential, y (Fig. 5.4). That is, we estimated:

^a Note: An example of the underlying ECG (in terms of an estimated template) is shown in Figure 5.6.

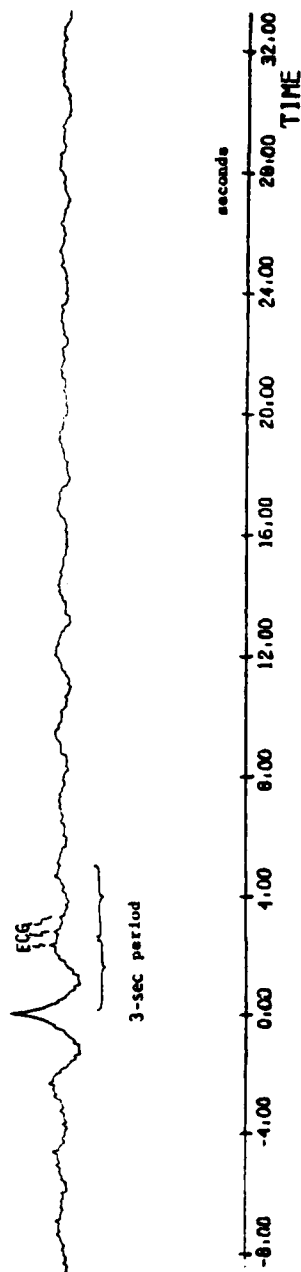


Figure 5.1. Slow components of EEG with 3-sec period; autocorrelation.

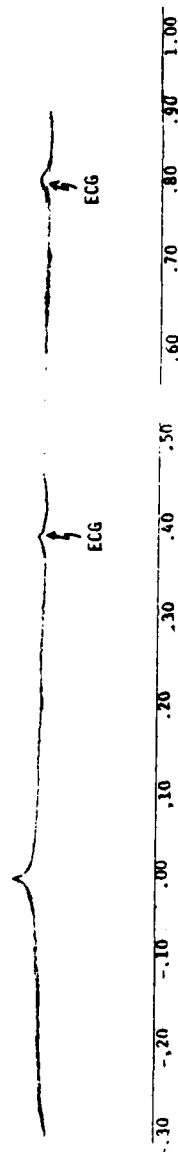


Figure 5.2. Strong serial dependency of EEG; same as Fig.5.1, but expanded time scale.
(Note: Heart rate is near 120 bpm; autocorrelation.)

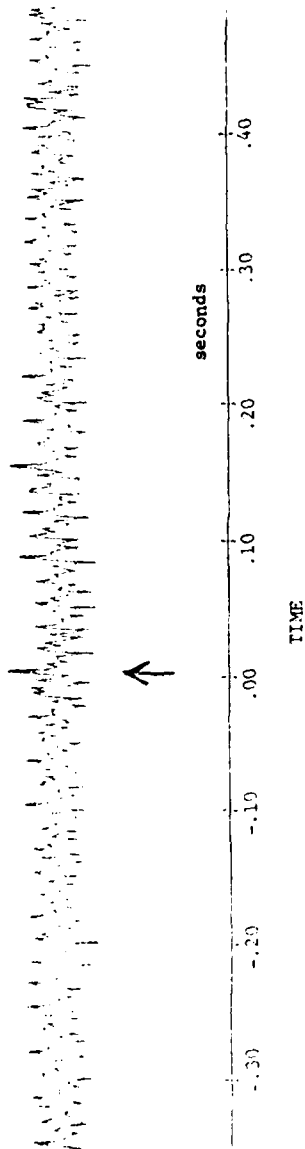


Figure 5.3. Cross-correlation between two channels shows strong 60-Hz noise (plus, pre-sumably, harmonics) which extends undiminished over some 30 sec.

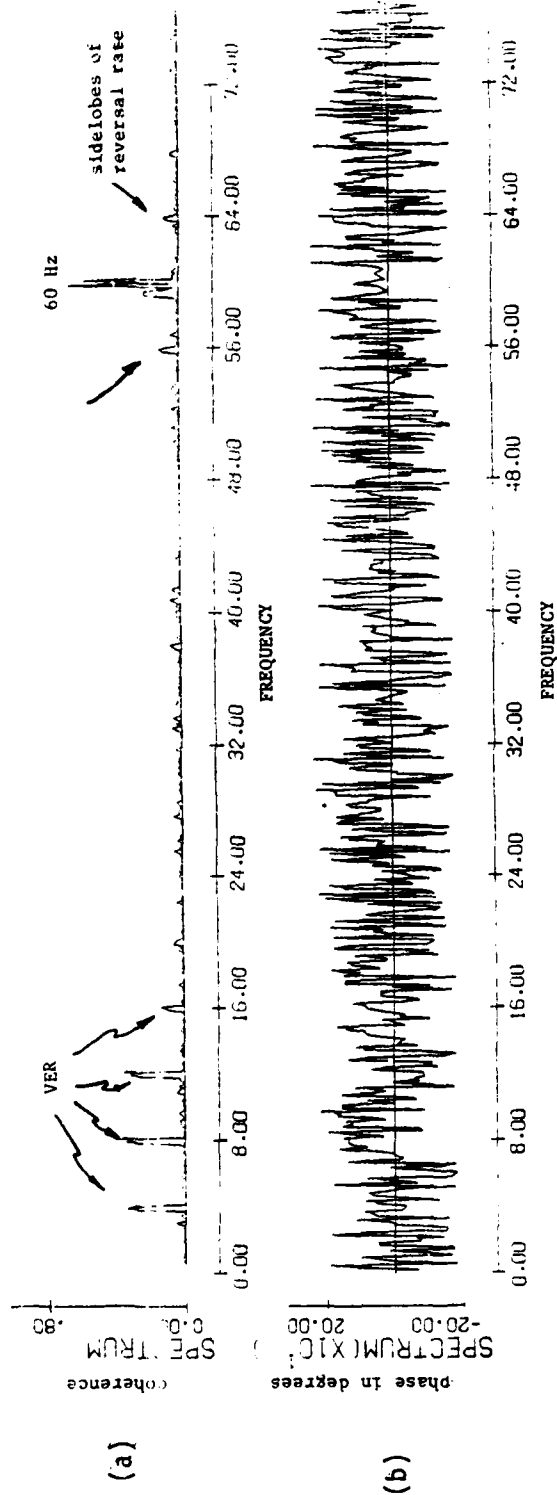


Figure 5.4: a and b. The coherence between the stimulus and the VER+EEG. The component at the 4-Hz reversal rate and harmonics up to 16 Hz are prominent. This observation suggests that the smoothing of the VER template should be limited to these significant components.

$$C(f) = \frac{S_{xy}(f)}{\sqrt{S_x(f)S_y(f)}}$$

where

$$0 \leq |C(f)| \leq 1.$$

Up to the third harmonic (as can be seen), our data show significant coherence (channel 2 of File 2). Thus, when smoothing the VER, we allow up to this harmonic in our template.

Next, we examined the coherence of the EEG between the electrodes. Our result can be summarized easily: Within each hemisphere, high coherence is observed up to high frequencies; e.g., 40 Hz, $C(f) > .5$. In contrast, the coherence between the left and right hemispheres is limited to low frequencies; e.g., above 8 Hz $C(f) < .2$ (Fig. 5.5).

These observations suggest that most information about the VER is carried in any pair of electrodes of opposite hemispheres. Adding any other channel will not provide much new information. Thus, as far as data acquisition and analysis are concerned, one may concentrate on only a pair of channels from opposite hemispheres -- without losing much information because of disregarding other channels.

5.3 THE SPECTRAL PROPERTIES OF THE ECG

The electrocardiogram consists of several wavelets, principally the P-wave, the QRS-complex, and the T-wave. All of these components are easily discernible, especially from the average of waveforms (Fig. 5.6). Most of the energy is contained in the R-wave. This short impulse-shaped wave generates harmonics of the heart rate well above 60 Hz.

Because of this wide spectrum (Fig. 5.5), some freedom exists in selecting a frequency window for the detection of the ECG, which is free of harmonics of the VER and of 60-Hz noise. From a rough analysis of the average ECG and its standard deviation (Fig. 5.6), we estimate the uncertainty in the time of detection of the ECG to be about 3 ms, which is slightly more than the sampling rate.

5.4 THE 60-Hz NOISE

Our data had been sampled at 512 samples/sec. This sampling rate allowed us to detect a 60-Hz component with its harmonics up to 300 Hz (which appears aliased at 212 Hz). Thus, we wish to emphasize that, in future digitization, the high-frequency cutoff of the filters has to be set to much lower frequencies and to a steeper rolloff.

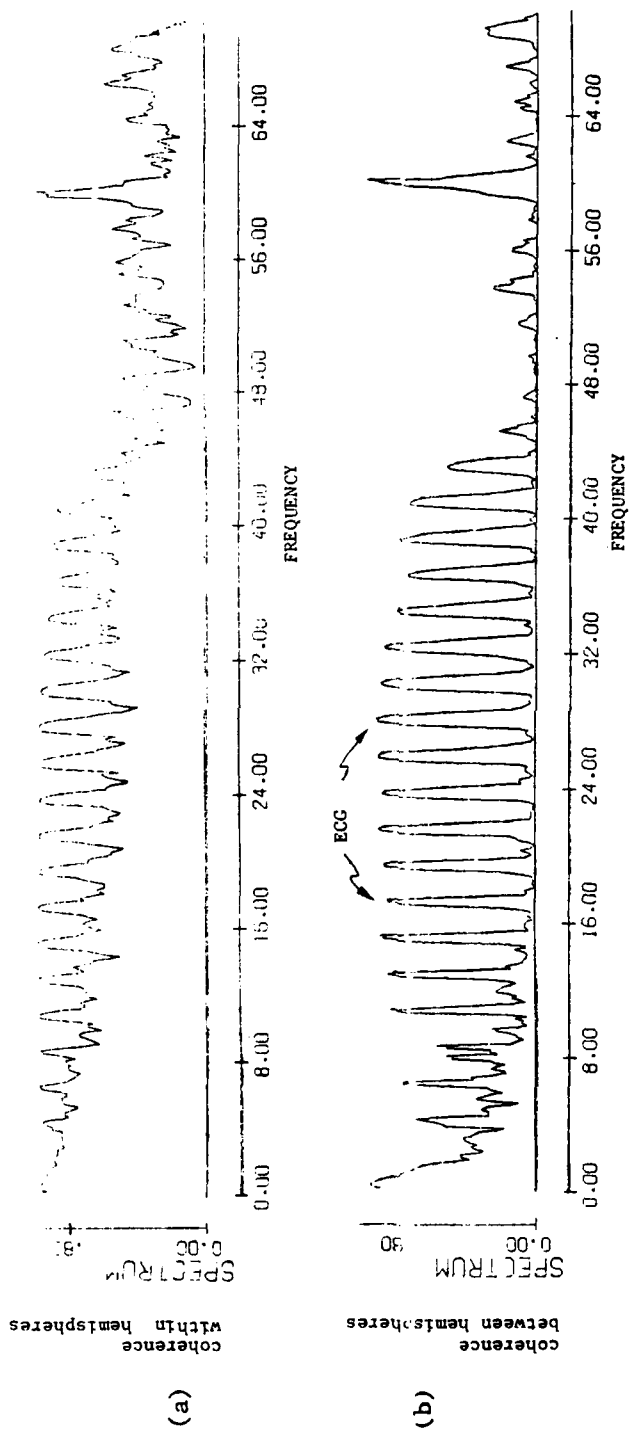


Figure 5.5: a and b. The coherence within and between the two hemispheres. Observe the coherence up to very high frequencies (e.g., 40 Hz) within a hemisphere. (Note: The periodic spectral components are due to the ECG.)

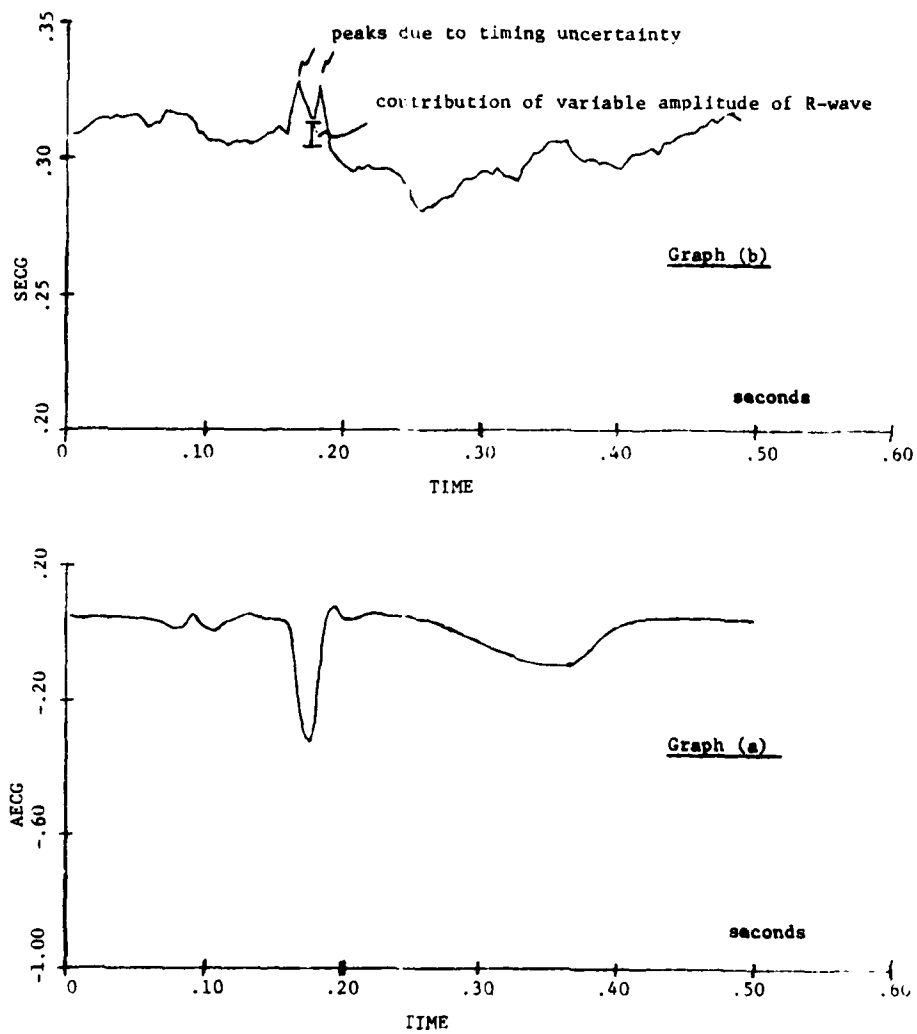


Figure 5.6: Graphs a and b. Average ECG (AECG) and standard deviation of the ECG (SECG) in channel 2.

Another observation was of interest: the 60-Hz noise has sidebands at 60 ± 4 Hz, coherent with the VER. These sidebands could be due to the nonlinearities of the recording equipment, or to some variation of the impedance of the visual cortex in synchrony to the VER. At the time, however, we could not pursue this lead any further. One way to discriminate between the two possibilities is to determine if the strong ECG also modulates the 60-Hz noise. If so, the recording equipment must be held responsible for these modulations.

If the ECG does not modulate the 60-Hz noise, then the recording equipment behaves linearly and cannot be responsible for modulation of the 60-Hz noise; possibly, impedance variations of the visual cortex are detectable.

5.5 CONCLUSION

The potential for a number of techniques to improve the signal-to-noise (S/N) ratio of the VER, versus other electrical activities, became apparent from these studies. Three aspects of these data made the analysis more difficult, however, than was anticipated in the original proposal:

- a. The VER was contained in all channels, not only in those placed above the foveal projections in area 17.
- b. Clippings, mainly associated with the occurrence of the QRS-complex of the ECG, occurred frequently in some of the channels and complicated removal of the ECG.
- c. A powerful 60-Hz component and its harmonics were encountered in all channels, and required appropriate prefiltering.

Despite these complications, significant enhancement of the extraction of the VER was possible. The analysis of these USAFSAM data provided, therefore, a good basis on which to begin analyzing the human subject data. Because the human subject data were yet to be recorded, the results of the foregoing analysis and the increased understanding of the nature of the problem could be used for improving the recording technique. In fact, the modified approach resulted in data of much better quality. In the following report sections, we address these human data, and demonstrate the significant improvements that are possible.

6. HUMAN SUBJECTS

In this phase of the research, we used human-scalp electrode tracings. For the recording of these data (by the present principal investigators at the USAFSAM) some important results from the previous epidural recordings on Macaca mulatta could be used in a beneficial manner.

The approach used for human subject data analysis follows, in general, the outline of our proposal. In summary, a rather drastic reduction of variability in response estimates has been attained, especially in the subject with high variability. Impressive results have been achieved despite the fact that the data exhibited a behavior somewhat different not only from the data available to us during the development of the proposal, but also from the data recorded on the Macaca mulatta.

The present report compares the current results of Scientific Systems, Inc., with the earlier USAFSAM results. The effectiveness of the individual layers in our approach is demonstrated. Then we turn to the details of the current processing method.

Finally, we discuss some of the interesting properties of the data. These properties -- which have been unraveled, in part, by separate statistical analysis of the data -- show that the concept of variability has to be viewed in a new light. For example, variability in itself is a predictor of stimulus condition and has a possible relation to hemispheric differences between the sexes (1, 2, and 3). We now begin our comparison of recording techniques.

6.1 RECORDING TECHNIQUES

The first step in recording is the placement of electrodes and the specification of the potential differentials which are to be measured. In the past, USAFSAM used the arrangement shown in Figure 6.1. The first set of data we had analyzed, recorded epidurally from Macaca mulatta, was based on that arrangement. Our analysis of that data revealed (in contrast to earlier information given to us) the presence of a VER on all electrodes. Furthermore, we found the responses to be nearly identical in the corresponding channels, much like a common mode. This situation results in a number of limitations when analyzing and interpreting VERs.

To combat such limitations, we set out to record in an arrangement from which we could anticipate good common mode rejection and thus facilitate analysis of data. The new arrangement (Fig. 6.2)--which assigns spatial differentials, relative to the center electrode, to individual channels (rather than relative to the ear)--proved also to be beneficial in regard to avoiding drift phenomena that lead to saturation of the preamplifier and FM-tape. An example of data recorded with this arrangement is shown in Figure 6.3.

A second refinement of our recording technique (also suggested by the analysis of earlier USAFSAM data) was the high-pass prefiltering of the data in the preamplifiers. These prefiltered data formed a second set of data (linearly dependent on the unfiltered data). Quite obvious during the recording was the fact that this technique avoided any risk of saturating the recording media due to electrode drift. Later, during analysis of these data, we confirmed an additional simplification with regard to the processing of these data (Figs. 6.4 and 6.5).

The new human subject data were recorded on FM-tape, along with the 15-Hz reversal-rate reference signal and an additional information channel for the EMG associated with eye blinking. The stimuli consisted of 10 repetitions of the following experiment: The subject was seated in a dark, electromagnetically shielded room in front of a computer-controlled TV display. At first, 60 sec of blank screen was displayed, followed by 80 sec of a checkerboard pattern at 30-percent contrast and 15-Hz reversal rate. The visual field was about 4 degrees, squared, with about 4 checks/degree. With these data we can demonstrate a drastic reduction of "variability" as compared with the earlier USAFSAM analysis.

6.2 COMPARISON OF VARIABILITY OF VER ESTIMATES

Our original idea of reducing variability in response estimates is based on extracting the information from the relevant information channel, more efficiently than by the original FFT method used by USAFSAM. Furthermore, "neighboring" channels should be used for reducing the effect of the EEG background activity. As mentioned before, however, all channels tend to contain VERs. Hence, information contained in these channels is also a mixture of VERs and EEG background activity.

To deal with this situation, we have modified our approach slightly. We treat all the individual channels with our matched filter before combining their outputs by a regression technique. [Note: Our original idea was, first, to use regression to remove background EEG activity from the information channel (carrying the VER); and second, to apply a matched filter.]

On the basis of our current understanding of the VER, it can easily be shown to be the current approach suboptimal--typical for such hierarchical schemes. (For a summary of our data processing, refer to Figure 6.6.)

Despite the suboptimal quality of the current scheme, we did achieve drastic improvements. To demonstrate the effect of the individual processing layers in the hierarchical approach, we begin with a short outline of the FFT method by USAFSAM, followed initially by the effect of the matched filter and, finally, by the effect of integration of the outputs of the matched filters.

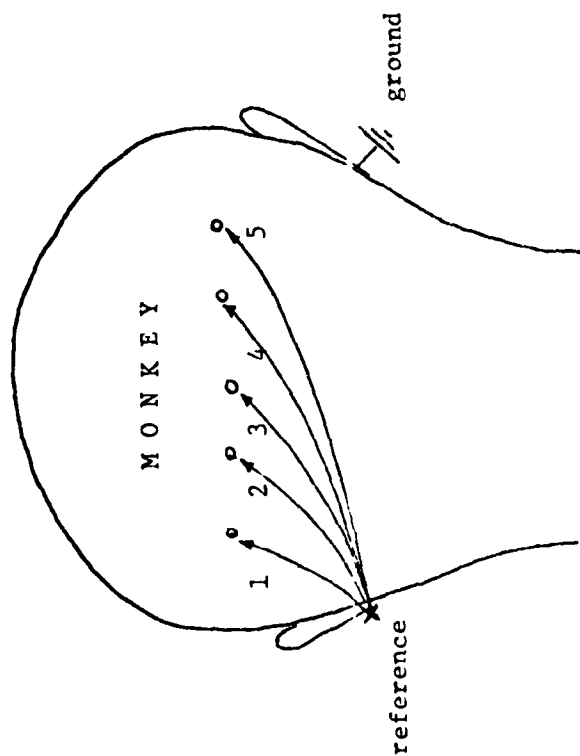


Figure 6.1. Arrangement of epidural electrodes in Macaca mulatta (used in previous experiments by USAFSAM).

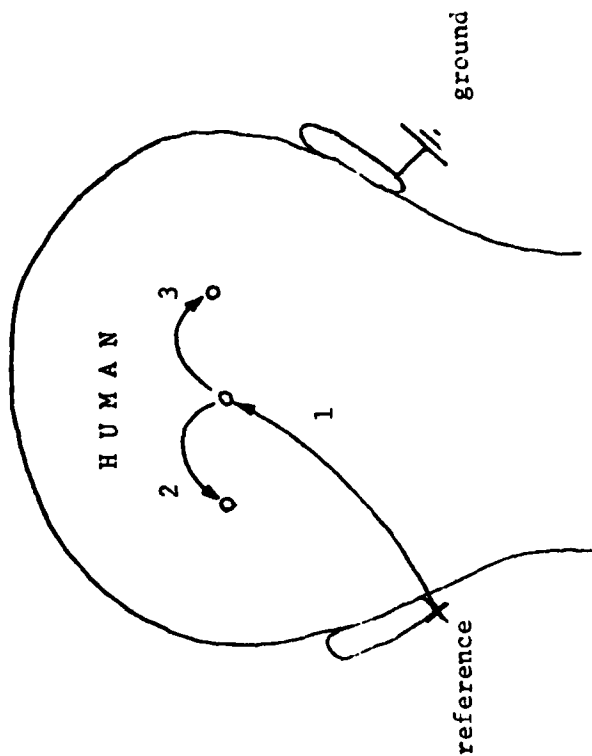


Figure 6.2. New arrangement, for reduced common mode of VER, based on analysis of previous USAFSAM recordings. Activity of left and right hemispheres can easily be distinguished. Note that, here, scalp electrodes were applied.

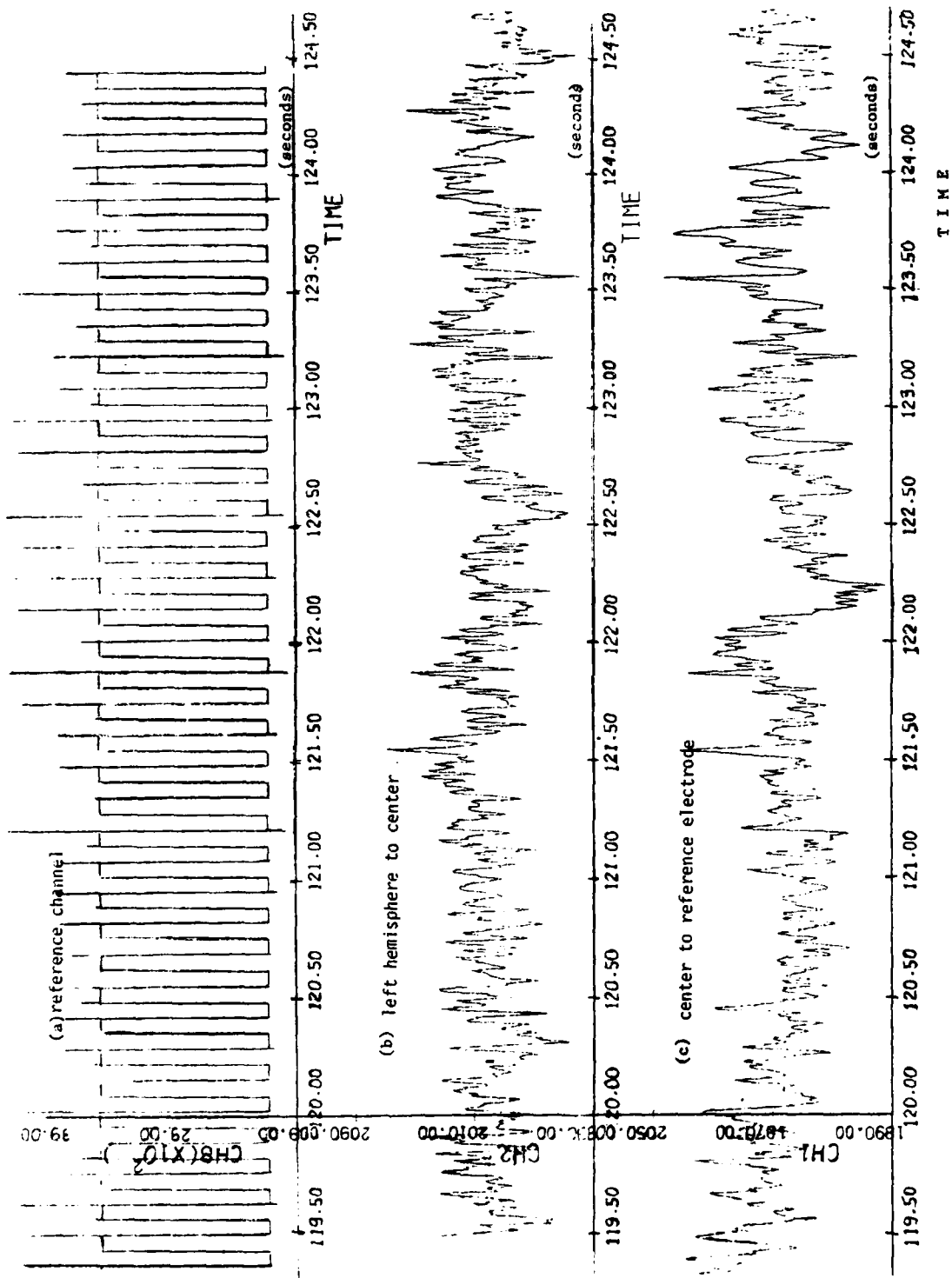


Figure 6.3: a - c. Raw data in the presence of 15-Hz reversal-rate stimulus.

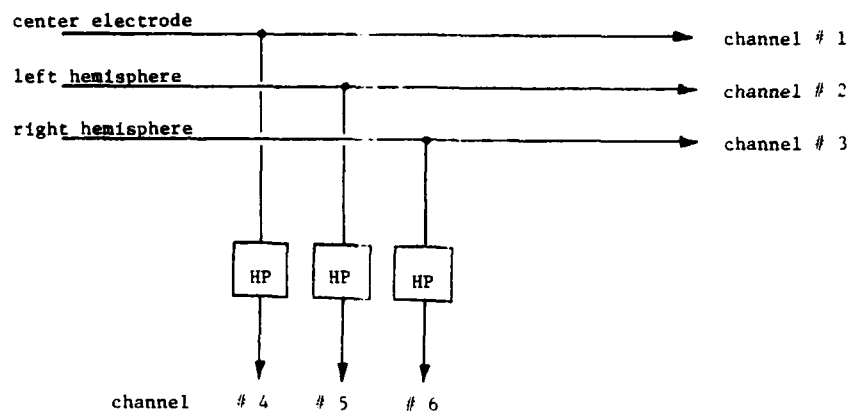


Figure 6.4. Specification of channels. HP indicates a high-pass filter which served preprocessing of the VER. Thus, compared with previous USAFSAM recording, data are differentiated in space and time.

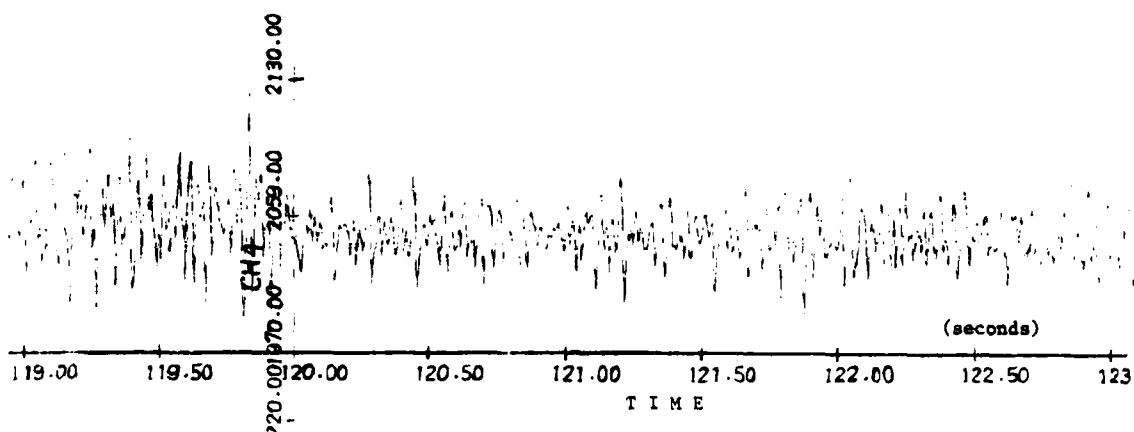


Figure 6.5. Example of high-pass filtered signal from center electrode. Obviously, electrode drift is no problem, and saturation of amplifiers can easily be avoided while retaining the information in the signal.

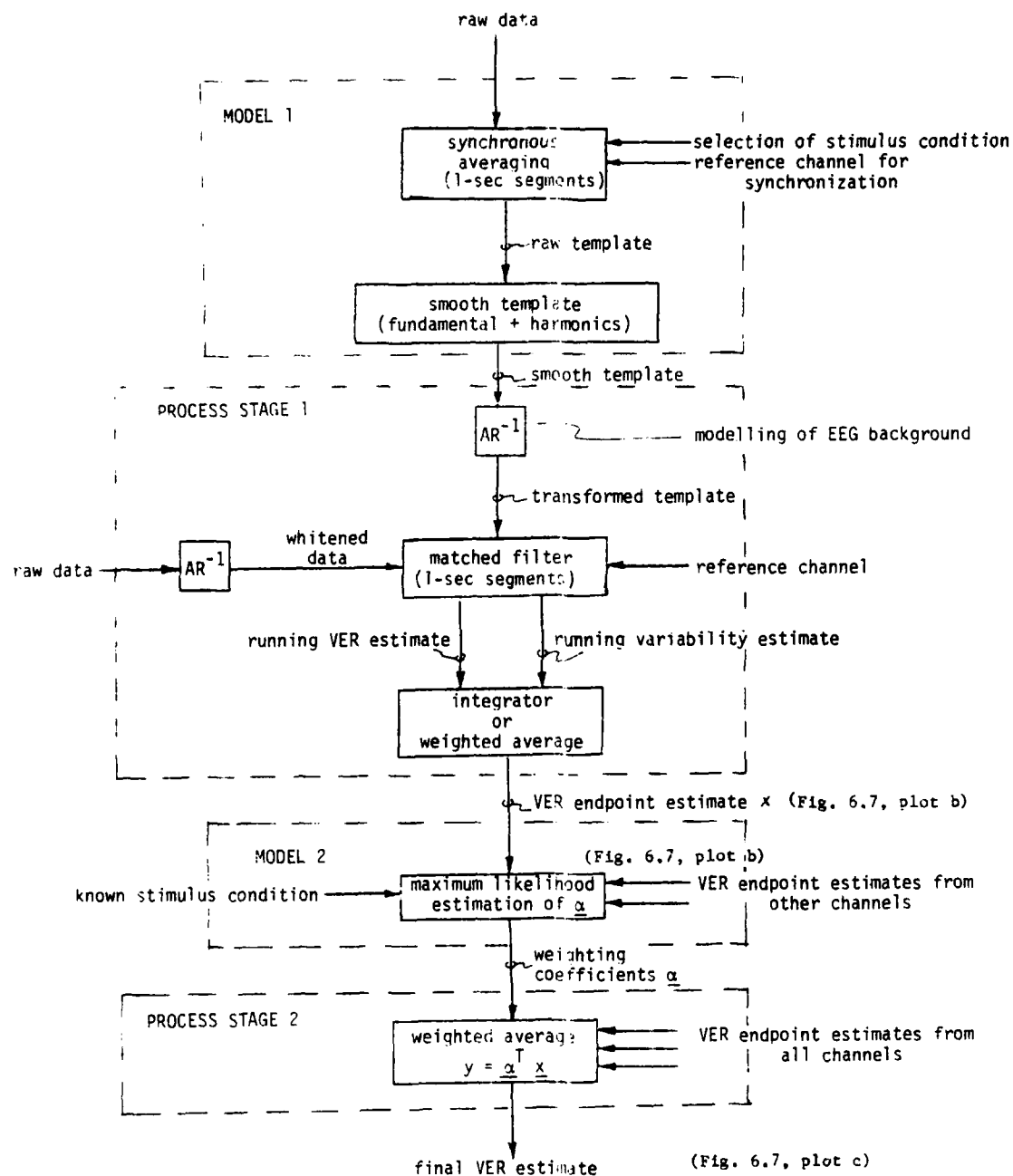


Figure 6.6. Summary of VER processing.

6.2.1 The FFT Method

The FFT method finds the response amplitude of the VER at the reversal rate--in this particular instance, at the 15-Hz reversal frequency. The actual computation is simplified by taking short segments of data (in our case, of 1-sec duration), and averaging a number of them in synchrony with the reference signal. For our comparison studies, 40 sec of data were thus averaged by averaging 40 segments of data. Following the averaging process, the 15-Hz amplitude was computed.

The result for the female subject is shown in Figure 6.7 (Plot a), and is labeled: FFTDJA1. The display shows the response estimates for the 10 experiments--first, giving the 10 estimates obtained from the no-stimulus situation; and, second, the 10 stimulus-present situations. The display shows the results for the center electrode (channel 1), which is believed to give some average response from the two hemispheres. To facilitate comparison of the FFT method with our method, we transformed the raw FFT outputs by removing the bias of the estimate (which is the non-zero estimate present when no stimulus is applied); and then we scaled the display to give an average unit response when the stimulus is present. When the necessary scaling coefficients are computed in this way, one obtains (for the sequence of 10 successive experiments) the outputs shown in Appendixes 1.1 - 1.4. In these Appendixes, observe the increase of the standard deviation SIG-Y of the estimate Y-HAT when a stimulus is present! The sequence of 10 sequential estimates listed in Appendix 1 are the estimates based on the FFT data up to (inclusive) the particular transformed FFT output, Y-HAT. Y-BAR is the average of the previous plus current, Y-HAT.

For accuracy we point out that, at execution of the FFT method--due to an oversight--5 percent more data were actually averaged than intended. This percentage corresponds to 42 sec of raw data for each displayed data point: one extra second of raw data had been added at the beginning and at the end of the data section.

The analysis of the individual data sections for each of the 10 experiments began at about 10 sec after the onset of the experiment, when no stimulus was present; or, alternatively, at about 80 sec, when a stimulus was present.

The equivalent results of the analysis for the male subject are shown in Figure 6.8: Plot a, and are labeled: FFTKJA1. Observe the high variability of the response estimate for this individual when compared with that for the female subject.

Having clarified our graphic display following the original USAFSAM approach, we now present the first level of processing by our matched filter approach.

6.2.2 The Matched Filter Approach for the Human Subjects

The matched filter approach requires a template of the VER and a model for the background noise. First, we compute a raw template by averaging over the data sections known to contain the VER. Second, the fundamental

reversal rate and the harmonics (up to 45 Hz, for now) are picked out and used to obtain the smoothed template. For the background noise, we rely on the previous analysis from the USAFSAM epidural recordings (in Macaca mulatta) which suggested that an autoregressive second-order process (although of variable variance) provided a good approximation. Through a few test runs, we found some good values for the present scalp-electrode recordings. These fixed values were used throughout our analysis. We point out, however, that apparently no such model is needed when the high-pass filtered information channels are used.

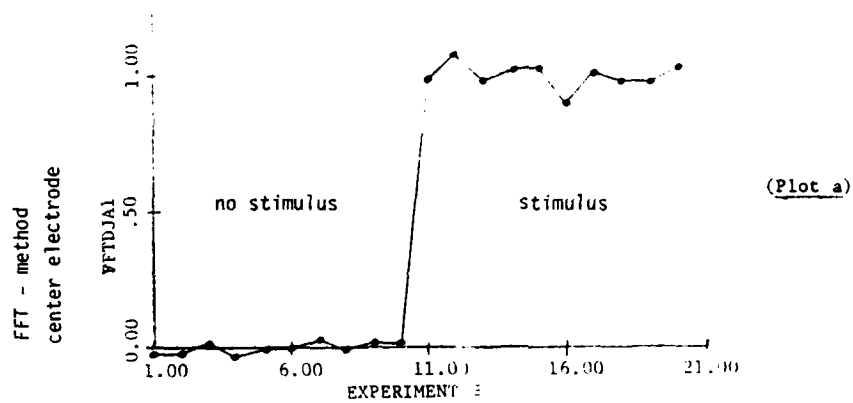
The results of using the matched filter for the same data sections and the center electrode (channel #1)--as just described for the FFT method (except that precisely 40 sec of data were used)--are shown in Figure 6.7, Plot b, for the female subject (labeled: VERDJA1), and in Figure 6.8, Plot b, for the male subject (labeled: VERKJ1). Observe the improvements, especially for the male subject. As for the FFT method, we computed standard deviation SIG-Y and average response Y-BAR for the individual response estimates Y-HAT. Numerical values are given in Appendixes 2.1 -2.4.

The factors in the figures refer to the improvement of the method over the FFT method, and indicate the time savings which can be achieved. For example, a factor of 10 implies the FFT method has to use measurement times 10 times as long to achieve the same accuracy as the particular alternative method. Conversely, by our method, measurement time can be cut to one-tenth that of the FFT method while achieving the same resolution. A summary of the standard deviations of the individual estimates is shown in Table 6.1. From these values the improvement factor is computed by taking the square of the ratio of corresponding standard deviations. The factors in the figures include the 5-percent correction factor, which is due to having used 5 percent more data windows in the FFT method than in the corresponding matched filter analysis.

Now that the improvement of estimation by use of the matched filter has been seen, the next interesting step is to combine the information from the individual channels by suitable regression.

6.2.3 Integrated Information of Response Estimates

Here, a suitable approach was to form a linear combination of the response estimates from the individual matched filters. The necessary coefficients are obtained by a method motivated by a maximum likelihood argument and regression, respectively. Although (for our current understanding of the VER), only part of the information contained in the outputs of the matched filters has actually been used, a significant further reduction of variability could be achieved. The results from combining the channels 1, 2, and 3 can be seen in the displays: in Figure 6.7, Plot e, for the female (labeled: VERDJ123); and in Figure 6.8, Plot c, for the male subject (labeled: VERKJ123). Compare, also, the standard deviations for these conditions as shown in Table 6.1. Given in section 6.4 are details of the estimation of the weighting factors for combining outputs from the matched filters. Numerical results are listed in Appendixes 3.1 - 3.4.



FEMALE
SUBJECT

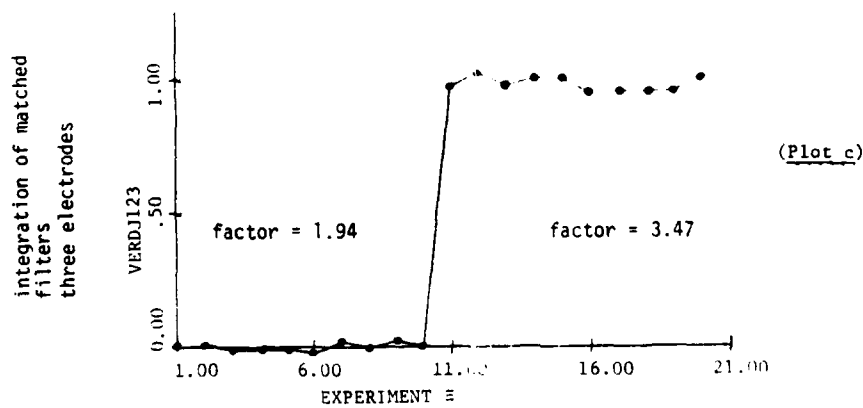
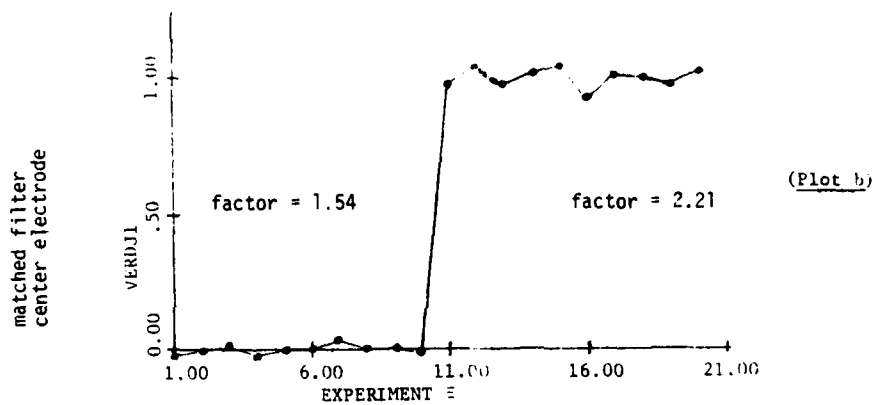


Figure 6.7: Plots a - c. Sequence of 20 experimental measurements for a female subject. Observe the variability of response estimates.

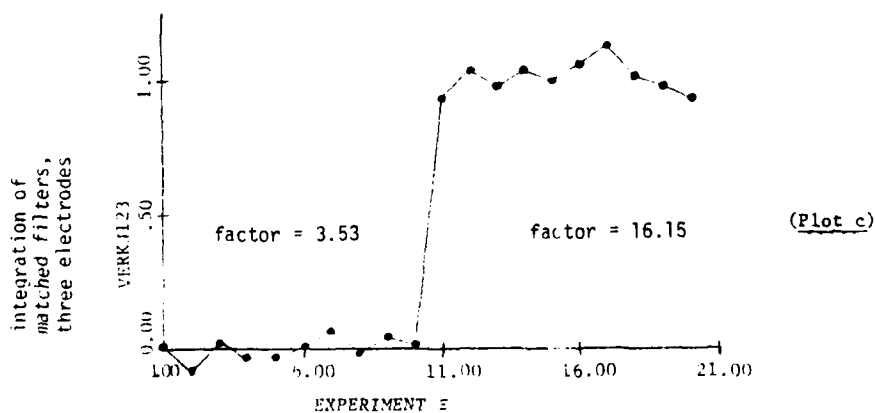
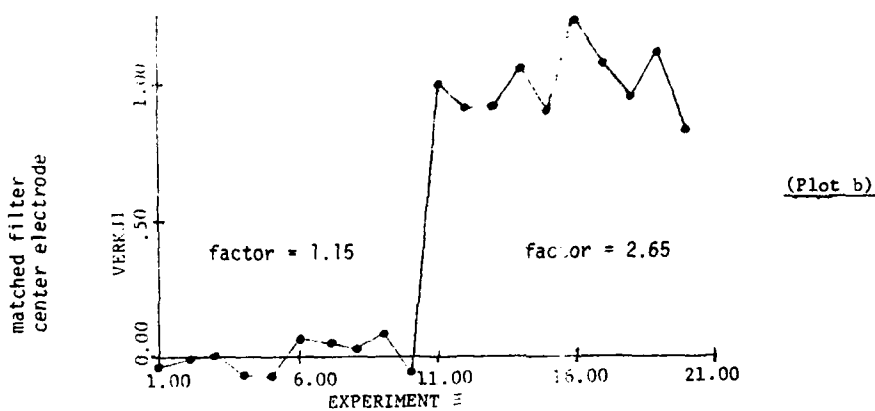
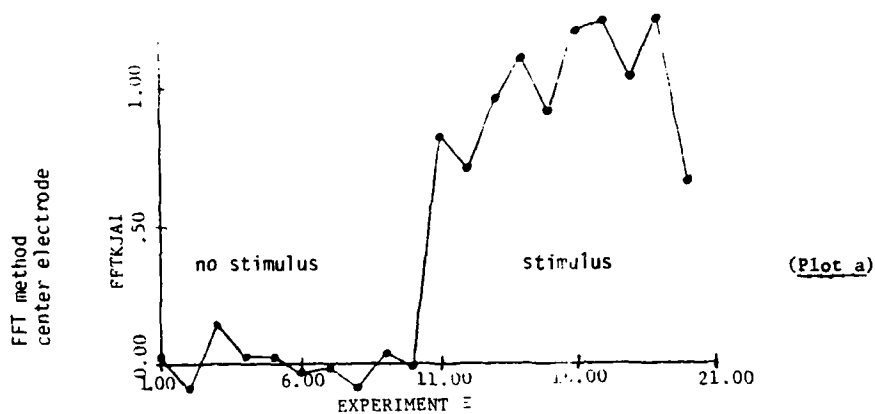


Figure 6.8: Plots a - c. Sequence of 20 experimental measurements for a male subject. Observe the variability of response estimates.

TABLE 6.1. STANDARD DEVIATIONS OF INDIVIDUAL ESTIMATES

Method	No stimulus	Stimulus
<u>Female subject: DJ</u>		
FFT	.0200	.0518
m-filt #1	.0165	.0381
m-filt #123	.0138	.0278

<u>Male subject: KJ</u>		
FFT	.0692	.2259
m-filt #1	.0589	.1232
m-filt #123	.0436	.0576

Note: FFT refers to the method described in section 6.2.1.
 m-filt #1 refers to center electrode method of section 6.2.2.
 m-filt #123 refers to combined electrode method of section 6.2.3.

Following this rather intuitive explanation of our approach, we now give a more technical presentation and evaluation of the methods we developed.

6.3 TECHNICAL ASPECTS OF MATCHED FILTER APPROACH FOR HUMAN SUBJECT DATA

This portion of the report deals with the individual programming steps of our hierarchical matched filter approach (described in more detail in the following section). Here, we give a brief description of the data processing, with some examples of typical results.

We begin with the extraction of the template, turn to the smoothing of the template, review the matched filter and, finally, describe the integration of the information from the individual data channels. A summary of the individual modeling and processing stages is shown in Figure 6.6. We also include a description of the results shown in Figures 6.7 and 6.8, and in Table 6.1.

6.3.1 Estimating the Template

The template of the VER is obtained in a two-step procedure.

First, a raw estimate is obtained by averaging, synchronously with the reference channel, a 1-sec segment of data over all data which are known to contain the VER; e.g., for each individual, the VER was present during about $T = 60$ sec to $T = 140$ sec in each of the 10 repetitions of the experiment. Thus, for each individual, a particular raw template is obtained. These raw templates for the male subject are displayed in Figure 6.9.

Second, this template is smoothed. The smoothing consists of a selection of the fundamental reversal frequency plus some of its harmonics. When the stimulus frequency is 15 Hz, we select typically only the 15-Hz, 30-Hz, and the 45-Hz components for this smoothed template. Thus, we avoid difficulties with 60-Hz interference. The selection is obtained by finding the FFT of the raw template, zeroing out the undesired frequencies, and back-transforming the template (Fig. 6.10). Observe the asymmetry of these templates.

We have not tried to use any higher harmonics at this time, although harmonics up to about 100 Hz may be present in VERs (4). Use of higher frequencies may possibly contribute to further reduction of the variability of VER estimates.

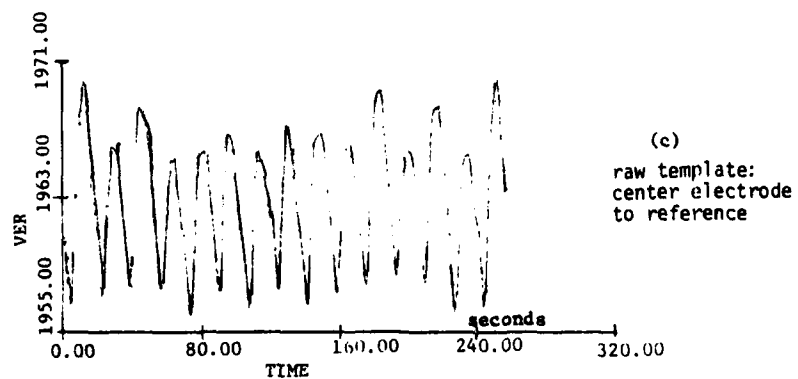
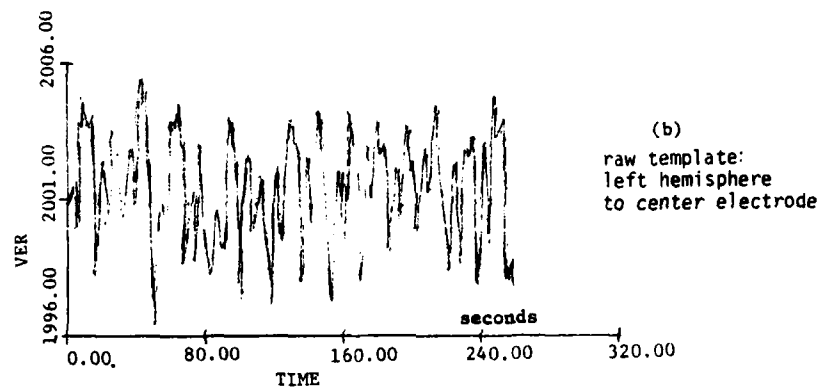
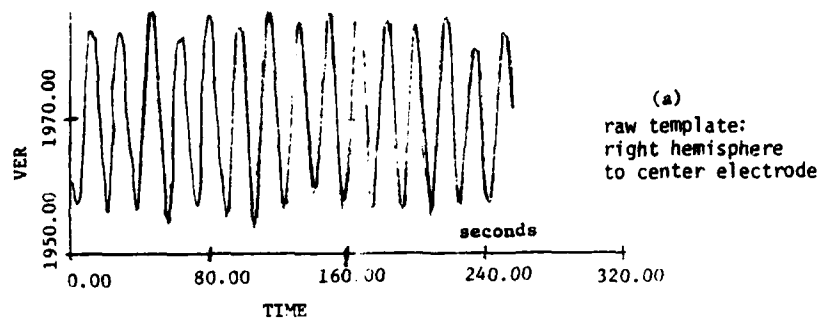


Figure 6.9: a - c. Raw templates for male subject.

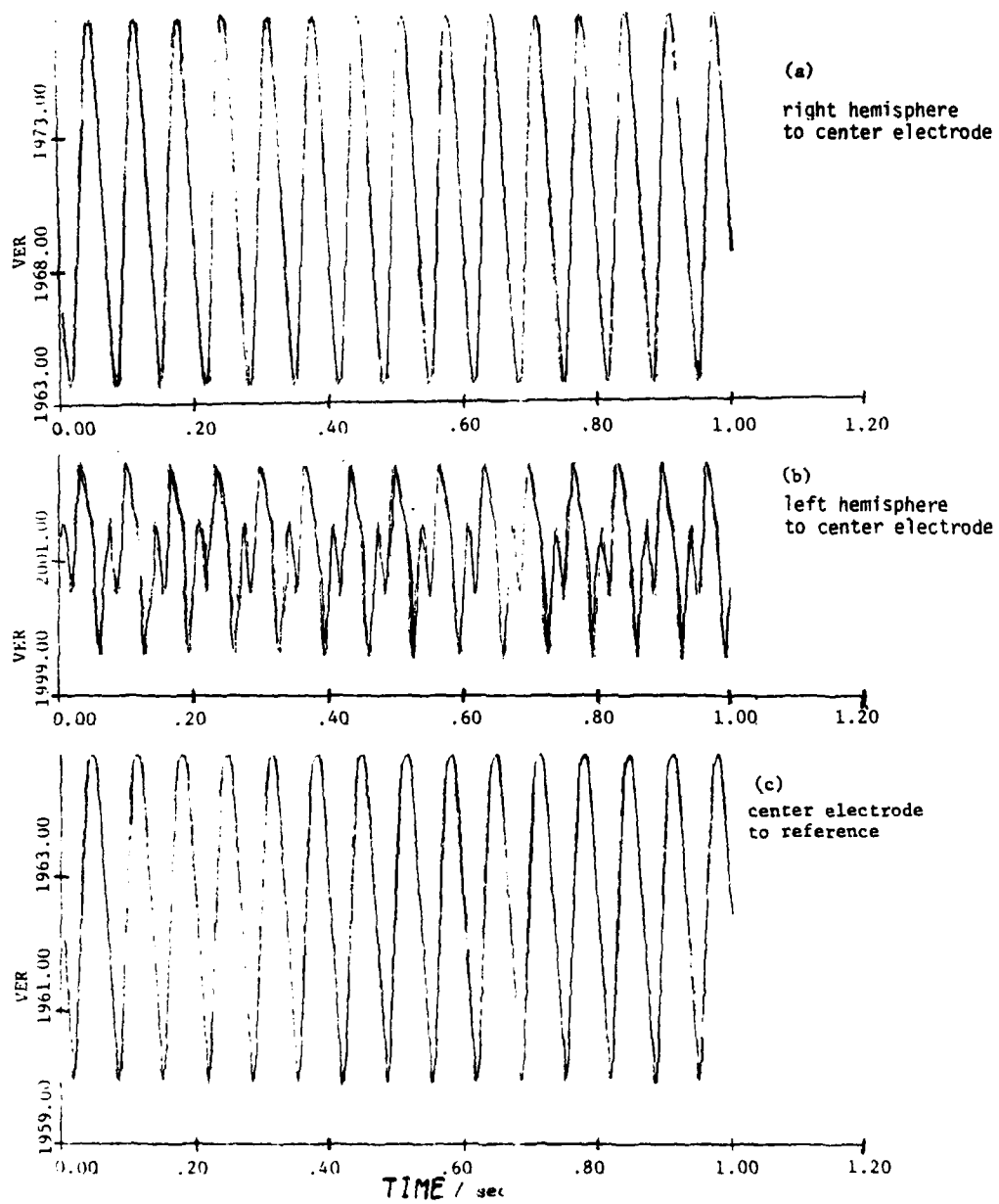


Figure 6.10: a - c. Smoothed templates for male subject.

6.3.2 The Matched Filter for the Human Subjects

A schematic drawing of the matched filter is shown in Figure 6.11. Observe that, prior to the matching, the raw data and the smoothed template are transformed by an inverse autoregressive process in order to whiten the background of the EEG--the noise for much of our analysis. The need for this whitening arises from the fact that the matched filter operates optimally only under these conditions.

For our purposes, we found that autoregressive model values $\alpha_1 = 1.6$ and $\alpha_2 = -.6$ gave good results regardless of the particular subject or scalp electrode. These values resulted in a slightly stronger high-pass filter effect than those we had derived for the epidural electrode recordings (6). Considering the low-pass filter characteristics of the transmission of VERs from the visual cortex to the scalp, these new autoregressive values were quite reasonable, even though they were found empirically. We also noted that, for the data which were recorded by means of the high-pass filter (Fig. 6.4), no preprocessing with the inverse autoregressive filter was needed to achieve near-optimal results. This finding was anticipated from the results we had obtained from the analysis of earlier recorded data (6). For an example of a typical output from the matched filter, see Figure 6.12.

An additional benefit may be obtained by use of the matched filter approach. We suspect physiological variability in the amplitudes of the individual evoked frequencies (e.g., 15 Hz and its harmonics) to be omnipresent but, apparently, either in an independent fashion or in some counter-phase fashion.

6.4 INTEGRATION OF INFORMATION FROM INDIVIDUAL INFORMATION CHANNELS

In this section, our objective is to relate the estimated VERs (from the individual information channels) to the stimulus in such a way that the stimulus can be estimated with minimal uncertainty. We may regard the condition of no stimulus to correspond to $y = 0$, and, when the 30-percent contrast stimulus is present, to $y = 1$, the "unit stimulus." All other potential stimuli would be scaled, in an appropriate way, relative to these two experimental conditions.

Given VER estimates, x , we may then ask how to combine them to estimate a stimulus condition (or some "generalized response") -- e.g., y -- with least variability. More formally, we wish to find a method to obtain.

$$\min [d(y-\hat{y})/x_1, x_2, \dots, x_N], \quad (6.1)$$

where d is some suitable metric. We are mainly interested in the usual least squares sense; that is,

$$d(y-\hat{y}) = (y-\hat{y})^2, \quad (6.2)$$

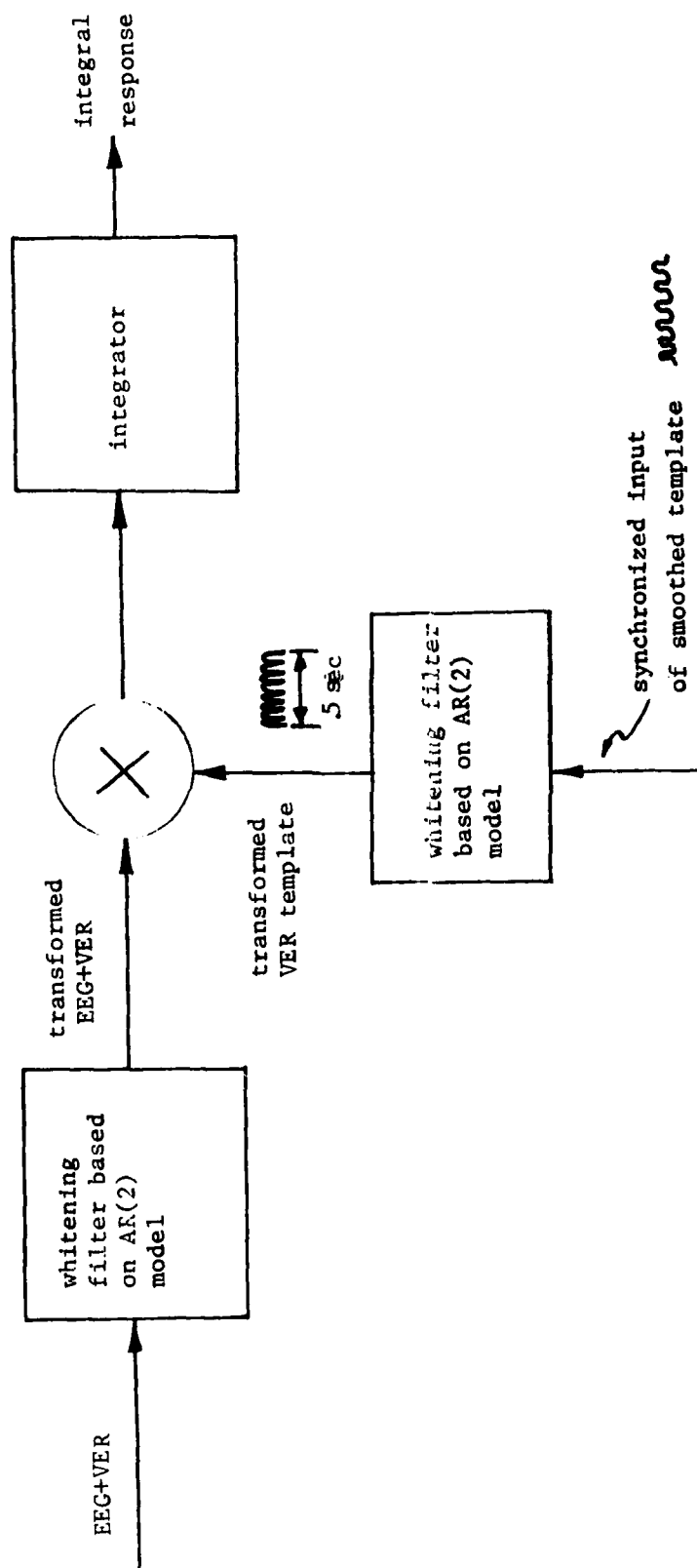


Figure 6.11. The matched filter approach applied to the VER signal for estimation of its (integrated) amplitude.

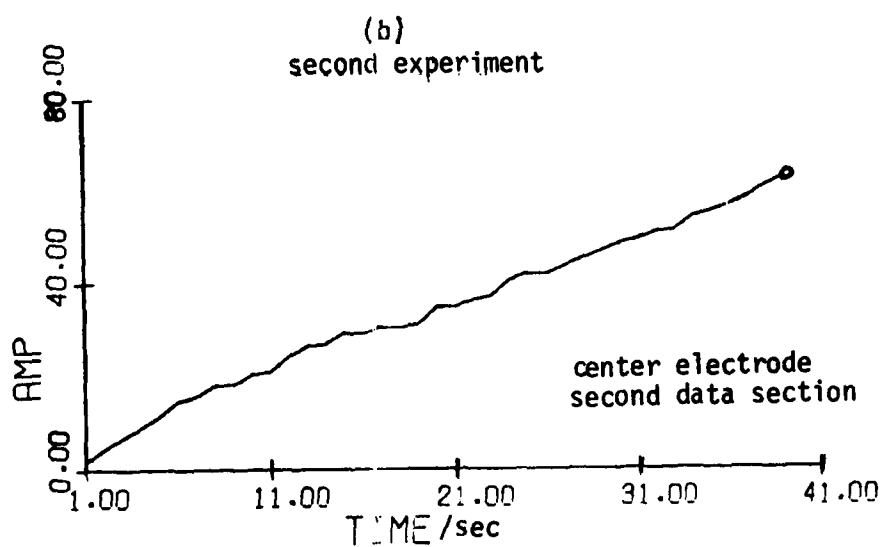
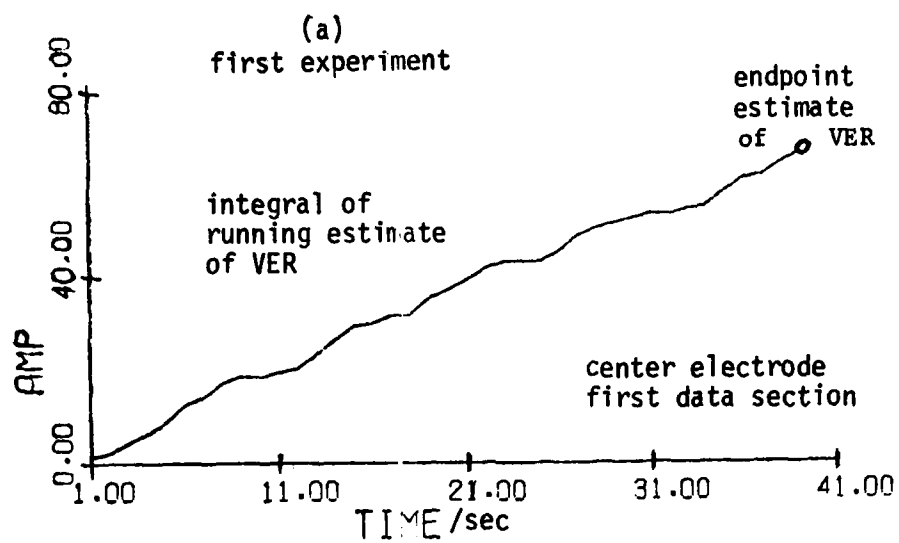


Figure 6.12: a and b. Output from matched filter (integral over time of response in a single channel).

which looks very much like the usual regression problem. However, here one has to be careful in obtaining weights β_1, \dots, β_n ; for the errors in the model do not lie in the stimulus condition, y (which is known from the experiment), as in the usual regression model:

$$y = \beta_0 + \beta_1 x_1 + \beta_2 x_2 + \dots + \beta_n x_n + \epsilon \quad (6.3)$$

but in the x 's, as in:

$$x_i = \gamma_i y + \epsilon_i \quad ; \quad i=1 \dots n \quad (6.4)$$

This situation is known as the "error invariable" problem. In many situations, the usual regression estimation for the parameters $\gamma_1, \dots, \gamma_n$ is still useful. In fact, it also leads to good estimation for our particular problem. Thus, we may obtain regression coefficients by use of:

$$\hat{\underline{\gamma}} = [\underline{X}' \underline{X}]^{-1} \underline{X}' \underline{y} \quad (6.5)$$

where, as usual, the rows of \underline{X} are formed by " \underline{x} " for the individual experiments.

Still, a more rigorous argument about the use of regression coefficients (or, equivalently, weight coefficients) is desirable. To clarify the situation, refer to the displays in Figure 6.13. The regression -- which is fit to such data, minimizing the residual error in y -- will tend to be too flat. Thus, when y is predicted on the basis of observations x , using the regression line, biased estimates will result.

In this particular case, two remedies are apparent: one appears to be a quick fix; the other is motivated by maximum likelihood estimation. As can easily be shown, they are identical here.

The quick fix, which seems to be to pull the regression line through the origin of the y and x space, may be done either by fitting a model without the regression constant β_0 , or, alternatively, by adding a lot or pseudo data points at the origin while fitting a model. This latter approach is convenient when standard regression packages, which often include β_0 , are to be used.

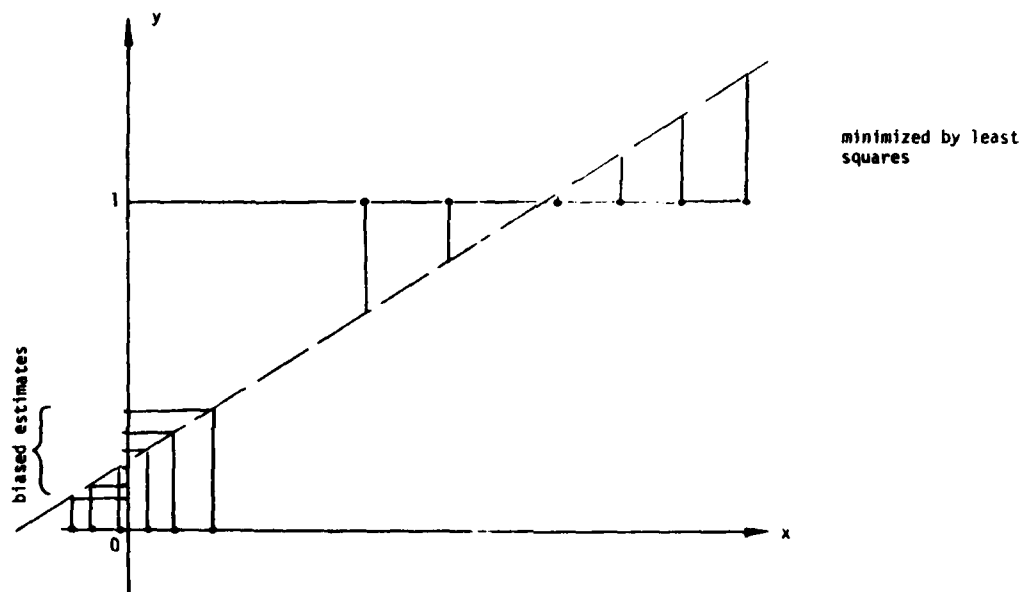


Figure 6.13. How error in the assumed independent variable, x , yields a biased regression line for assumed dependent variable, y (which will usually be identified with the stimulus strength).

With regard to the maximum likelihood (ML) estimation (MLE), consider the following simple model for n -correlated channels (Fig. 6.14) for two stimulus conditions $y = 0$ and $y = 1$:

$$x_i = \gamma_i y_j + \epsilon_i; i=1 \dots n, j=0,1, \quad (6.6)$$

and

$$\text{cov} [\underline{\epsilon}, \underline{\epsilon}'] = C, \quad (6.7)$$

where γ_i stands for the fixed part of the relation between x_i and y , while ϵ_i stands for the random part of that relationship. Then,

$$p(x / y, \underline{\gamma}, C) = c \exp \{-1/2 (x - \underline{\gamma} y)' C^{-1} (x - \underline{\gamma} y)\}. \quad (6.8)$$

The maximum likelihood estimate of $\underline{\gamma}$, given the stimulus present condition ($y = 1$), is simply:

$$\hat{\underline{\gamma}} = \underline{\bar{x}} / y, \quad (6.9)$$

where the averaging is performed over independent (for us, successive) experiments. When these gain factors, summarized in $\underline{\gamma}$, have been obtained, one may conversely proceed to estimate y , given \underline{x} . The maximum likelihood estimate for y is by equation 6.8, and by replacing the estimate $\hat{\underline{\gamma}}$ for $\underline{\gamma}$:

$$y = \hat{\underline{\gamma}}' C^{-1} \underline{x} / \hat{\underline{\gamma}}' C^{-1} \hat{\underline{\gamma}}. \quad (6.10)$$

We can show, fairly simply, that estimation, via equation 6.10 leads to the same estimates as use of the regression formula, equation 6.5, when an infinitely large number of points at the origin is added. This finding is due to the equivalence (up to a multiplicative factor, in this case) of $\underline{x}' \underline{y}$ with $\hat{\underline{\gamma}}$, and $(\underline{x}' \underline{x})$ with C .

We should point out at this time that the model of the estimates of VERs, as shown in equation 6.7, is not quite realistic in view of our current data analysis: that C changes, generally speaking, increases monotonic with stimulus intensity (Fig. 6.15). We presume, also, that the contours of the distribution of estimates change with stimulus intensity. Some preliminary investigations along these lines showed the usefulness of a variability measure for predicting stimulus condition. Since these aspects exceed by far the scope of our current effort, however, we have to leave further investigation for the future.

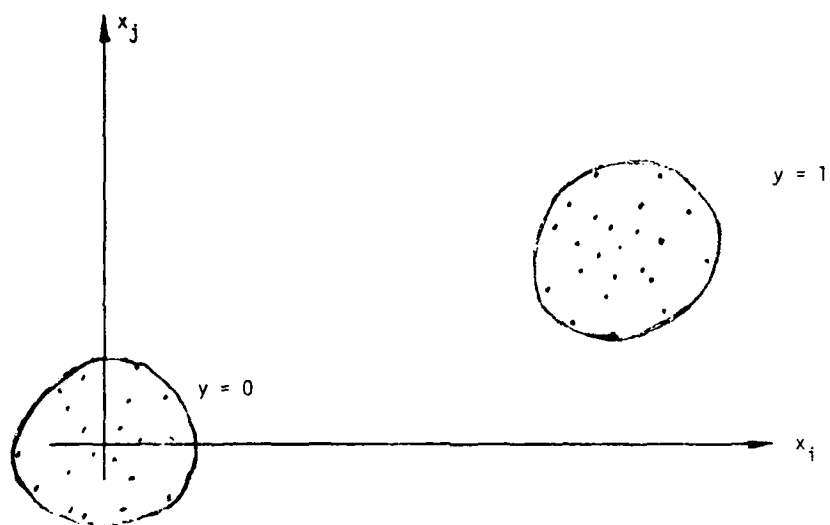


Figure 6.14. Simple model for the relation between visual evoked response, x_j , and stimulus, y .

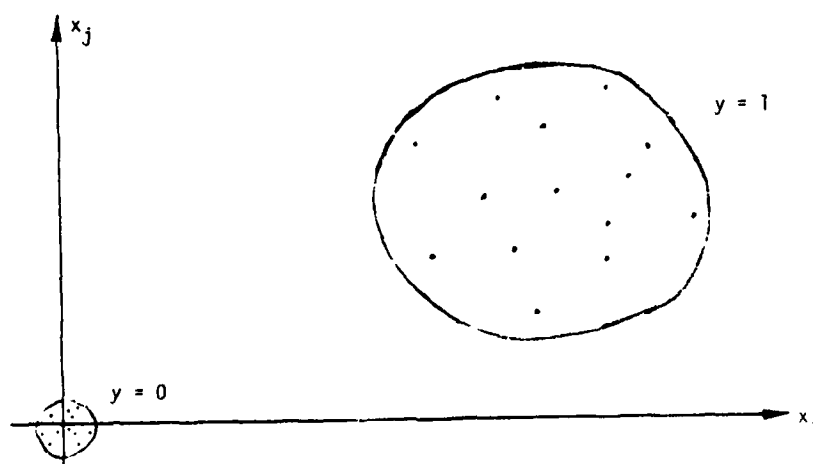


Figure 6.15. A more realistic model for the relation between visual evoked response, x_j , and stimulus, y . Observe variance of the x_j 's.

In summary, significant reduction of the estimation of VERs is possible by a combined matched filter and maximum likelihood approach. However, the current approach is hierarchical and should not be presumed to be optimal with regard to potential reduction of variability. One of the important questions is how one might go about finding an integrated (not hierarchical) approach which has the potential to yield near optimal performance. The necessary approach seems to be dictated by our improved understanding of the VER. Some of the important findings, which will lead eventually to near optimal assessment of visual performance, are discussed in the following pages.

7. SOME BASIC STUDIES AND PROPERTIES OF THE HUMAN VER

Three properties of the data appear particularly interesting for refining our understanding of the VER. They concern: the variability of the VER; the mutual dependencies of harmonic frequencies and fundamental frequency; and the effect of blinking on the phase angle of the VER. The observations are in accordance with our understanding of the underlying physiology of information processing, and are discussed here in this context.

7.1 THE CONCEPT OF VARIABILITY

As already mentioned (Figs. 6.13 and 6.15), the variability of response estimates in individual channels (corresponding to differential voltages between electrodes) increases when a stimulus is presented. This finding is true for both individual channels. The increase is strong enough to be useful for predicting stimulus condition.

In general, we computed, for individual 40-sec segments of data, the standard deviation of individual VER estimates based on 10-sec subsegments. Thus, the variability of 4 subsegments generated a variability index. This index could be used, in turn, in the (already described) maximum likelihood estimation for assessing stimulus condition. In fact, we found from regression analysis that some 50 - 70 percent of the regression model was explained by this variable.

Conceptually, what appears to happen is that the "gain" of the visual system varies in a random fashion. Thus, the larger an input signal (e.g., no-contrast = 0 vs. unit-contrast = 1), the larger will be the absolute variation of the response. Thus, such variation relates to the amplitude of the stimulus intensity.

A second aspect was highly interesting to us. It concerns the hemispheric differences of the VER. We found that, for the female subject, mainly the left hemisphere gave large variability -- while the right hemisphere delivered a much more constant response. In the male subject, the converse was true: the right hemisphere gave highly variable responses -- while the left hemisphere provided a very constant response. This result, which may be a pure fluke of the "random sampling of the population" (not of our data processing), is in accordance with the general outline in our final report for phase I(5). There, we discussed the hemispheric differences. In accord with Beaumont et al. (1), Ben-Dov and Carmon (2), and others, the female utilizes her left hemisphere more, as compared with the male; and, conversely, the male utilizes more of his right hemisphere than does the female. Thus, in the male, the right hemisphere appears to be more complex; and, in the female, the left hemisphere, associated with the differing functions of these hemispheres. This finding is in accordance with our observation and has an obvious bearing on what might be expected from the VER in these hemispheres--the VER in the more complex hemisphere is expected to be more variable. Substantiating this finding with more representative random samples of the general population will be important.

The increased variability was reflected in a much smaller weight factor for that hemisphere when the individual channels were combined in the maximum likelihood estimation. In fact, a slightly negative weight factor was estimated, both for the female and the male. The fact that the coefficients are not significantly negative might be an indication of a counter-phase variation of the VER between the hemispheres: when one hemisphere receives more input, the other one receives less. Such a model has to be considered in view of the known existence of competing neural networks (mutual inhibitory innervation).

7.2. RELATION OF FUNDAMENTAL AND HARMONIC FREQUENCIES

This study was of limited nature, and was performed only in the female because of her strong and clear VERs. Basically, we tried to determine any systematic relation in the variation of the fundamental and harmonic variability of response estimates (or better estimators of stimulus condition) could be reduced. For this purpose, we checked the autocorrelation of 15-Hz amplitude estimates from successive 1-sec data windows with the corresponding amplitude estimates at 30 Hz (Fig. 7.1.). From a statistical viewpoint, no significant correlation could be observed, for example, on a 95-percent level. Thus, for the present, we disregarded any potential relation.

In retrospect, the situation may be different for the male subject, because variability of the "true" VER seems to be a much more significant component when compared with the variability induced by the noisy background EEG. Thus, a possible relationship may become statistically more significant.

7.3 THE EFFECT OF BLINKING

For some time, blinking has been our concern as one of the contributing factors in variability of response estimates in human subjects. Thus, we performed an additional experiment, in which the individual was asked to blink, self-controlled, every 5 sec. Accuracy was verified from a separate EMG signal channel (described earlier).

The major finding of this limited effort was the change of the phase angle of the VER during blinking. For both subjects, the phase angle was reduced (for the fundamental reversal rate and, in corresponding fashion, for the harmonics). This reduction in phase angle corresponds to a faster response to the stimulus. For the male subject, the change corresponded to some 7 ms; and, in the female, about 1.2 ms. Although these changes may appear small, they are significant.

We came to this conclusion in the following way: We computed, in synchrony with the reference channel, the FFT of successive 1-sec complex planes. In the event that no stimulus was present, a random walk of this sum developed (Fig. 7.2). On the other hand, when a stimulus is present, a consistent component will be in one particular direction. These results are shown for both subjects in Figures 7.3 and 7.4.

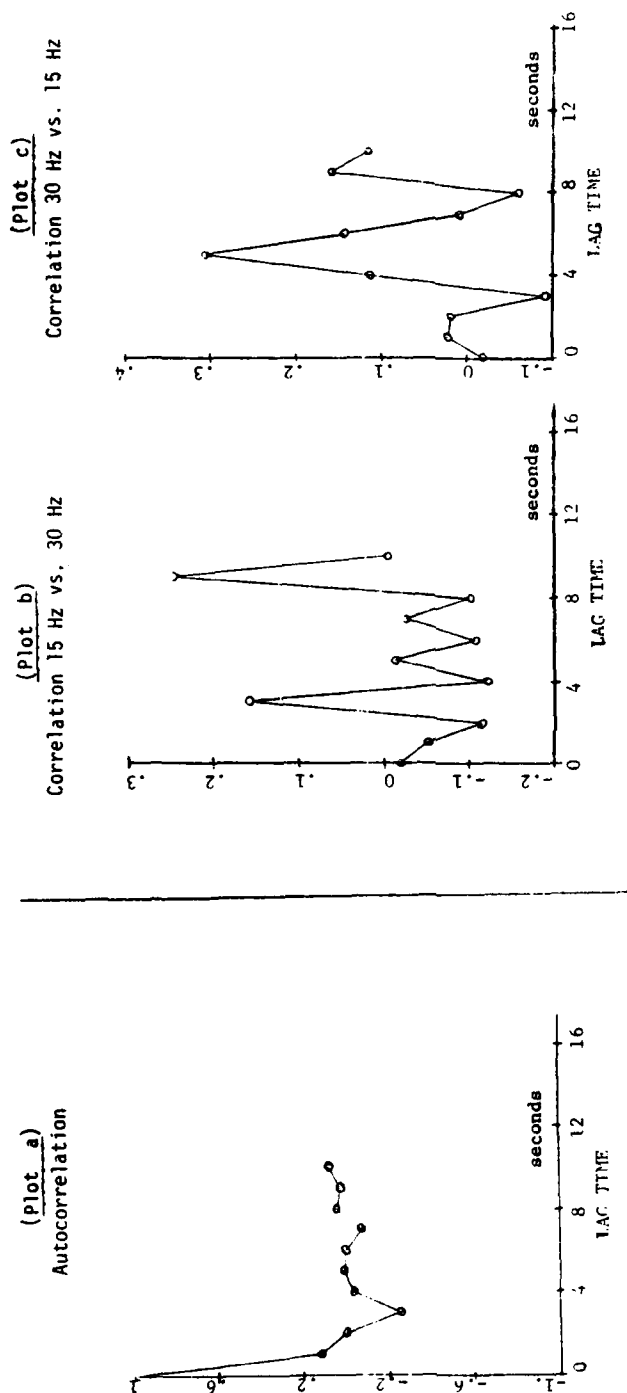


Figure 7.1: Plots a - c. Autocorrelation and cross-correlation of amplitude of 15-Hz and 30-Hz components, when estimated from 1-sec segments of data (during stimulus). No particular correlation of the response within or between successive data segments is apparent. Subject: female; center electrode; data file DJ1701; time, 79 - 129 sec.

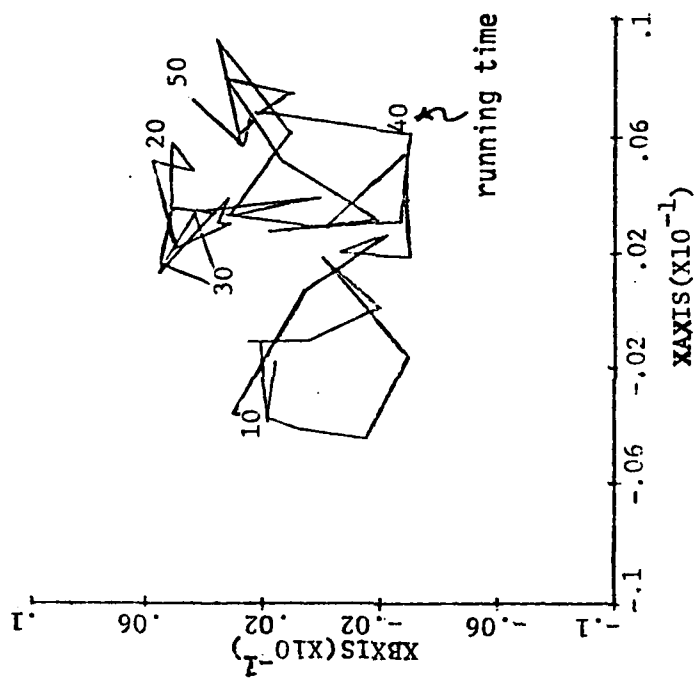


Figure 7.2. Random walk, in complex plane of the integrated 15-Hz component, when stimulus is absent.

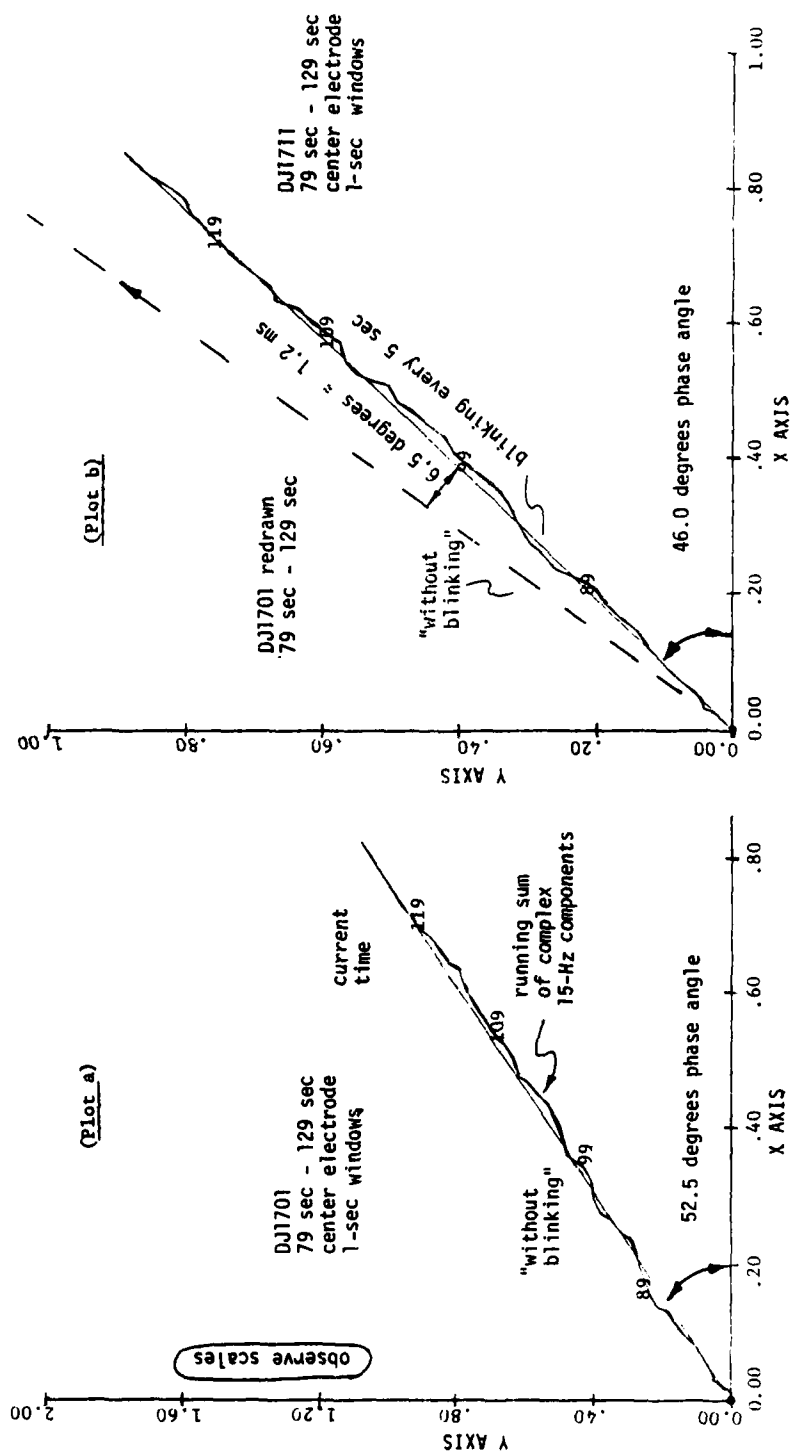


Figure 7.3: Plots a and b. Comparison of phase angle of VER with and without blinking. Blinking reduces the phase angle. The corresponding change of delay time is 1.2 ms. Subject: female; 15-Hz reversal rate.

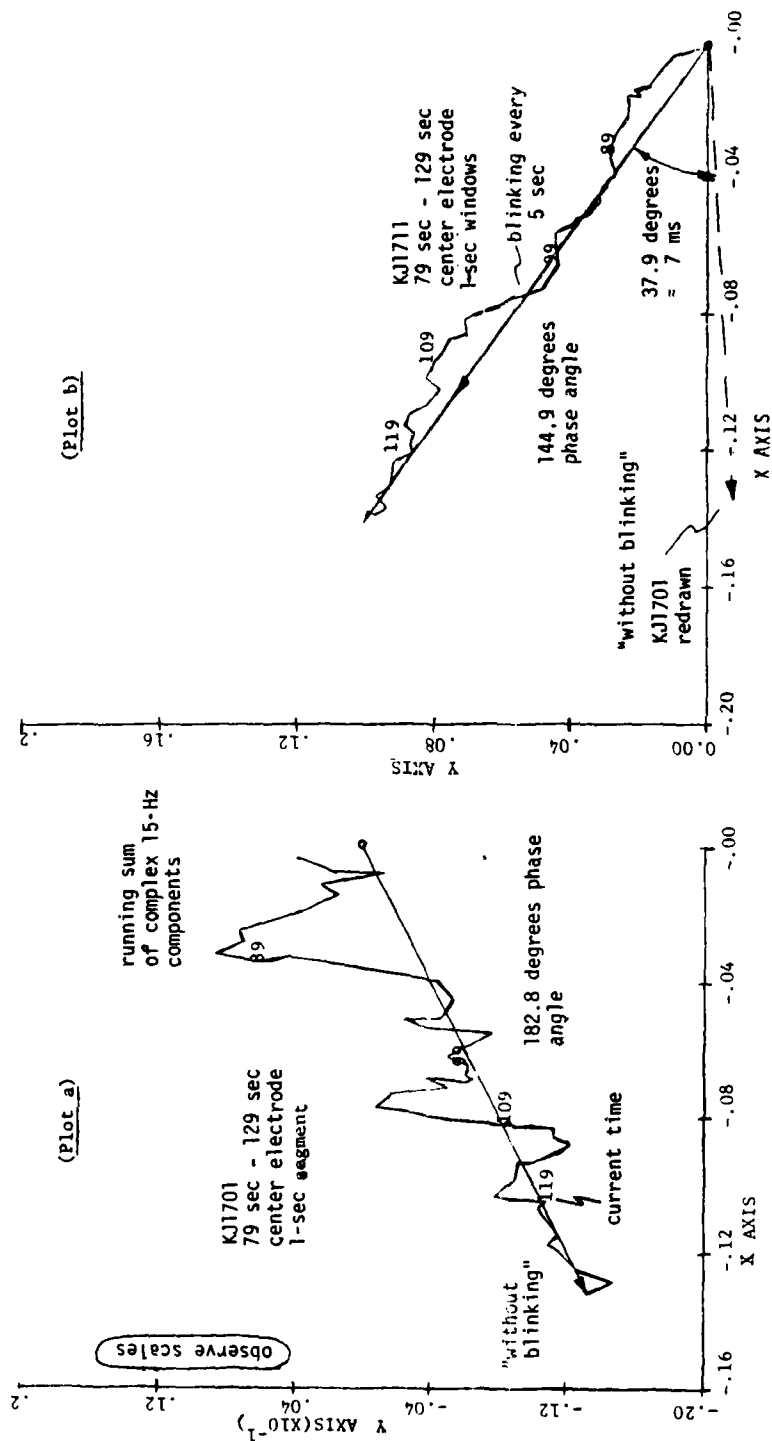


Figure 7.4: Plots a and b. Comparison of phase angle of VER with and without blinking. Blinking reduces the phase angle. The corresponding change of delay time is 7 ms. Subject: male; 15-Hz reversal rate.

The left-hand side shows the results of integrating the complex vectors when the subject suppressed blinking (reduced to some 2 to 3 times/min), while the right-hand side displays the result for regular blinking every 5 sec. For both subjects, a drastic reduction of the phase angle results. (When interpreting the figures, observe the unequal scales in the left-hand part.) The result is interesting, especially because one will usually associate late responses with fatigue and, possibly, more variability.

In any event, for reducing variability in response estimates in the presence of blinking, the incorporation of the effect of blinking on the phase lag of the VER seems to be important. The importance is more striking when one considers higher harmonics. There, changes of phase angle in excess of 90 degrees are observed. Clearly, from the properties of the matched filter, this knowledge about phase shifts is crucial.

At this time, however, we could not find any indication for reducing variability of response estimates by incorporating phase variation into estimation of the VER when the subject is not blinking. Over periods of more than 2 min, in the present recordings, blinking seemed to occur rarely (e.g., 3 or 4 times). Due to our doubt about the accuracy of our channel for recording blinking, we decided to verify performance of that channel by encouraging the subject to blink regularly every 5 sec. We can only suspect that, when the subject is encouraged to blink freely, the consideration of phase lags becomes important for modeling the VER. Inducing a subject to blink freely may be attractive because of the aforementioned faster response, which may be an expression of increased alertness.

In summary, we made a number of interesting observations with regard to the variability of the VER and its causes. Because of time constraints, however, a number of questions could not be thoroughly investigated. These had to be left to future analysis and to new experimental setups.

7.4 STUDY OF SEGMENTING

Following our observation of the possible clusters of the variance of the EEG background activity in data of *Macaca mulatta* (Fig. 4.12), we tested the significance of weighing data according to the residual power in the matched filter (the sum of squares of the residuals within 1-sec segments of data). The following two opposing models were tried--

First: The relative weight of the contribution of an amplitude estimate was reduced when the residual power increased. This processing counteracts a model in which corrupting noise is assumed to be superimposed on the VER. Such a processing method is attractive, because it leads naturally to a robust procedure (one which is not too badly affected by sudden artifacts, such as possible loosening of electrodes). Second: We tested a processing which increases the weight of amplitude estimates within these 1-sec data windows when the residual power increases. Interestingly,

we did not find any statistically significant differences in these two alternative processing methods compared to the plain integration in time of the matched filter output. We assume, therefore, that the current method must be in a sense close to optimal. However, one should keep in mind that this attempt was not based on any of the (in this respect) possibly varying properties of the human subject data. Following a more rigorous analysis, a more sophisticated data processing might improve estimation. This question has, however, to be left to future investigation.

DISCUSSION

According to the results we have obtained to date, our approach appears to be a valid way to reduce the variability of response estimates. Our analysis had impact: on the selection of the differentials between electrodes which were to be used as information channels; on the prewhitening of recorded data by a high-pass filtering process (eliminating the problem of amplifier saturation, and simplifying subsequently the matched filter which does not require the inverse autoregressive filter); and on the ultimate structure of our hierarchical processing method.

The present data indicate that hemispheric differences--possibly linked to the sex of the subject--and the effect of blinking may be some of the next variables to be investigated. Other variables are day-to-day variations which may, in part, be due to variation in electrode locations.

A word should also be said about the current data-acquisition method. We found the time resolution to be somewhat of a limiting factor because of:

- (a) considerable random tape-speed variations up to 10 ms/sec; and
- (b) a sampling rate of only 256 samples/sec.

This low sampling rate results, in view of the random tape-speed variations, in a large uncertainty in phase angles at higher harmonics of the VER.

The problem can be cured, to some extent, by more sophisticated software which synchronizes the data processing with the reference channel more often than once per second. Possibly a simple model of the tape-speed-sensitive FM decoder of the tape deck should be included, and interpolation of data and reference signal between sample points (for proper phase alignment relative to previous data sections) should be performed. Of course, if data acquisition did not have to go through this replay procedure with the tape machine (as with the use of a separate computer for data acquisition), these problems would disappear automatically. Hence, the software would remain much simpler.

Beyond the current methodology, we feel that importance lies in developing more rigorous dynamic models of the VER (not just a fixed matched filter), which make explicit use of the variability of the VER. The use of different stimulus conditions--possibly a superposition of two reversal rates at, e.g., 14 Hz and 17 Hz--may permit the identification of mechanisms which contribute to the variability of the VER. When a model for variability of components and their mutual relation can be developed, further reduction of uncertainty associated with the VER can be expected. From a philosophical point of view, feeding a more complex stimulus into the visual system (viz., 14 Hz and 17 Hz) might permit us to extract more information from the VER (provided the channel capacity of the system is not exceeded), and to surpass the results we were able to achieve so far in terms of reduced variability and/or necessary experimental measurement time.

REFERENCES

1. Beaumont, J. G., A. R. Mayes, and M. D. Rugg. Asymmetry in EEG alpha coherence and power: Effects of task and sex. *Electroencephalogr Clin Neurophysiol* 45: 93-101 (1978).
2. Ben-Dov, G., and A. Carmon. On time space and the cerebral hemispheres: A theoretical note. *Int J Neurosci* 7: 29-33 (1976).
3. Carmon, A. The two human hemispheres acting as separate parallel and sequential processors, pp. 219-233. In G. F. Inbar (ed.). *Proc. Int. Symp.*, Haifa, New York, Toronto: A Halsted Press Book, John Wiley & Sons, 1974.
4. Desmedt, J. E. Visual evoked potentials in man: New developments. Oxford: Clarendon Press, 1977.
5. Gustafson, D. E., J. S. Eterno, and W. Jarisch. Signal analysis techniques for interpreting electroencephalograms. SAM-TR-80-33, Dec 1980.
6. Jarisch, W., and K. Hsu. Signal analysis of visual evoked responses. 2nd Quarterly Progress Report, under USAF contract #F33615-81-C-0602, July 1981. (Unpublished)

APPENDIXES 1.1 - 4.2

APPENDIX 1.1: STATISTICS FOR FFT METHOD, CENTER ELECTRODE, NO STIMULUS--FOR FEMALE SUBJECT

\$ R REGMOD

LU OF DATA FILE

90

OF INDEPENDENT VARIABLES, E.G. 3

1

OF DIFFERENT STIMULUS CONDITIONS, E.G. 2

2

OF POINTS IN GROUP, E.G. 10

10

DJ

1

true value - contrast level of experiment

DJ

1

x

y

FFTDJAL

amplitude from
15 Hz FFT comp.

0.3903E+00	0.0000E+00
0.4905E+00	0.0000E+00
0.1176E+01	0.0000E+00
0.2819E+00	0.0000E+00
0.7652E+00	0.0000E+00
0.8057E+00	0.0000E+00
0.1412E+01	0.0000E+00
0.7720E+00	0.0000E+00
0.1250E+01	0.0000E+00
0.1124E+01	0.0000E+00
0.1980E+02	0.1000E+01
0.2174E+02	0.1000E+01
0.1963E+02	0.1000E+01
0.2050E+02	0.1000E+01
0.2073E+02	0.1000E+01
0.1798E+02	0.1000E+01
0.2043E+02	0.1000E+01
0.1967E+02	0.1000E+01
0.1958E+02	0.1000E+01
0.2067E+02	0.1000E+01

GIVE STIMULUS CONDITIONS, E.G. Y=1

0

REG-CONSTANT + COEFFICIENTS

-.044033138

.052005596

from regression analysis

SIG-Y/Y-BAR

Y-HAT =	-J.0440 +	0.0520 X1 +				
NSAMP = 1	Y-HAT = -0.0237	Y-BAR = -0.0217	SIG-Y = 0.0000	Y-SHARP = 0.0000		
NSAMP = 2	Y-HAT = -0.0185	Y-BAR = -0.0211	SIG-Y = 0.0037	Y-SHARP = -0.1744		
NSAMP = 3	Y-HAT = 0.0171	Y-BAR = -0.0084	SIG-Y = 0.0222	Y-SHARP = -2.6535		
NSAMP = 4	Y-HAT = -0.0294	Y-BAR = -0.0136	SIG-Y = 0.0210	Y-SHARP = -1.5388		
NSAMP = 5	Y-HAT = -0.0042	Y-BAR = -0.0118	SIG-Y = 0.0186	Y-SHARP = -1.5864		
NSAMP = 6	Y-HAT = -0.0021	Y-BAR = -0.0101	SIG-Y = 0.0171	Y-SHARP = -1.6881		
NSAMP = 7	Y-HAT = 0.0294	Y-BAR = -0.0045	SIG-Y = 0.0216	Y-SHARP = -4.8046		
NSAMP = 8	Y-HAT = -0.0039	Y-BAR = -0.0044	SIG-Y = 0.0200	Y-SHARP = -4.5260		
NSAMP = 9	Y-HAT = 0.0290	Y-BAR = -0.0016	SIG-Y = 0.0206	Y-SHARP = -12.8072		
NSAMP = 10	Y-HAT = 0.0144	Y-BAR = 0.0000	SIG-Y = 0.0200	Y-SHARP = *****		

\hat{y} given x

\bar{y}

$\sigma_y = \sqrt{(y-\bar{y})^2}$

current
estimates
plotted in
Figure 6.7

average
given the
past

estimate
given past
experiments

PREVIOUS PAGE
IS BLANK

APPENDIX 1.2: STATISTICS FOR FFT METHOD, CENTER ELECTRODE, WITH STIMULUS--FOR FEMALE SUBJECT

```

$ R REGMOD
LU OF DATA FILE
90
# OF INDEPENDENT VARIABLES, E.G. 3
1
# OF DIFFERENT STIMULUS CONDITIONS, E.G. 2
2
# OF POINTS IN GROUP, E.G. 10
10
DJ      1
DJ      1

```

x	y	
0.3903E+00	0.0000E+00	
0.4905E+00	0.0000E+00	
0.1176E+01	0.0000E+00	
0.2819E+00	0.0000E+00	
0.7652E+00	0.0000E+00	
0.8057E+00	0.0000E+00	
0.1412E+01	0.0000E+00	
0.7720E+00	0.0000E+00	
0.1250E+01	0.0000E+00	
0.1124E+01	0.0000E+00	
0.1980E+02	0.1000E+01	
0.2174E+02	0.1000E+01	
0.1963E+02	0.1000E+01	
0.2050E+02	0.1000E+01	
0.2073E+02	0.1000E+01	
0.1798E+02	0.1000E+01	
0.2043E+02	0.1000E+01	
0.1967E+02	0.1000E+01	
0.1958E+02	0.1000E+01	
0.2067E+02	0.1000E+01	

selected here the unit stimulus (~30% contrast)

GIVE STIMULUS CONDITIONS, E.G. Y=1

1

REG-CONSTANT + COEFFICIENTS

-.044033138 .052005596

Y-HAT =	-0.0440 +	0.0520 X1 +			
NSAMP = 1	Y-HAT = 0.9856	Y-BAR = 0.9856	SIG-Y = 0.0000	Y-SHARP = 0.0000	
NSAMP = 2	Y-HAT = 1.0868	Y-BAR = 1.0362	SIG-Y = 0.0715	Y-SHARP = 0.0690	
NSAMP = 3	Y-HAT = 0.9771	Y-BAR = 1.0165	SIG-Y = 0.0610	Y-SHARP = 0.0600	
NSAMP = 4	Y-HAT = 1.0222	Y-BAR = 1.0179	SIG-Y = 0.0499	Y-SHARP = 0.0490	
NSAMP = 5	Y-HAT = 1.0342	Y-BAR = 1.0212	SIG-Y = 0.0438	Y-SHARP = 0.0429	
NSAMP = 6	Y-HAT = 0.8913	Y-BAR = 0.9995	SIG-Y = 0.0659	Y-SHARP = 0.0660	
NSAMP = 7	Y-HAT = 1.0184	Y-BAR = 1.0022	SIG-Y = 0.0606	Y-SHARP = 0.0605	
NSAMP = 8	Y-HAT = 0.9790	Y-BAR = 0.9993	SIG-Y = 0.0567	Y-SHARP = 0.0568	
NSAMP = 9	Y-HAT = 0.9744	Y-BAR = 0.9965	SIG-Y = 0.0537	Y-SHARP = 0.0539	
NSAMP = 10	Y-HAT = 1.0311	Y-BAR = 1.0000	SIG-Y = 0.0518	Y-SHARP = 0.0518	

y given x y σ_y relative variability
current estimates σ/y
plotted in Figure 6.7

APPENDIX 1.3: STATISTICS FOR FFT METHOD, CENTER ELECTRODE, NO STIMULUS--FOR MALE SUBJECT

\$ R REGMOD
LU OF DATA FILE
90

OF INDEPENDENT VARIABLES, E.G. 3

1

OF DIFFERENT STIMULUS CONDITIONS, E.G. 2

2

OF POINTS IN GROUP, E.G. 10

10

KJ

1

KJ

1

FFTKJAI

x	y
0.3026E+00	0.0000E+00
0.8686E-01	0.0000E+00
0.5277E+00	0.0000E+00
0.3045E+00	0.0000E+00
0.3095E+00	0.0000E+00
0.1950E+00	0.0000E+00
0.2368E+00	0.0000E+00
0.9807E-01	0.0000E+00
0.3344E+00	0.0000E+00
0.2404E+00	0.0000E+00
0.1791E+01	0.1000E+00
0.1549E+01	0.1000E+01
0.2016E+01	0.1000E+01
0.2309E+01	0.1000E+01
0.1937E+01	0.1000E+01
0.2511E+01	0.1000E+01
0.2592E+01	0.1000E+01
0.2167E+01	0.1000E+01
0.2611E+01	0.1000E+01
0.1477E+01	0.1000E+01

selected

GIVE STIMULUS CONDITION, E.G. Y = 1,

0

REG-CONSTANT + COEFFICIENTS

-0.14385505 0.54573237

Y-HAT =	-0.1439 +	0.5457 X1 +		
NSAMP = 1	Y-HAT = 0.0213	Y-BAR = 0.0213	SIG-Y = 0.0000	Y-SHARP = 0.0000
NSAMP = 2	Y-HAT = -0.0965	Y-BAR = -0.376	SIG-Y = 0.0832	Y-SHARP = -2.2141
NSAMP = 3	Y-HAT = 0.1441	Y-BAR = 0.0230	SIG-Y = 0.1203	Y-SHARP = 5.2365
NSAMP = 4	Y-HAT = 0.0223	Y-BAR = 0.0228	SIG-Y = 0.0982	Y-SHARP = 4.3072
NSAMP = 5	Y-HAT = 0.0250	Y-BAR = 0.233	SIG-Y = 0.0851	Y-SHARP = 3.6584
NSAMP = 6	Y-HAT = -0.0374	Y-BAR = 0.0131	SIG-Y = 0.0800	Y-SHARP = 6.0894
NSAMP = 7	Y-HAT = -0.0146	Y-BAR = 0.0092	SIG-Y = 0.0738	Y-SHARP = 8.0446
NSAMP = 8	Y-HAT = -0.0903	Y-BAR = -0.0033	SIG-Y = 0.0768	Y-SHARP = -23.5287
NSAMP = 9	Y-HAT = 0.0386	Y-BAR = 0.0014	SIG-Y = 0.0732	Y-SHARP = 52.7674
NSAMP = 10	Y-HAT = -0.0126	Y-BAR = 0.0000	SIG-Y = 0.0692	Y-SHARP = -4768.6792

^
y
current
estimates
plotted in
Figure 6.8

APPENDIX 1.4: STATISTICS FOR FFT METHOD, CENTER ELECTRODE, WITH STIMULUS--FOR MALE SUBJECT

\$ R REGMOD
LU OF DATA FILE

90

OF INDEPENDENT VARIABLES, E.G. 3

1

OF DIFFERENT STIMULUS CONDITIONS, E.G. 2

2

OF POINTS IN GROUP, E.G. 10

10

KJ

1

KJ

1

x	y
0.3026E+00	0.0000E+00
0.8686E-01	0.0000E+00
0.5277E+00	0.0000E+00
0.3045E+00	0.0000E+00
0.3095E+00	0.0000E+00
0.1950E+00	0.0000E+00
0.2368E+00	0.0000E+00
0.9807E-01	0.0000E+00
0.3344E+00	0.0000E+00
0.2404E+00	0.0000E+00
0.1791E+01	0.1000E+00
0.1549E+01	0.1000E+01
0.2016E+01	0.1000E+01
0.2309E+01	0.1000E+01
0.1937E+01	0.1000E+01
0.2511E+01	0.1000E+01
0.2592E+01	0.1000E+01
0.2167E+01	0.1000E+01
0.7611E+01	0.1000E+01
0.1477E+01	0.1000E+01

selected

GIVE STIMULUS CONDITION, E.G. Y = 1,

1

REG-CONSTANT + COEFFICIENTS

-0.14385505 0.54573237

Y-HAT =	-0.1439 +	0.5457 X1 +			
NSAMP = 1	Y-HAT = 0.8337	Y-BAR = 0.8337	SIG-Y = 0.0000	Y-SHARP = 0.0000	
NSAMP = 2	Y-HAT = 0.7017	Y-BAR = 0.7677	SIG-Y = 0.0934	Y-SHARP = 0.1216	
NSAMP = 3	Y-HAT = 0.9565	Y-BAR = 0.8306	SIG-Y = 0.1274	Y-SHARP = 0.1534	
NSAMP = 4	Y-HAT = 1.1161	Y-BAR = 0.9020	SIG-Y = 1.766	Y-SHARP = 0.1958	
NSAMP = 5	Y-HAT = 0.9130	Y-BAR = 0.9042	SIG-Y = 0.1530	Y-SHARP = 0.1693	
NSAMP = 6	Y-HAT = 1.2268	Y-BAR = 0.9580	SIG-Y = 0.1899	Y-SHARP = 0.1983	
NSAMP = 7	Y-HAT = 1.2708	Y-BAR = 1.0027	SIG-Y = 0.2099	Y-SHARP = 0.2093	
NSAMP = 8	Y-HAT = 1.0386	Y-BAR = 1.0072	SIG-Y = 0.1947	Y-SHARP = 0.1933	
NSAMP = 9	Y-HAT = 1.2811	Y-BAR = 1.0376	SIG-Y = 0.2037	Y-SHARP = 0.1964	
NSAMP = 10	Y-HAT = 0.6619	Y-BAR = 1.0000	SIG-Y = 0.2259	Y-SHARP = 0.2259	

^
y
current
estimates
plotted in
Figure 6.8

APPENDIX 2.1: STATISTICS FOR MATCHED FILTER METHOD, CENTER ELECTRODE, NO STIMULUS--FOR FEMALE SUBJECT

LUROREGMOD FILE

90

OF INDEPENDENT VARIABLES, E.G. 3

3

OF DIFFERENT STIMULUS CONDITIONS, E.G. 2

2

OF POINTS IN GROUP, E.G. 10

VERDJI

10

TEMP1D.OUT 1
TEMP2D.OUT 2
TEMP3D.OUT 3
TEMP1D.OUT 1
TEMP2D.OUT 2
TEMP3D.OUT 3

stimulus condition

x_1	x_2	x_3	y
0.9931E-03	0.6960E-01	0.3915E-01	0.0000E+00
0.3194E-01	0.6296E-01	0.1829E-02	0.0000E+00
0.6406E-01	-0.8106E-02	-0.1875E+00	0.0000E+00
0.2677E-02	0.2856E-01	0.2438E+00	0.0000E+00
0.3547E-01	0.1780E-01	-0.1254E+00	0.0000E+00
0.3902E-01	-0.3840E-01	-0.4314E-01	0.0000E+00
0.1096E+00	0.6040E-01	-0.8432E-01	0.0000E+00
0.4794E-01	0.3290E-01	-0.6859E-01	0.0000E+00
0.4677E-01	0.1066E+00	0.1987E+00	0.0000E+00
0.1385E-01	0.5961E-01	0.9772E-01	0.0000E+00
0.1941E+01	0.2001E+01	0.1639E+01	0.1000E+01
0.2072E+01	0.2103E+01	0.1995E+01	0.1000E+01
0.1939E+01	0.2029E+01	0.1860E+01	0.1000E+01
0.2014E+01	0.2056E+01	0.1869E+01	0.1000E+01
0.2068E+01	0.2039E+01	0.1986E+01	0.1000E+01
0.1826E+01	0.1993E+01	0.1806E+01	0.1000E+01
0.2012E+01	0.1916E+01	0.1671E+01	0.1000E+01
0.1987E+01	0.1933E+01	0.2117E+01	0.1000E+01
0.1934E+01	0.1965E+01	0.2377E+01	0.1000E+01
0.2024E+01	0.2081E+01	0.2496E+01	0.1000E+01

selected

the x_i 's are the
endpoint estimates from
the matched filter output

GIVE STIMULUS CONDITION, E.G. Y=1

0

REG-CONSTANT + COEFFICIENTS

-.02019 .5148 0 0

neglected

Y-HAT =	-0.0202 +	0.5148 x_1 +	0.0000 x_2 +	0.0000 x_3 +
NSAMP = 1	Y-HAT = -0.0197	Y-BAR = -0.0197	SIG-Y = 0.0000	Y-SHARP = 0.0000
NSAMP = 2	Y-HAT = -0.0037	Y-BAR = -0.0117	SIG-Y = 0.0113	Y-SHARP = -0.9618
NSAMP = 3	Y-HAT = 0.0128	Y-BAR = -0.0035	SIG-Y = 0.0162	Y-SHARP = -4.5775
NSAMP = 4	Y-HAT = -0.0188	Y-BAR = -0.0074	SIG-Y = 0.0153	Y-SHARP = -2.0774
NSAMP = 5	Y-HAT = -0.0019	Y-BAR = -0.0063	SIG-Y = 0.0135	Y-SHARP = -2.1459
NSAMP = 6	Y-HAT = -0.0001	Y-BAR = -0.0052	SIG-Y = 0.0123	Y-SHARP = -2.3454
NSAMP = 7	Y-HAT = 0.0362	Y-BAR = 0.0007	SIG-Y = 0.0193	Y-SHARP = 28.3809
NSAMP = 8	Y-HAT = 0.0045	Y-BAR = 0.0012	SIG-Y = 0.0179	Y-SHARP = 15.4908
NSAMP = 9	Y-HAT = 0.0039	Y-BAR = 0.0015	SIG-Y = 0.0168	Y-SHARP = 11.4932
NSAMP = 10	Y-HAT = -0.0131	Y-BAR = 0.0000	SIG-Y = 0.0165	Y-SHARP = 2069.2251

\hat{y} given x_1
plotted in Figure 6.7

APPENDIX 2.2: STATISTICS FOR MATCHED FILTER METHOD, CENTER ELECTRODE, WITH STIMULUS--FOR FEMALE SUBJECT

R REGMOD
LU OF DATA FILE
90

OF INDEPENDENT VARIABLES, E.G. 3

3

OF DIFFERENT STIMULUS CONDITIONS, E.G. 2

2

OF POINTS IN GROUP, E.G. 10

10

TEMP1D.OUT 1
TEMP2D.OUT 2
TEMP3D.OUT 3
TEMP1D.OUT 1
TEMP2D.OUT 2
TEMP3D.OUT 3

VERDJ1

x_1	x_2	x_3	y
0.9931E-03	0.6960E-01	0.3915E-01	0.0000E+00
0.3194E-01	0.6296E-01	0.1829E-02	0.0000E+00
0.6406E-01	-0.8106E-02	-0.1875E+00	0.0000E+00
0.2677E-02	0.2856E-01	0.2438E+00	0.0000E+00
0.3547E-01	0.1780E-01	-0.1254E+00	0.0000E+00
0.3902E-01	-0.3840E-01	-0.4314E-01	0.0000E+00
0.1096E+00	0.6040E-01	-0.8432E-01	0.0000E+00
0.4794E-01	0.3290E-01	-0.6859E-01	0.0000E+00
0.4677E-01	0.1066E+00	0.1987E+00	0.0000E+00
0.1385E-01	0.5961E-01	0.9772E-01	0.0000E+00
0.1941E+01	0.2001E+01	0.1639E+01	0.1000E+01
0.2072E+01	0.2103E+01	0.1995E+01	0.1000E+01
0.1939E+01	0.2029E+01	0.1860E+01	0.1000E+01
0.2014E+01	0.2056E+01	0.1869E+01	0.1000E+01
0.2068E+01	0.2039E+01	0.1986E+01	0.1000E+01
0.1826E+01	0.1993E+01	0.1806E+01	0.1000E+01
0.2012E+01	0.1916E+01	0.1671E+01	0.1000E+01
0.1987E+01	0.1933E+01	0.2117E+01	0.1000E+01
0.1934E+01	0.1965E+01	0.2377E+01	0.1000E+01
0.2024E+01	0.2081E+01	0.2496E+01	0.1000E+01

the x_i 's are the
endpoint estimates from
the matched filter output

selected

GIVE STIMULUS CONDITION, E.G. Y=1

1
REG-CONSTANT + COEFFICIENTS
-.02019 .5148 0 0

		neglected			
Y-HAT =	-0.0202 +	0.5148 X1 +	0.0000 X2 +	0.0000 X3 +	
NSAMP = 1	Y-HAT = 0.9791	Y-BAR = 0.9791	SIG-Y = 0.0000	Y-SHARP =	0.0000
NSAMP = 2	Y-HAT = 1.0465	Y-BAR = 1.0128	SIG-Y = 0.0476	Y-SHARP =	0.0470
NSAMP = 3	Y-HAT = 0.9778	Y-BAR = 1.0012	SIG-Y = 0.0393	Y-SHARP =	0.0392
NSAMP = 4	Y-HAT = 1.0166	Y-BAR = 1.0050	SIG-Y = 0.0330	Y-SHARP =	0.0328
NSAMP = 5	Y-HAT = 1.0445	Y-BAR = 1.0129	SIG-Y = 0.0336	Y-SHARP =	0.0332
NSAMP = 6	Y-HAT = 0.9199	Y-BAR = 0.9974	SIG-Y = 0.0484	Y-SHARP =	0.0486
NSAMP = 7	Y-HAT = 1.0154	Y-BAR = 1.0000	SIG-Y = 0.0447	Y-SHARP =	0.0447
NSAMP = 8	Y-HAT = 1.0028	Y-BAR = 1.0003	SIG-Y = 0.0414	Y-SHARP =	0.0414
NSAMP = 9	Y-HAT = 0.9756	Y-BAR = 0.9976	SIG-Y = 0.0396	Y-SHARP =	0.0397
NSAMP = 10	Y-HAT = 1.0217	Y-BAR = 1.0000	SIG-Y = 0.0381	Y-SHARP =	0.0381

^
y given x_1
plotted in Figure 6.7

APPENDIX 2.3: STATISTICS FOR MATCHED FILTER METHOD, CENTER ELECTRODE, NO STIMULUS--FOR MALE SUBJECT

```

$ R REGMOD
LU OF DATA FILE
90
# OF INDEPENDENT VARIABLES, E.G. 3
3
# OF DIFFERENT STIMULUS CONDITIONS, E.G. 2
2
# OF POINTS IN GROUP, E.G. 10
10
TEMP1K.OUT      1
TEMP2K.OUT      2
TEMP3K.OUT      3
TEMP1K.OUT      1
TEMP2K.OUT      2
TEMP3K.OUT      3

```

VERKJ1

x ₁	x ₂	x ₃	y
0.1864E+01	0.1881E+01	0.1748E+01	0.1000E+01
0.1699E+01	0.2101E+01	0.2152E+01	0.1000E+01
0.1713E+01	0.1763E+01	0.1920E+01	0.1000E+01
0.1965E+01	0.2074E+01	0.1985E+01	0.1000E+01
0.1672E+01	0.1302E+01	0.1936E+01	0.1000E+01
0.2297E+01	0.2983E+01	0.1990E+01	0.1000E+01
0.1999E+01	0.1824E+01	0.2178E+01	0.1000E+01
0.1763E+01	0.1483E+01	0.1953E+01	0.1000E+01
0.2073E+01	0.2428E+01	0.1824E+01	0.1000E+01
0.1558E+01	0.1715E+01	0.1882E+01	0.1000E+01
-0.1849E+01	0.1645E+00	0.2773E-01	0.0000E+00
0.2925E-01	0.2912E+00	-0.2559E+00	0.0000E+00
0.6134E-01	-0.1876E-01	-0.2101E-01	0.0000E+00
-0.7798E-01	0.2049E-01	-0.7963E-01	0.0000E+00
-0.8653E-01	-0.6413E-01	-0.7649E-01	0.0000E+00
0.1701E+00	-0.9510E+00	-0.633E+00	0.0000E+00
0.1413E+00	0.3667E+00	0.1326E+00	0.0000E+00
0.1007E+00	-0.1195E+00	-0.1432E+00	0.0000E+00
0.2050E+00	0.2188E+00	0.5784E-02	0.0000E+00
-0.6515E-01	-0.1447E+00	0.2094E-01	0.0000E+00

selected

GIVE STIMULUS CONDITION, E.G. Y=1

0

REG-CONSTANT + COEFFICIENTS

-.02535 .55115 0 0

neglected

Y-HAT =	-0.0254 +	0.5512 X1 +	0.0000 X2 +	0.0000 X3 +
NSAMP = 1	Y-HAT = -0.0355	Y-BAR = -0.0355	SIG-Y = 0.0000	Y-SHARP = 0.0000
NSAMP = 2	Y-HAT = -0.0092	Y-BAR = -0.0224	SIG-Y = 0.0186	Y-SHARP = -0.8312
NSAMP = 3	Y-HAT = 0.0085	Y-BAR = -0.0121	SIG-Y = 0.0221	Y-SHARP = -1.8292
NSAMP = 4	Y-HAT = -0.0683	Y-BAR = -0.0262	SIG-Y = 0.0334	Y-SHARP = -1.2777
NSAMP = 5	Y-HAT = -0.0730	Y-BAR = -0.0355	SIG-Y = 0.0357	Y-SHARP = -1.0058
NSAMP = 6	Y-HAT = 0.0684	Y-BAR = -0.0182	SIG-Y = 0.0531	Y-SHARP = -2.9174
NSAMP = 7	Y-HAT = 0.0525	Y-BAR = -0.0081	SIG-Y = 0.0554	Y-SHARP = -6.8311
NSAMP = 8	Y-HAT = 0.0302	Y-BAR = -0.0033	SIG-Y = 0.0530	Y-SHARP = -15.9608
NSAMP = 9	Y-HAT = 0.0877	Y-BAR = 0.0068	SIG-Y = 0.0581	Y-SHARP = 8.5662
NSAMP = 10	Y-HAT = -0.0613	Y-BAR = 0.0000	SIG-Y = 0.0589	Y-SHARP = -3349.4158

ŷ given x₁

plotted in Figure 6.8

APPENDIX 2.4: STATISTICS FOR MATCHED FILTER METHOD, CENTER ELECTRODE, WITH STIMULUS--FOR MALE SUBJECT

```

$ R REGMOD
LU OF DATA FILE
90
# OF INDEPENDENT VARIABLES, E.G. 3
3Y
# OF DIFFERENT STIMULUS CONDITIONS, E.G. 2
2
# OF POINTS IN GROUP, E.G. 10
10
TEMP1K.OUT      1
TEMP2K.OUT      2
TEMP3K.OUT      3
TEMP1K.OUT      1
TEMP2K.OUT      2
TEMP3K.OUT      3

```

VERKJ1

x_1	x_2	x_3	y	
0.1864E+01	0.1881E+01	0.1748E+01	0.1000E+01	selected
0.1699E+01	0.2101E+01	0.2152E+01	0.1000E+01	
0.1713E+01	0.1763E+01	0.1920E+01	0.1000E+01	
0.1965E+01	0.2074E+01	0.1985E+01	0.1000E+01	
0.1672E+01	0.1302E+01	0.1936E+01	0.1000E+01	
0.2297E+01	0.2983E+01	0.1990E+01	0.1000E+01	
0.1999E+01	0.1824E+01	0.2178E+01	0.1000E+01	
0.1763E+01	0.1483E+01	0.1953E+01	0.1000E+01	
0.2073E+01	0.2428E+01	0.1824E+01	0.1000E+01	
0.1558E+01	0.1715E+01	0.1882E+01	0.1000E+01	
-0.1849E+01	0.1645E+00	0.2773E-01	0.0000E+00	
0.2925E-01	0.2912E+00	-0.2559E+00	0.0000E+00	
0.6134E-01	-0.1876E-01	-0.2101E-01	0.0000E+00	
-0.7798E-01	0.2049E-01	-0.7963E-01	0.0000E+00	
-0.8653E-01	-0.6413E-01	-0.7649E-01	0.0000E+00	
0.1701E+00	-0.9510E+00	-0.633E+00	0.0000E+00	
0.1413E+00	0.3667E+00	0.1326E+00	0.0000E+00	
0.1007E+00	-0.1195E+00	-0.1432E+00	0.0000E+00	
0.2050E+00	0.2188E+00	0.5784E-02	0.0000E+00	
-0.6515E-01	-0.1447E+00	0.094E-01	0.0000E+00	

GIVE STIMULUS CONDITION, E.G. Y=1

1
REG-CONSTANT + COEFFICIENTS
-.02535 .55115 0 0

neglected

	$-0.0254 +$	$0.5512 X_1 +$	$0.0000 X_2 +$	$0.0000 X_3 +$	
NSAMP = 1	Y-HAT = 1.0023	Y-BAR = 1.0023	SIG-Y = 0.0000	Y-SHARP = 0.0000	
NSAMP = 2	Y-HAT = 0.9110	Y-BAR = 0.9566	SIG-Y = 0.0646	Y-SHARP = 0.0675	
NSAMP = 3	Y-HAT = 0.9188	Y-BAR = 0.9440	SIG-Y = 0.0506	Y-SHARP = 0.0536	
NSAMP = 4	Y-HAT = 1.0576	Y-BAR = 0.9724	SIG-Y = 0.0702	Y-SHARP = 0.0722	
NSAMP = 5	Y-HAT = 0.8964	Y-BAR = 0.9572	SIG-Y = 0.0697	Y-SHARP = 0.0728	
NSAMP = 6	Y-HAT = 1.2405	Y-BAR = 1.0044	SIG-Y = 0.1314	Y-SHARP = 0.1308	
NSAMP = 7	Y-HAT = 1.0766	Y-BAR = 1.0147	SIG-Y = 0.1230	Y-SHARP = 0.1212	
NSAMP = 8	Y-HAT = 0.9463	Y-BAR = 1.0062	SIG-Y = 0.1164	Y-SHARP = 0.1157	
NSAMP = 9	Y-HAT = 1.1173	Y-BAR = 1.0185	SIG-Y = 0.1150	Y-SHARP = 0.1129	
NSAMP = 10	Y-HAT = 0.8335	Y-BAR = 1.0000	SIG-Y = 0.1232	Y-SHARP = 0.1232	

^
y given x_1
plotted in Figure 6.8

APPENDIX 3.1: STATISTICS FOR MATCHED FILTERS, ALL ELECTRODES, BOTH STIMULI--FOR FEMALE SUBJECT

TEMP1D.OUT 1
TEMP2D.OUT 2
TEMP3D.OUT 3
TEMP1D.OUT 1
TEMP2D.OUT 2
TEMP3D.OUT 3

x_1	x_2	x_3	y
0.9931E-03	0.6960E-01	0.3915E-01	0.0000E+00
0.3194E-01	0.6296E-01	0.1829E-02	0.0000E+00
0.6406E-01	-0.8106E-02	-0.1875E+00	0.0000E+00
0.2677E-02	0.2856E-01	0.2138E+00	0.0000E+00
0.3547E-01	0.1780E-01	-0.1254E+00	0.0000E+00
0.3902E-01	-0.3840E-01	-0.4314E-01	0.0000E+00
0.1096E+00	0.6040E-01	-0.8432E-01	0.0000E+00
0.4794E-01	0.3290E-01	-0.6859E-01	0.0000E+00
0.4677E-01	0.1066E+00	0.1987E+00	0.0000E+00
0.1385E-01	0.5961E-01	0.9772E-01	0.0000E+00
0.1941E+01	0.2001E+01	0.1639E+01	0.1000E+01
0.2072E+01	0.2103E+01	0.1995E+01	0.1000E+01
0.1939E+01	0.2029E+01	0.1860E+01	0.1000E+01
0.2014E+01	0.2056E+01	0.1869E+01	0.1000E+01
0.2068E+01	0.2039E+01	0.1986E+01	0.1000E+01
0.1826E+01	0.1993E+01	0.1806E+01	0.1000E+01
0.2012E+01	0.1916E+01	0.1671E+01	0.1000E+01
0.1987E+01	0.1933E+01	0.2117E+01	0.1000E+01
0.1934E+01	0.1965E+01	0.2377E+01	0.1000E+01
0.2024E+01	0.2081E+01	0.2496E+01	0.1000E+01

VERDJ123

GIVE STIMULUS CONDITION, E.G. Y=1
0

REG-CONSTANT + COEFFICIENTS constant response in
left hemisphere-important

model values → -0.0198 .1736 .3332 -.0078

Y-HAT =	-0.0198 +	0.1736 X1 +	0.3332 X2 +	-0.0078 X3 +
NSAMP = 1	Y-HAT = 0.0033	Y-BAR = 0.0033	SIG-Y = 0.0000	Y-SHARP = 0.0000
NSAMP = 2	Y-HAT = 0.0067	Y-BAR = 0.0050	SIG-Y = 0.0024	Y-SHARP = 0.4894
NSAMP = 3	Y-HAT = -0.0099	Y-BAR = 0.0000	SIG-Y = 0.0088	Y-SHARP = 544.2001
NSAMP = 4	Y-HAT = -0.0117	Y-BAR = -0.0029	SIG-Y = 0.0093	Y-SHARP = -3.1736
NSAMP = 5	Y-HAT = -0.0067	Y-BAR = -0.0037	SIG-Y = 0.0082	Y-SHARP = -2.2275
NSAMP = 6	Y-HAT = -0.0255	Y-BAR = -0.0073	SIG-Y = 0.0115	Y-SHARP = -1.5767
NSAMP = 7	Y-HAT = 0.0200	Y-BAR = -0.0034	SIG-Y = 0.0147	Y-SHARP = -4.3235
NSAMP = 8	Y-HAT = 0.0000	Y-BAR = -0.0030	SIG-Y = 0.0137	Y-SHARP = -4.5969
NSAMP = 9	Y-HAT = 0.0223	Y-BAR = -0.0002	SIG-Y = 0.0153	Y-SHARP = -87.7774
NSAMP = 10	Y-HAT = 0.0017	Y-BAR = 0.0000	SIG-Y = 0.0145	Y-SHARP = 1107.8656

no stimulus

TERMINATE = -1, SAME FILE = 0, NEW FILE = 1

GIVE STIMULUS CONDITION, E.G. Y=1

1

y given x

Y-HAT =	Y-BAR =	SIG-Y =	Y-SHARP =
NSAMP = 1	Y-HAT = 0.9711	Y-BAR = 0.9711	SIG-Y = 0.0000
NSAMP = 2	Y-HAT = 1.0252	Y-BAR = 0.9981	SIG-Y = 0.0383
NSAMP = 3	Y-HAT = 0.9782	Y-BAR = 0.9915	SIG-Y = 0.0294
NSAMP = 4	Y-HAT = 1.0001	Y-BAR = 0.9937	SIG-Y = 0.0244
NSAMP = 5	Y-HAT = 1.0033	Y-BAR = 0.9956	SIG-Y = 0.0216
NSAMP = 6	Y-HAT = 0.9472	Y-BAR = 0.9875	SIG-Y = 0.0276
NSAMP = 7	Y-HAT = 0.9547	Y-BAR = 0.9828	SIG-Y = 0.0281
NSAMP = 8	Y-HAT = 0.9528	Y-BAR = 0.9791	SIG-Y = 0.0281
NSAMP = 9	Y-HAT = 0.9522	Y-BAR = 0.9761	SIG-Y = 0.0278
NSAMP = 10	Y-HAT = 1.0055	Y-BAR = 0.9790	SIG-Y = 0.0278

stimulus

TERMINATE = -1, SAME FILE = 0, NEW FILE = 1

-1
X-SC 1.000000 5.000000
Y-SC -1.000000 1.000000
O.K. = 1
0

APPENDIX 3.2 (Cont'd.)

```

RLMUL IER =      0
      DF      DF-RES  DF-TOT    SS-REG    SS-RES    SS-TOT    MS-REG
3.0000 26.0000 29.0000 0.6660E+01 0.6952E-02 0.6667E+01 0.2220E+01
      MS-RES      F-VALUE    P-EXC HO %-EXPL  STDV-RES  %-R-MEAN  OK=4
0.2674E-03 0.8303E+04 0.0000 99.8957 0.1635E-01 0.4906E+01 4.0000

```

```

B-MATRIX
REG-COEFF      L-LIM      U-LIM      STDV-ERR      PART-F-VALUE      P-EXC HO
0.1736E+00 0.2250E-01 0.3248E+00 0.7353E-01 0.1491E-02 0.5577E+01
0.3332E+00 0.1829E+00 0.4836E+00 0.7315E-01 0.5548E-02 0.2075E+02
-0.7805E-02 -0.4906E-01 0.3345E-01 0.2007E-01 0.4044E-04 0.1512E+00
0.3476E-03 -0.7167E-02 0.7862E-02 0.3656E-02 0.0000E+00 0.0000E+00

```

```

VARB
0.2022E+02
-0.1936E+02 0.2002E+02
-0.5575E+00 -0.9352E+00 0.1506E+01

```

```

Y-HAT = 0.0003 + 0.1736 X1 + 0.3332 X2 + -0.0078 X3 +
          may be slightly      model values used
          readjusted

```

APPENDIX 3.3: STATISTICS FOR MATCHED FILTERS, ALL ELECTRODES, BOTH STIMULI--FOR MALE SUBJECT

TEMP1K.OUT 1
TEMP2K.OUT 2
TEMP3K.OUT 3
TEMP1K.OUT 1
TEMP2K.OUT 2
TEMP3K.OUT 3

x ₁	x ₂	x ₃	y
0.1864E+01	0.1881E+01	0.1748E+01	0.1000E+01
0.1699E+01	0.2101E+01	0.2152E+01	0.1000E+01
0.1713E+01	0.1763E+01	0.1920E+01	0.1000E+01
0.1965E+01	0.2074E+01	0.1985E+01	0.1000E+01
0.1672E+01	0.1302E+01	0.1936E+01	0.1000E+01
0.2297E+01	0.2983E+01	0.1990E+01	0.1000E+01
0.1999E+01	0.1824E+01	0.2178E+01	0.1000E+01
0.1763E+01	0.1483E+01	0.1953E+01	0.1000E+01
0.2073E+01	0.2428E+01	0.1824E+01	0.1000E+01
0.1558E+01	0.1715E+01	0.1882E+01	0.1000E+01
-0.1849E+01	0.1645E+00	0.2773E-01	0.0000E+00
0.2925E-01	0.2912E+00	-0.2559E+00	0.0000E+00
0.6134E-01	-0.1876E-01	-0.2101E-01	0.0000E+00
-0.7798E-01	0.2049E-01	-0.7963E-01	0.0000E+00
-0.8653E-01	-0.6413E-01	-0.7649E-01	0.0000E+00
0.1701E+00	-0.9510E+00	-0.2633E+00	0.0000E+00
0.1413E+00	0.3667E+00	0.1326E+00	0.0000E+00
0.1007E+00	-0.1195E+00	-0.1432E+00	0.0000E+00
0.2050E+00	0.2188E+00	0.5784E-02	0.0000E+00
-0.6515E-01	-0.1447E+00	0.2094E-01	0.0000E+00

VERKJ123

GIVE STIMULUS CONDITION, E.G. Y=1

0
REG-CONSTANT + COEFFICIENTS
0.0133 0.2077 -0.0550 0.3662

constant response in right hemisphere - important

model values	Y-HAT	Y-BAR	SIG-Y	Y-SHARP
NSAMP = 1	0.0133	0.0106	0.0106	0.0000
NSAMP = 2	-0.0903	-0.0399	0.0714	-1.7889
NSAMP = 3	0.0194	-0.0201	0.0610	-3.0281
NSAMP = 4	-0.0359	-0.0241	0.0504	-2.0928
NSAMP = 5	-0.0292	-0.0251	0.0437	-1.7415
NSAMP = 6	0.0045	-0.0202	0.0409	-2.0300
NSAMP = 7	0.0710	-0.0071	0.0508	-7.1292
NSAMP = 8	-0.0116	-0.0077	0.0471	-6.1200
NSAMP = 9	0.0460	-0.0017	0.0475	-27.4603
NSAMP = 10	0.0154	0.0000	0.0451	-2442.5129

no stimulus

TERMINATE = -1, SAME FILE = 0, NEW FILE = 1

0
GIVE STIMULUS CONDITION, E.G. Y=1

model values	Y-HAT	Y-BAR	SIG-Y	Y-SHARP
NSAMP = 1	0.9373	0.9373	0.0000	0.0725
NSAMP = 2	1.0385	0.9879	0.0716	0.0520
NSAMP = 3	0.9753	0.9837	0.0512	0.0490
NSAMP = 4	1.0341	0.9963	0.0488	0.0424
NSAMP = 5	0.9978	0.9966	0.0423	0.0444
NSAMP = 6	1.0549	1.0063	0.0447	0.0595
NSAMP = 7	1.1260	1.0234	0.0609	0.0553
NSAMP = 8	1.0132	1.0221	0.0565	0.0539
NSAMP = 9	0.9783	1.0173	0.0548	0.0578
NSAMP = 10	0.9318	1.0087	0.0583	

stimulus

TERMINATE = -1, SAME FILE = 0, NEW FILE = 1

-1
X-SC 1.000000 5.000000
Y-SC -1.000000 1.000000
O.K.=1
0

APPENDIX 3.4: EXAMPLE OF AUGMENTING DATA FOR APPROXIMATE MAXIMUM
LIKELIHOOD ESTIMATION, ALL CHANNELS--FOR MALE SUBJECT

```
# OF INDEPENDENT VARIABLES, E.G. 3
3
# OF DIFFERENT STIMULUS CONDITIONS, E.G. 2
3
# OF POINTS IN GROUP, E.G. 10                                regress KJ
10
TEMP1K.OUT              1
TEMP2K.OUT              2
TEMP3K.OUT              3
EMP00                   0
EMP00                   0
EMP00                   0
EMP00                   0
EMP00                   0
EMP00                   0
EMP00                   0
0.1864E+01   0.1881E+01   0.1748E+01   0.1000E+01
0.1699E+01   0.2101E+01   0.2152E+01   0.1000E+01
0.1713E+01   0.1763E+01   0.1920E+01   0.1000E+01
0.1965E+01   0.2074E+01   0.1985E+01   0.1000E+01
0.1672E+01   0.1302E+01   0.1936E+01   0.1000E+01
0.2297E+01   0.2983E+01   0.1990E+01   0.1000E+01
0.1999E+01   0.1824E+01   0.2178E+01   0.1000E+01
0.1763E+01   0.1483E+01   0.1953E+01   0.1000E+01
0.2073E+01   0.2428E+01   0.1824E+01   0.1000E+01
0.1558E+01   0.1715E+01   0.1882E+01   0.1000E+01
0.0000E+00   0.0000E+00   0.0000E+00   0.0000E+00
0.0000E+00   0.0000E+00   0.0000E+00   0.0000E+00
0.0000E+00   0.0000E+00   0.0000E+00   0.0000E+00
0.0000E+00   0.0000E+00   0.0000E+00   0.0000E+00
0.0000E+00   0.0000E+00   0.0000E+00   0.0000E+00
0.0000E+00   0.0000E+00   0.0000E+00   0.0000E+00
0.0000E+00   0.0000E+00   0.0000E+00   0.0000E+00
0.0000E+00   0.0000E+00   0.0000E+00   0.0000E+00
0.0000E+00   0.0000E+00   0.0000E+00   0.0000E+00
0.0000E+00   0.0000E+00   0.0000E+00   0.0000E+00
0.0000E+00   0.0000E+00   0.0000E+00   0.0000E+00
0.0000E+00   0.0000E+00   0.0000E+00   0.0000E+00
0.0000E+00   0.0000E+00   0.0000E+00   0.0000E+00
0.0000E+00   0.0000E+00   0.0000E+00   0.0000E+00
0.0000E+00   0.0000E+00   0.0000E+00   0.0000E+00
0.0000E+00   0.0000E+00   0.0000E+00   0.0000E+00
0.0000E+00   0.0000E+00   0.0000E+00   0.0000E+00
0.0000E+00   0.0000E+00   0.0000E+00   0.0000E+00
0.0000E+00   0.0000E+00   0.0000E+00   0.0000E+00
SIGNIFICANCE ALFA, E.G..05
.05
BECOVN IER =          0
A-MATRIX
  0.2352E+02
  0.2504E+02   0.2757E+02
  0.2429E+02   0.2553E+02   0.2568E+02
  0.1240E+02   0.1303E+02   0.1304E+02   0.6667E+01
RLMUL IER =          0
ANOVA
      DF       DF-RES     DF-TOT    SS-REC        SS-RES         SS-TOT      MS-REG
3.0000    26.0000    29.0000   0.6636E+01   0.3077E-01   0.6667E+01   0.2212E+01
MS-RES           F-VALUE   P-EXC HO   %-EXPL  STDV-RES  %R-MEAN  OK=4
0.1183E-02    0.1869E+04   0.0000   99.5385   0.3440E-01   0.1032E+02   4.0000
```

(Cont'd on next page)

APPENDIX 3.4 (Cont'd.)

B-MATRIX

REG-COEFF	L-LIM	U-LIM	STDV-ERR	PART-F-VALUE	P-EXC HO
0.2077E+00	0.4567E-01	0.3698E+00	0.7883E-01	0.8216E-02	0.6942E+01
-0.5504E-01	-0.1367E+00	0.2665E-01	0.3974E-01	0.2270E-02	0.1918E+01
0.3662E+00	0.2657E+00	0.4668E+00	0.4891E-01	0.6634E-01	0.5605E+02
0.1539E-02	-0.1426E-01	0.1734E-01	0.7686E-02	0.0000E+00	0.0000E+00

VARB

0.5251E+01		
-0.2145E+01	0.1335E+01	
-0.2834E+01	0.7014E+00	0.2022E+01

Y-HAT = 0.0015 + 0.2077 X1 + -0.0550 X2 + 0.3662 X3 + model KJ

model values used

APPENDIX 4.1: USEFULNESS OF VARIABILITY MEASURE-- FOR FEMALE SUBJECT

```

R REGRESS
LU OF DATA FILE
90
# OF INDEPENDENT VARIABLES, E.G. 3
3
# OF DIFFERENT STIMULUS CONDITIONS, E.G. 2
2
# OF POINTS IN GROUP, E.G. 10
10
VERDJVV
TEMP1D.OUT      1
TEMP2K.OUT      2
TEMP3D.OUT      3
TEMP1D.OUT      1
TEMP2K.OUT      2
TEMP3D.OUT      3
                                stimulus condition

      z1      z2      z3      y
0.3747E-02  0.3559E-02  0.1104E-01  0.0000E+00
0.3873E-02  0.1041E-01  0.4610E-02  0.0000E+00
0.1695E-02  0.5232E-02  0.1454E-01  0.0000E+00
0.8106E-02  0.5737E-02  0.1219E-01  0.0000E+00
0.7576E-02  0.4068E-02  0.1013E+00  0.0000E+00
0.9514E-02  0.5407E-02  0.1111E-01  0.0000E+00
0.1090E-01  0.6532E-02  0.1675E-01  0.0000E+00
0.1369E-01  0.1804E-02  0.9163E-02  0.0000E+00
0.1902E-02  0.9029E-02  0.9211E-01  0.0000E+00
0.7406E-02  0.5252E-02  0.2258E+00  0.0000E+00
0.6244E-02  0.1617E-01  0.2427E-01  0.1000E+01
0.4223E-01  0.2207E-01  0.2985E-01  0.1000E+01
0.1353E-01  0.6600E-01  0.2260E+00  0.1000E+01
0.3528E-01  0.1180E-01  0.1693E-01  0.1000E+01
0.5051E-01  0.6275E-02  0.2333E+00  0.1000E+01
0.3528E-01  0.1105E-01  0.4538E-01  0.1000E+01
0.1457E-01  0.2269E-01  0.5961E-01  0.1000E+01
0.1958E-01  0.1376E-01  0.1881E+00  0.1000E+01
0.2853E-01  0.4474E-01  0.6369E-01  0.1000E+01
0.2771E-01  0.1310E-03  0.5115E-01  0.1000E+01
SIGNIFICANCE ALFA, E.G..05
.05
BECOVN IER =      0
A-MATRIX
0.3990E-02
0.6276E-03  0.4802E-02
0.4885E-02  0.8257E-02  0.1224E+00
0.1025E+00  0.7883E-01  0.2198E+00  0.5000E+01
RLMUL IER =      0
ANOVA
      DF      DF-RES      DF-TOT      SS-REG      SS-RES      SS-TOT      MS-REG
3.0000  16.0000  19.0000  0.3471E+01  0.1529E+01  0.5000E+01  0.1157E+01
      MS-RES      F-VALUE      P-EXC HO      %-EXPL      STDV-RES      %-R-MEAN      OK=4
0.9557E-01  0.1211E+02  0.0002  69.4173  0.3901E+00  0.6183E+02  4.0000
                                variability z is related to stimulus

B-MATRIX
0.2365E+02  0.1298E+02  0.3432E+02  0.5032E+01  0.1211E+01  0.2209E+02
0.1342E+02  0.3330E+01  0.2350E+02  0.4758E+01  0.7599E+00  0.7952E+01
-0.5328E-01 -0.2080E+01  0.1974E+01  0.9563E+00  0.2966E-03  0.3104E-02
-0.8277E-01 -0.3443E+00  0.1788E+00  0.1234E+00  0.0000E+00  0.0000E+00
VARB
0.2650E+03
-0.1861E+02  0.2369E+03
-0.9320E+01 -0.1524E+02  0.9568E+01
Y-HAT =  -0.0828 +  23.6526 X1 +  13.4174 X2 +  -0.0533 X3 +
                                center      left hemisphere      right
                                more variable
                                than right

```


APPENDIX 4.2: USEFULNESS OF VARIABILITY MEASURE-- FOR MALE SUBJECT

LU OF DATA FILE

90

OF INDEPENDENT VARIABLES, E.G. 3

3

OF DIFFERENT STIMULUS CONDITIONS, E.G. 2

2

OF POINTS IN GROUP, E.G. 10

10

TEMP1K.OUT 1

TEMP2K.OUT 2

TEMP3K.OUT 3

VERKJVV

TEMP1K.OUT 1

TEMP2K.OUT 2

TEMP3K.OUT 3

z_1	z_2	z_3	y
0.9354E+00	0.5004E-01	0.1019E+00	0.0000E+00
0.7964E+00	0.1912E+00	0.6059E-01	0.0000E+00
0.7046E+00	0.3850E+00	0.4898E-01	0.0000E+00
0.1252E+00	0.2421E+00	0.1624E-01	0.0000E+00
0.1737E+01	0.1029E+00	0.4250E-01	0.0000E+00
0.3046E+00	0.1029E+01	0.5255E-01	0.0000E+00
0.4322E+00	0.1029E+01	0.4749E-01	0.0000E+00
0.8312E+00	0.33E+00	0.2058E+00	0.0000E+00
0.8436E+00	0.2217E+00	0.2985E-01	0.0000E+00
0.1105E+01	0.2338E-01	0.1348E+00	0.0000E+00
0.5642E-01	0.3131E+00	0.3875E-01	0.1000E+01
0.1492E+00	0.1244E+00	0.1989E-01	0.1000E+01
0.1652E+00	0.6974E+00	0.4122E-01	0.1000E+01
0.1554E+00	0.8784E-01	0.1984E-01	0.1000E+01
0.9855E+00	0.1420E+00	0.2439E+00	0.1000E+01
0.5516E+00	0.1642E+01	0.1220E+00	0.1000E+01
0.3278E-01	0.1367E+01	0.2906E+00	0.1000E+01
0.3021E+00	0.2310E+00	0.1102E+00	0.1000E+01
0.7830E-00	0.8025E+00	0.7498E-01	0.1000E+01
0.5214E+00	0.8611E+00	0.6018E-01	0.1000E+01

SIGNIFICANCE ALFA, E.G..05

.05

BECOVN IER = 0

A-MATRIX

0.3889E+01			
-0.1068E+00	0.3975E+01		
0.1428E+00	0.2379E+00	0.8428E-01	
-0.2444E+01	0.1488E+01	0.7495E-01	0.5000E+01

RLMUL IER = 0

ANOVA

DF	DF-RES	DF-TOT	SS-REG	SS-RES	SS-TOT	MS-REG
3.0000	16.0000	19.0000	0.2139E+01	0.2861E+01	0.5000E+01	0.7130E+00
MS-RES	F-VALUE	P-EXC HO	χ^2 -EXPL	STDV-RES	χ -R-MEAN	OK=4
0.1788E+00	0.3988E+01	0.0268	42.7825	0.4229E+00	0.8457E+02	4.0000

variability z is related to stimulus

B-MATRIX

REG-COEFF	L-LIM	U-LIM	STDV-ERR	PART-F-VALUE	P-EXC HO
-0.6653E+00	-0.1140E+01	-0.1908E+00	0.2339E+00	0.1580E+01	0.8834E+01
0.2836E+00	-0.2150E+00	0.7822E+00	0.2352E+00	0.2599E+00	0.1454E-01
0.1216E+01	-0.2219E+01	0.4750E+01	0.1667E+01	0.9506E-01	0.5316E+00
0.6175E+00	0.2108E+00	0.1024E+01	0.1918E+00	0.0000E+00	0.0000E+00

VARB

0.2803E+00			
0.4226E+01	0.3094E+00		
-0.5969E+00	-0.9468E+00	0.1555E+02	
Y-RAT = 0.6175 +	-0.6653 X1 +	0.2836 X2 +	1.2157 X3 +
	center	left	right hemisphere more variable than left

END

FILMED

1984

DATIC